

NACA
TN
4303

TECH LIBRARY KADS, NM



0067140

NATIONAL ADVISORY COMMITTEE FOR AERONAUTICS

LOAN COPY: 5
AFWL C
TECHNICAL NOTE 4303 KIRTLAND AF

MEASUREMENTS AND POWER SPECTRA OF
RUNWAY ROUGHNESS AT AIRPORTS IN COUNTRIES OF
THE NORTH ATLANTIC TREATY ORGANIZATION

By Wilbur E. Thompson

Langley Aeronautical Laboratory
Langley Field, Va.



Washington

July 1958



0067140

NATIONAL ADVISORY COMMITTEE FOR AERONAUTICS

TECHNICAL NOTE 4303

MEASUREMENTS AND POWER SPECTRA OF
RUNWAY ROUGHNESS AT AIRPORTS IN COUNTRIES OF
THE NORTH ATLANTIC TREATY ORGANIZATION

By Wilbur E. Thompson

SUMMARY

Measurements of runway roughness obtained by a profile-survey method are presented. A variety of runway lengths or sections and degrees of roughness were measured. The results are presented as elevation profiles of the runways surveyed and in the form of power spectra.

INTRODUCTION

Because of concern regarding taxiing loads due to runway roughness, various programs have been undertaken to accumulate data on runway profiles. An initial step in this endeavor was the roughness measurement of two runways at Langley Air Force Base, Va. These data are presented in reference 1. An additional aid in this study was the roughness measurement of runways at four commercial airports which have large amounts of traffic. These data are presented in the form of elevation profiles in reference 2.

In order to increase the amount of data available for runway roughness studies, the National Advisory Committee for Aeronautics has agreed to process runway-profile data obtained through the Advisory Group for Aeronautical Research and Development on runways located in member countries of the North Atlantic Treaty Organization. These data are compiled by the surveying method described in reference 1. As a first step in this program, measurements have been obtained for 28 runways. This report presents measurements of these 28 runways and 6 additional runways as elevation profiles and power spectral densities.

SYMBOLS

- m number of uniformly spaced points over frequency range at which power estimates are desired

n	number of equally spaced elevations taken over runway
x	distance, ft
Δx	space interval, ft
y(x)	random function of distance (runway elevation)
λ	wavelength, ft
σ	root-mean-square value of y
$\Phi(\Omega)$	power-spectral-density function, $\frac{\text{ft}^2}{\text{radian}/\text{ft}}$
Ω	reduced frequency, $2\pi/\lambda$, radians/ft

SURVEY OF RUNWAY ELEVATIONS

The elevation-profile graphs and power-spectral-density graphs for the 34 runways evaluated herein are presented in figures 1 to 56. Runways 5R and 5L (figs. 8 and 9) constitute measurements along both the right and left sides of one runway. Runways 10-I and 10-II (figs. 17 and 18) constitute measurements of two sections or portions of one runway; and likewise, runways 22-I and 22-II (figs. 35 and 36) represent two sections of one runway. On runways 33 and 34 (figs. 53 and 54), measurements were made each month for a period of nine consecutive months.

The elevation-profile measurements were obtained by the profile-survey method described in references 1 and 2, that is, by means of a surveyor's level, rod, and tape, and by using an interval of 2 feet with the exception of the measurements on runway 8 (fig. 14) where an interval of 0.6 meter (approximately 1.97 feet) was used. As explained in reference 1, the selected measurement interval of 2 feet is one-half the shortest wavelength considered and adequately specifies the disturbance. This 4-foot wavelength corresponds to approximately 35 cycles per second at 100 miles per hour.

The runway elevations for runways 7 and 8 (figs. 13 and 14) were tabulated in meters in the original data and were converted to feet for use in this paper.

The measurements were taken along a line parallel to the runway center line, approximately along the path of a main landing gear of an aircraft landing or taking off.

The elevation references are arbitrary; however, the zero reference for measurement of several of the runways was close to sea level.

POWER SPECTRA OF RUNWAY ELEVATIONS

The power spectral densities which provide a description of the frequency characteristics of the runway roughness were computed by the method described in reference 3. Specifically, the computation of the power spectra involved the following steps:

- (1) The measured profile data were first prewhitened by the relation

$$y'(x) = y(x) - \theta y(x - \Delta x) \quad (\theta = 1)$$

This linear operation corresponds to the multiplication in the frequency plane by the frequency response function $F(\Omega)$ given by

$$F(\Omega) = 1 - e^{-i\Omega\Delta x}$$

- (2) The mean lagged products or autocovariance functions R_p were determined from

$$R_p = \frac{1}{n-p} \sum_{q=1}^{n-p} y'_q y'_{q+p} \quad (p = 0, 1, 2, \dots, m)$$

- (3) Initial or "raw" estimates of power I_h were determined by

$$I_h = \frac{2 \Delta x}{\pi} \sum_{p=0}^m \epsilon_p \cos \frac{hp\pi}{m} R_p \quad (h = 0, 1, 2, \dots, m)$$

where

$$\epsilon_p = \begin{cases} 1 & (0 < p < m) \\ 1/2 & (p = 0 \text{ or } m) \end{cases}$$

(4) Final or "smoothed" estimates of power Φ_h were determined as follows:

$$\Phi_h = \frac{1}{2} L_0 + \frac{1}{2} L_1 \quad (h = 0)$$

$$\Phi_h = \frac{1}{4} L_{h-1} + \frac{1}{2} L_h + \frac{1}{4} L_{h+1} \quad (1 \leq h \leq m - 1)$$

$$\Phi_h = \frac{1}{2} L_{m-1} + \frac{1}{2} L_m \quad (h = m)$$

(5) The results of the previous step are then divided by

$$|F(\Omega)|^2 = 2(1 - \cos \Omega \Delta x)$$

to compensate for the prewhitening operation.

Evaluation was made with $m = 40$, which is the number of uniformly spaced points over the frequency range investigated. Power-spectral-density values are plotted as a function of the reduced frequency

$\Omega = \frac{2\pi}{\lambda}$. Each point on the power-spectral-density graphs represents the

average power in a frequency interval $\pm \frac{\pi}{80}$ about the value plotted.

The cut-off frequency at the high-frequency end of the power curves is $\frac{\pi}{2}$ radians per foot, with the exception of runway 8 (fig. 15) where the

cut-off frequency was $\frac{\pi}{1.97}$ radians per foot.

The root-mean-square values were derived from the equation

$$\sigma^2 = \sum_{r=1}^m \Phi(\Omega)_r \frac{\pi}{80}$$

since the mean square of runway elevation is represented by the area under the power estimate curves. However, a lower limit of zero frequency is neither attainable nor desired; therefore, the root-mean-square values presented herein are approximations for comparison of average roughness within the frequency range investigated. The root mean square of runway elevation, σ , which is a convenient measure of average roughness, is presented for each runway on the respective power-spectral-density graphs.

Langley Aeronautical Laboratory,
National Advisory Committee for Aeronautics,
Langley Field, Va., April 28, 1958.

REFERENCES

1. Walls, James H., Houbolt, John C., and Press, Harry: Some Measurements and Power Spectra of Runway Roughness. NACA TN 3305, 1954.
2. Potter, Dexter M.: Measurements of Runway Roughness of Four Commercial Airports. NACA RM L56I26, 1957.
3. Press, Harry, and Tukey, John W.: Power Spectral Methods of Analysis and Their Application to Problems in Airplane Dynamics. Vol. IV of AGARD Flight Test Manual, Pt. IV C, Enoch J. Durbin, ed., North Atlantic Treaty Organization, pp. IVC:1 - IVC:41.

$$\text{Re} = \frac{2\pi}{\lambda} \text{ where } \lambda = 80 \text{ ft}$$

$$f_{\text{ref}} = \frac{\omega}{2\pi} = \frac{133}{80} = 1.66 \text{ Hz}$$

$$\omega_0 = \frac{\pi}{2\lambda} = \frac{\pi}{2 \cdot 80} \text{ rad/sec}$$

$$\omega_0 = \frac{\pi}{2 \cdot 80} = \frac{\pi}{160} \text{ rad/sec}$$

$$\omega_0 = \frac{\pi}{2 \cdot 80} = \frac{\pi}{160} \text{ rad/sec}$$

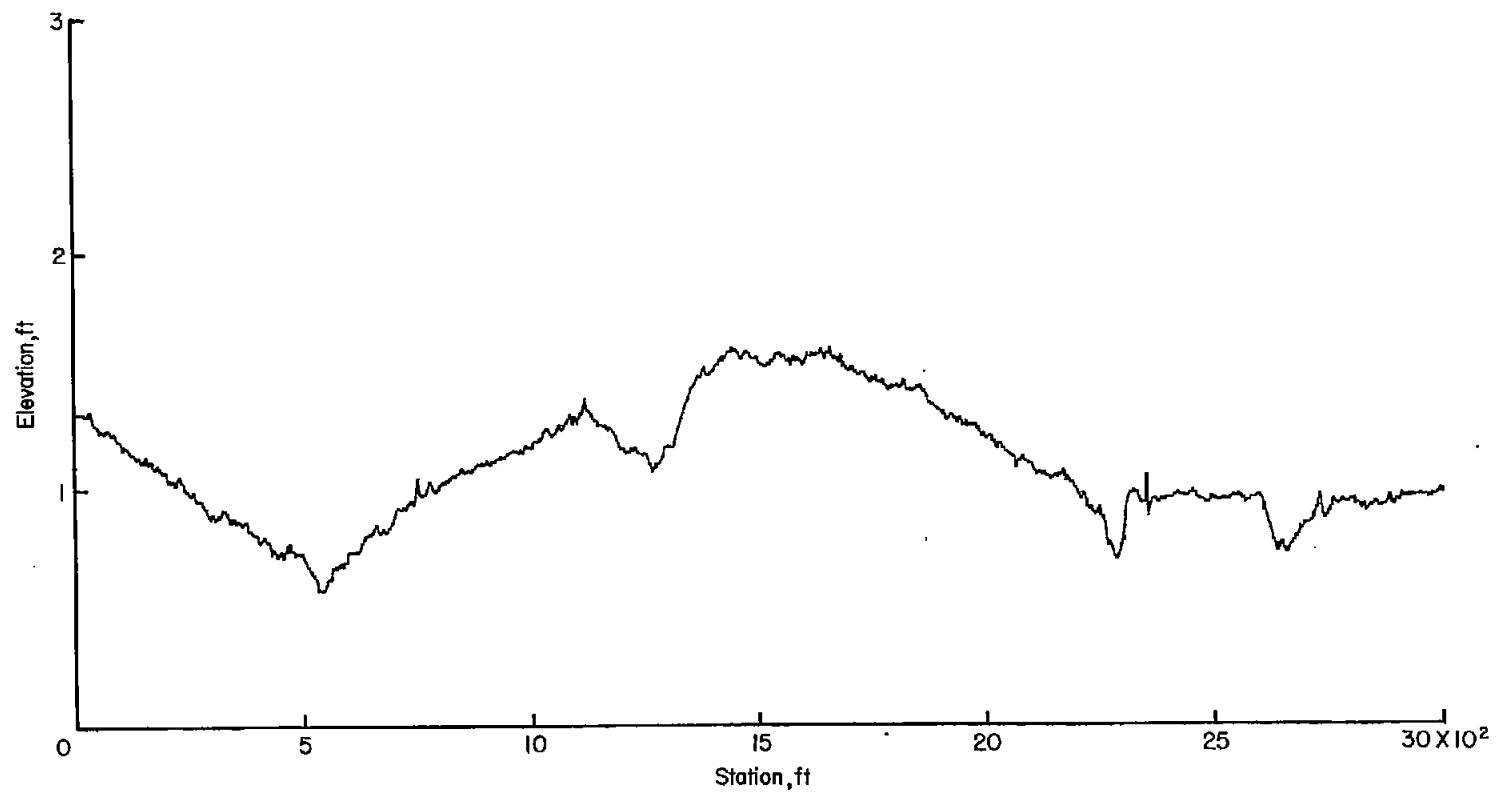


Figure 1.- Profile of runway 1.

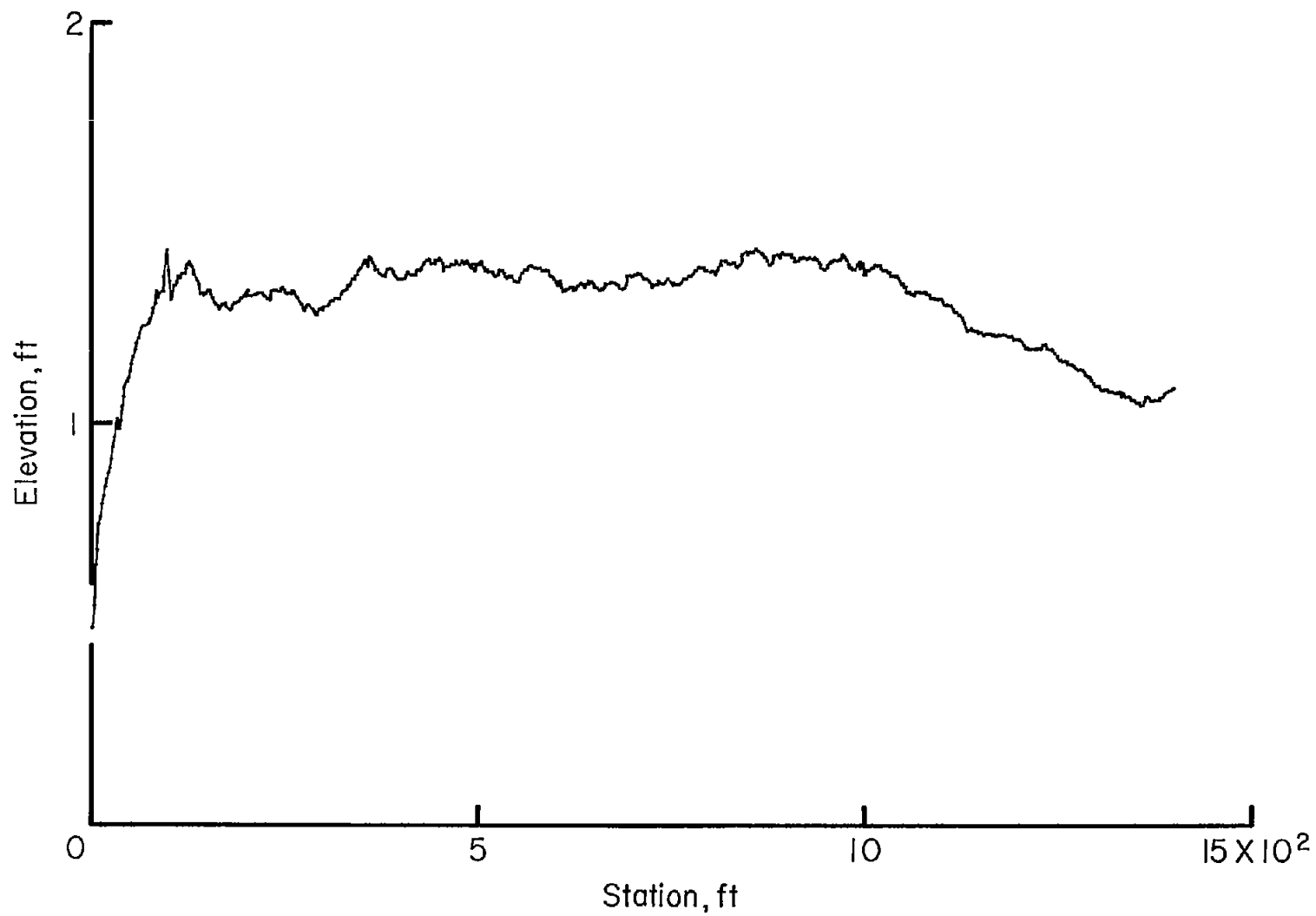


Figure 2.- Profile of runway 2.

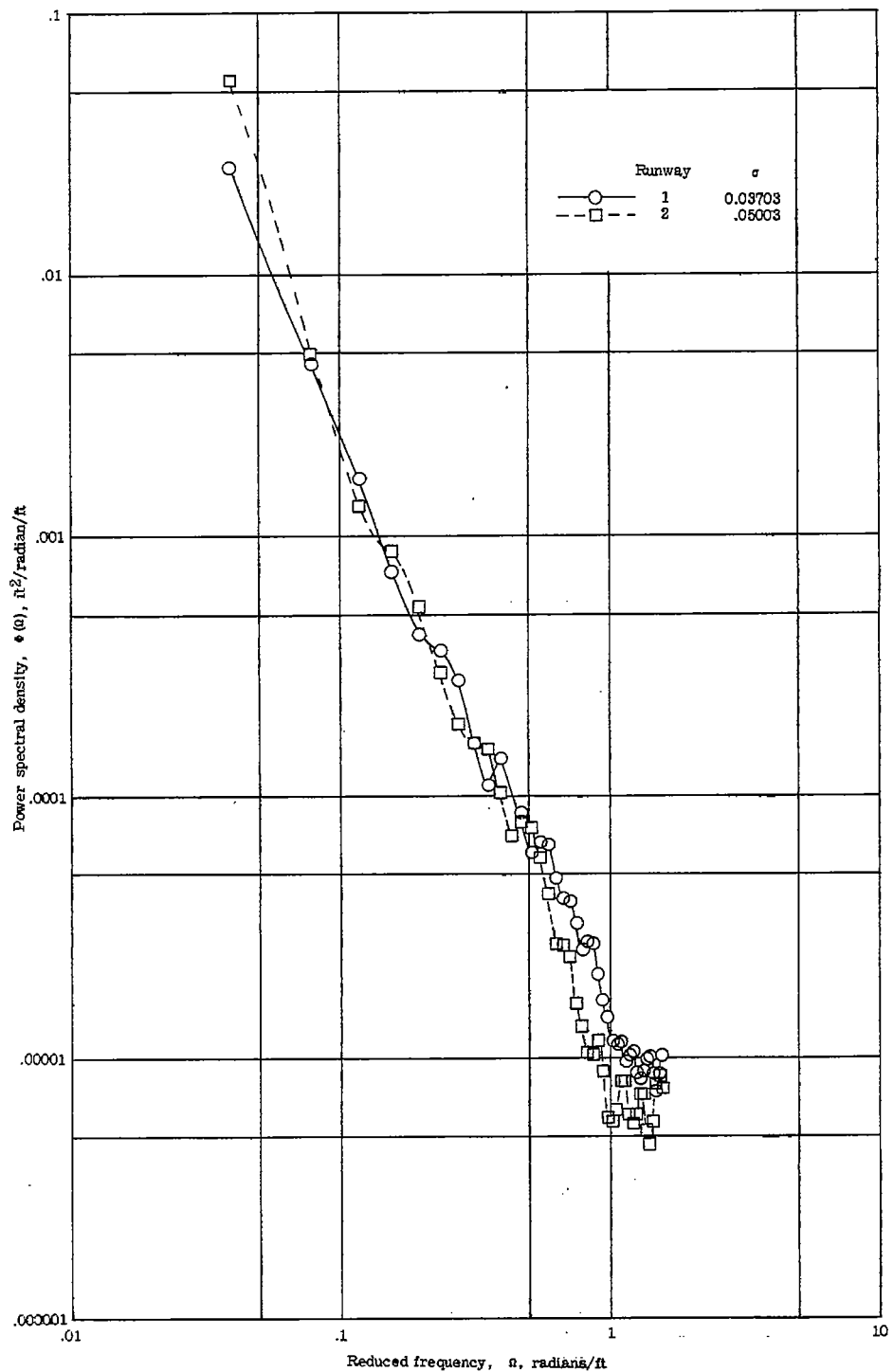


Figure 3.- Power-spectral-density functions for runways 1 and 2.

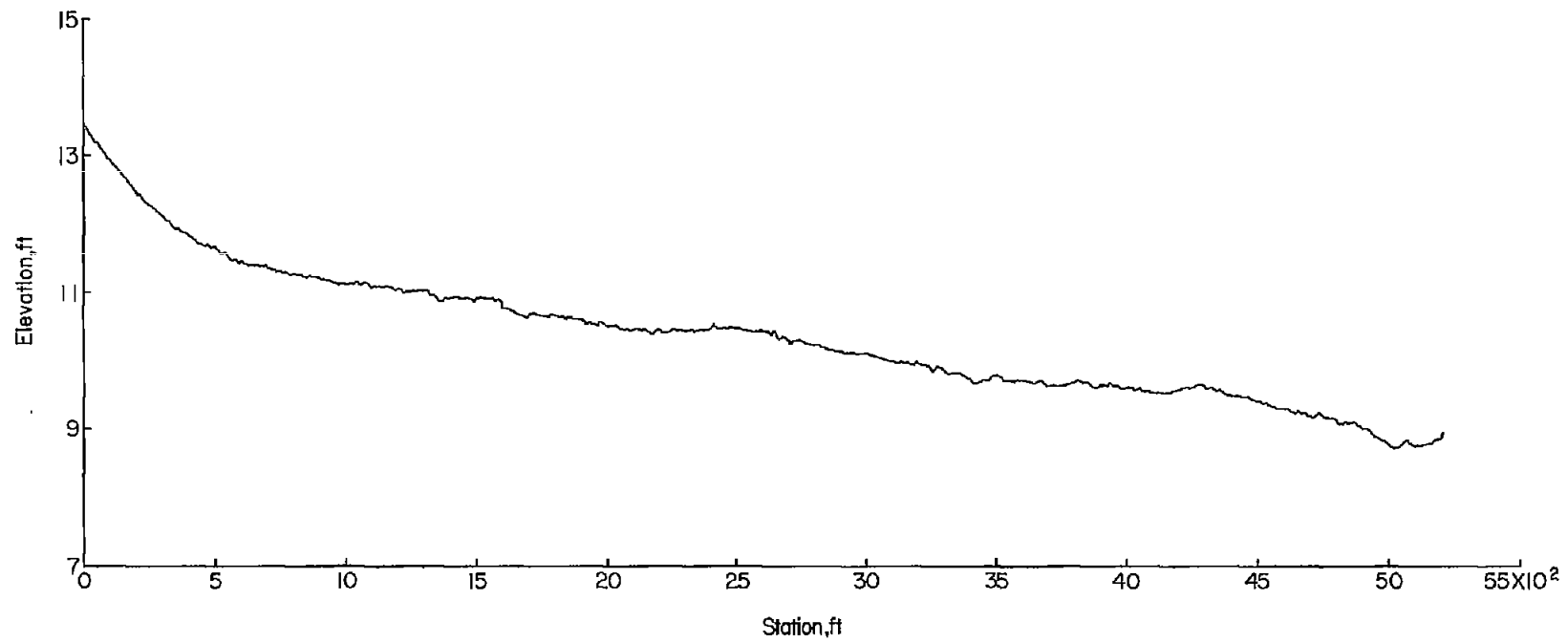


Figure 4.- Profile of runway 3.

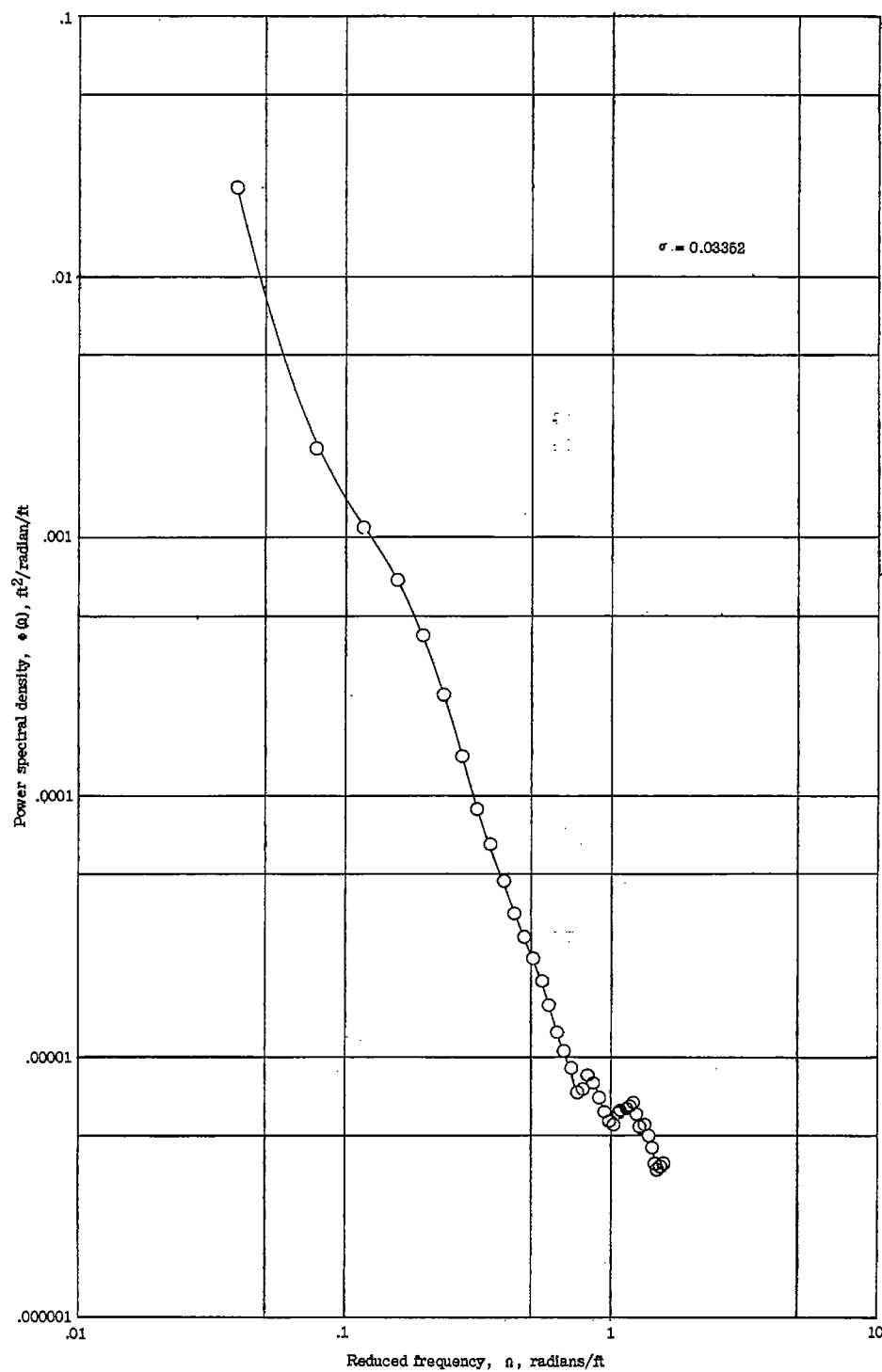


Figure 5.- Power-spectral-density functions for runway 3.

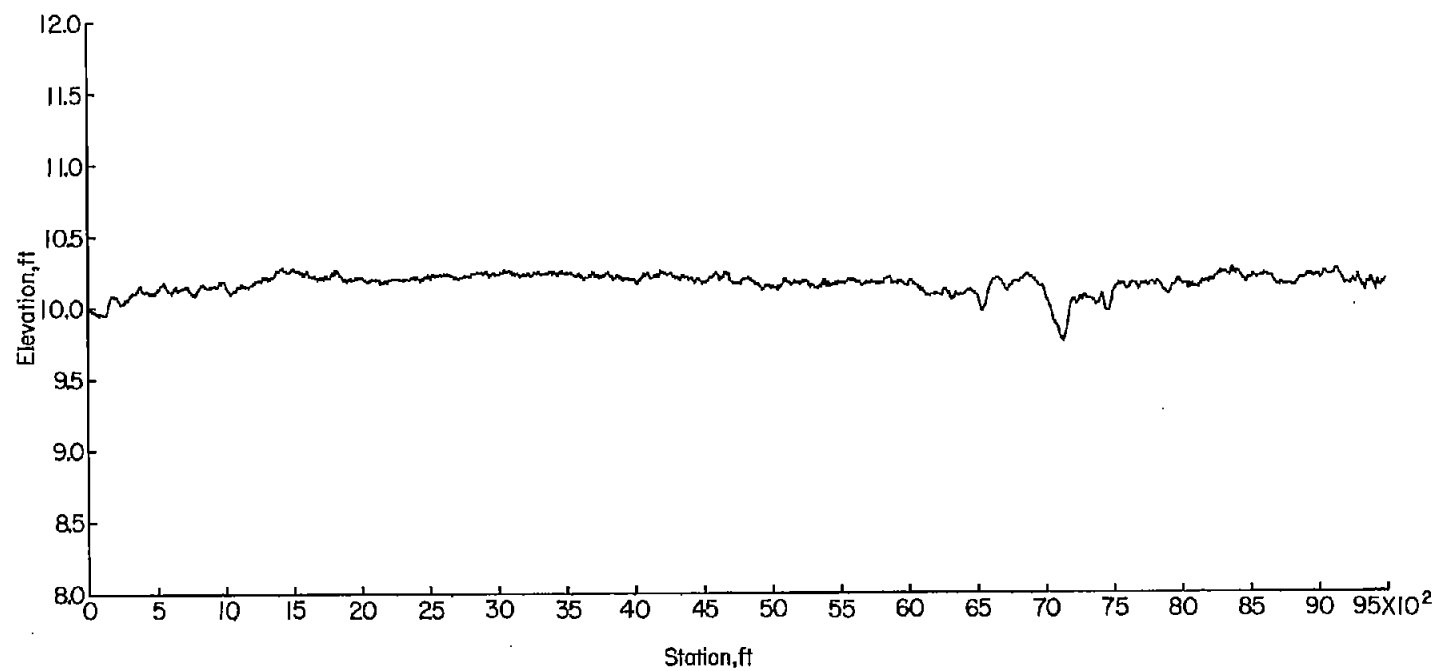


Figure 6.- Profile of runway 4.

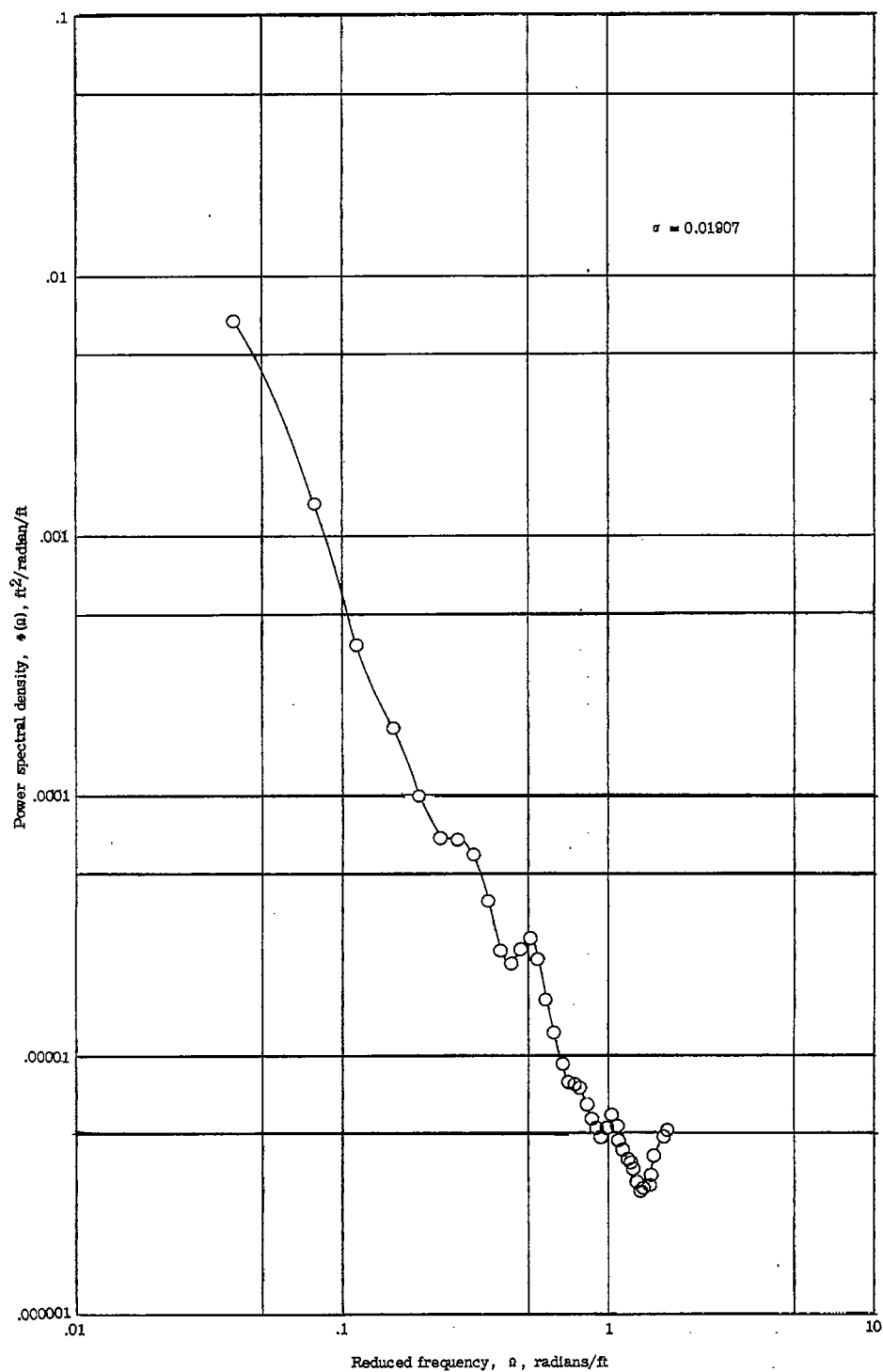


Figure 7.- Power-spectral-density functions for runway 4.

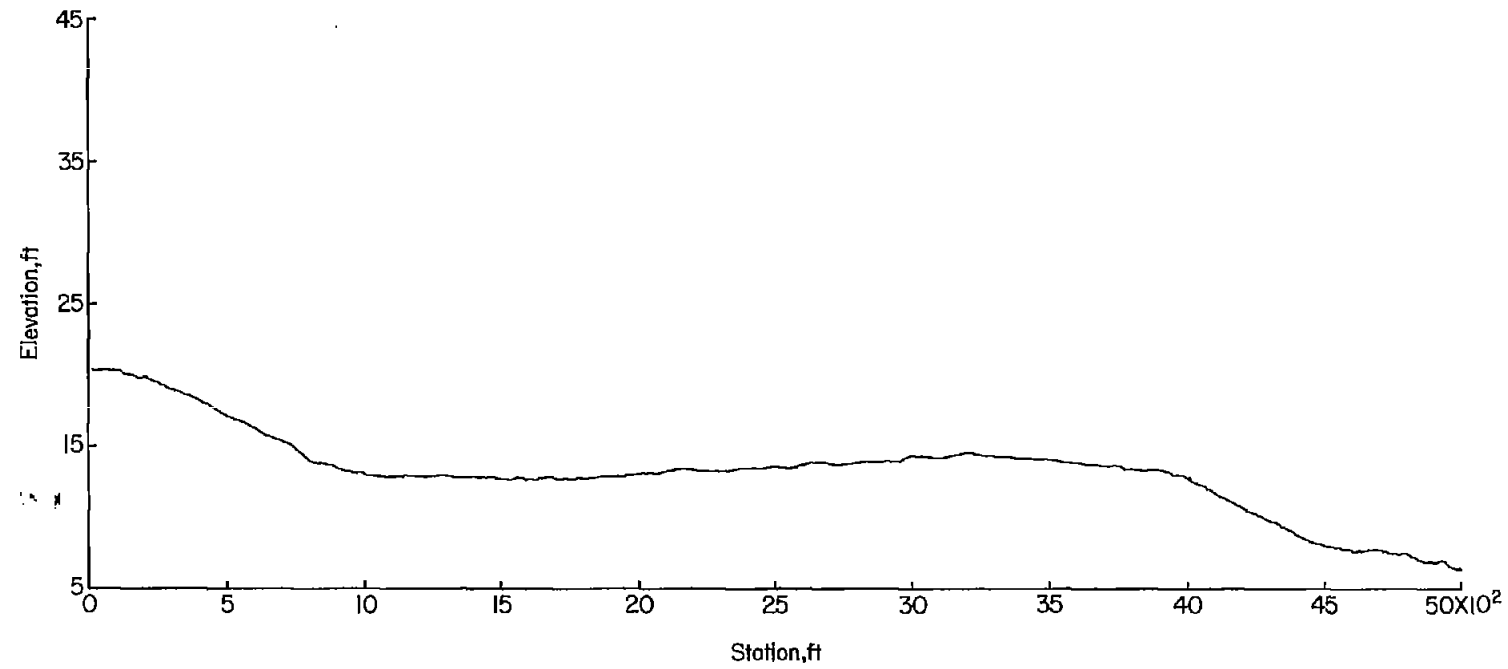


Figure 8.- Profile of runway 5R.

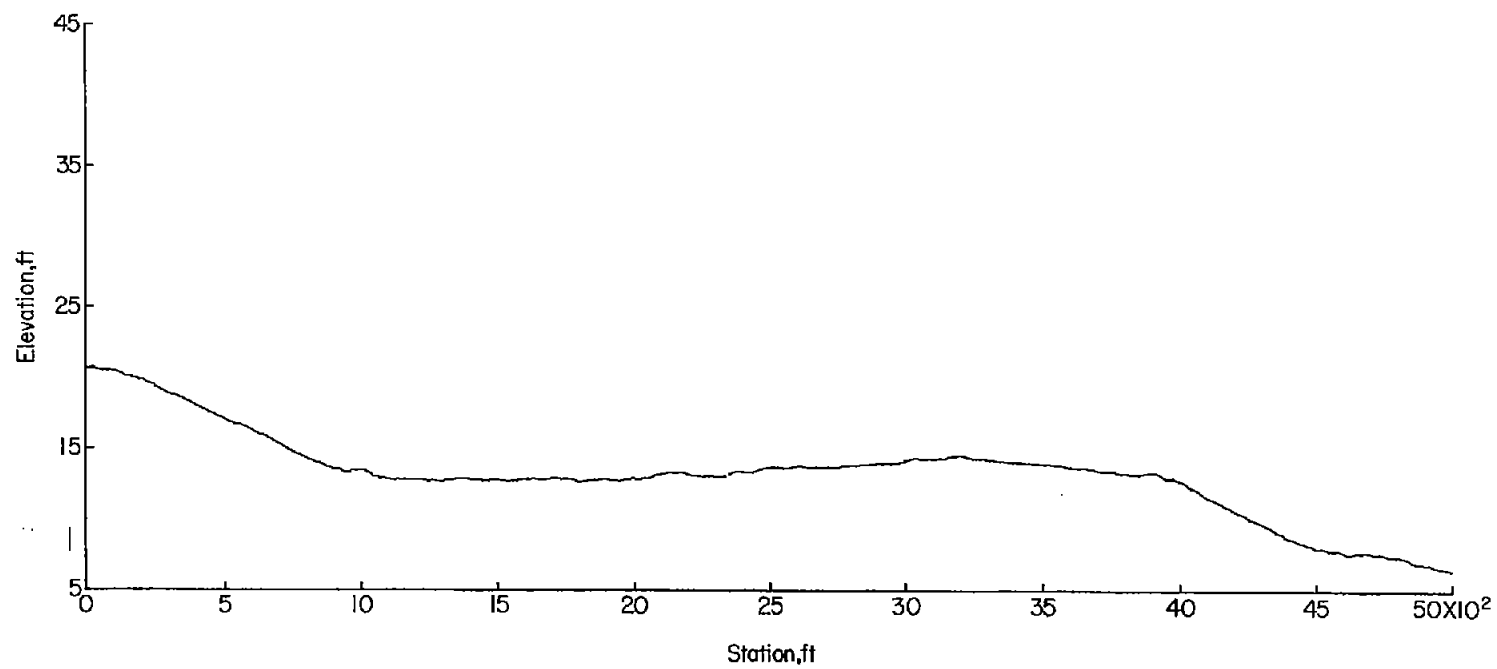


Figure 9.- Profile of runway 5L.

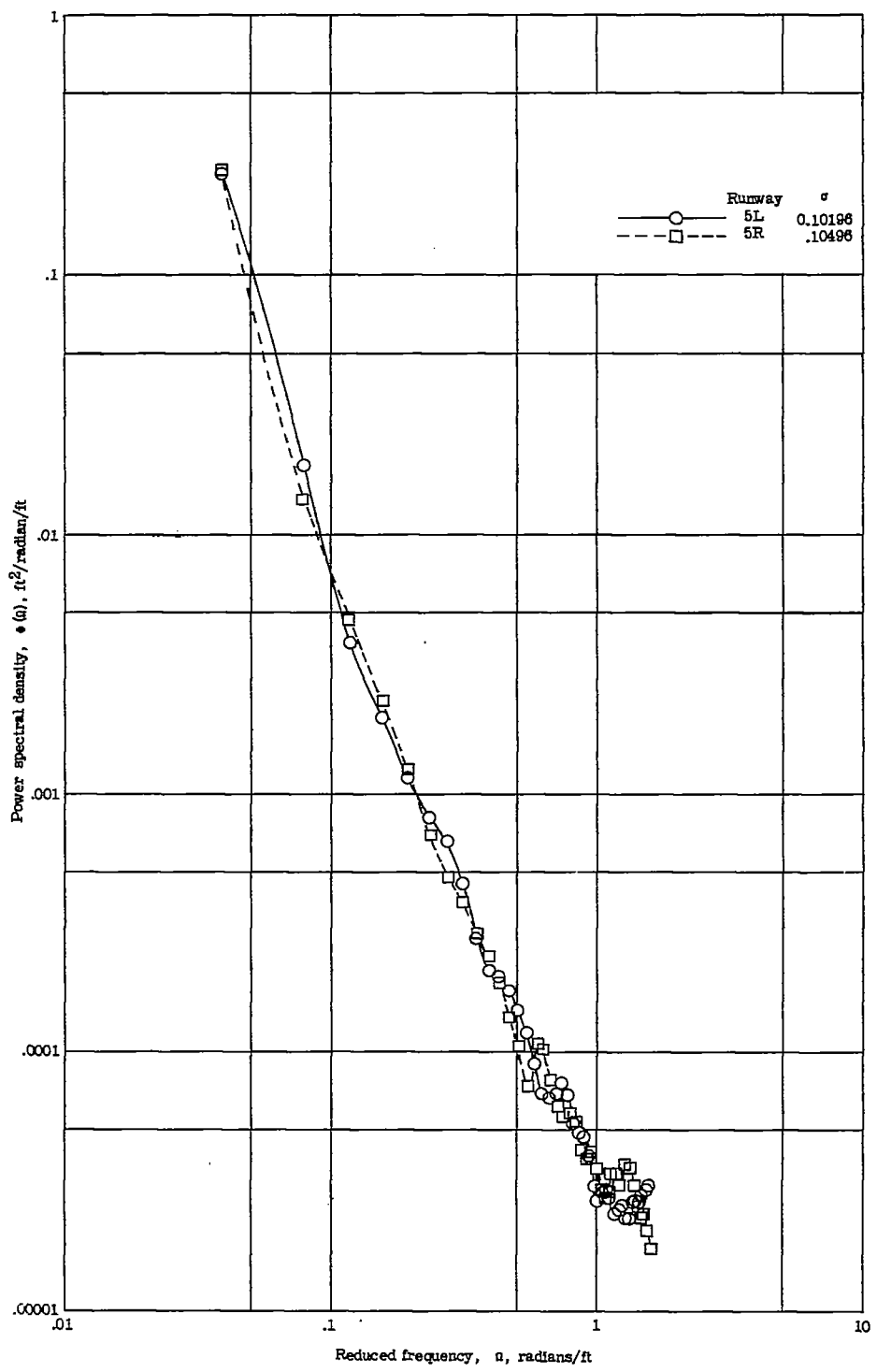


Figure 10.- Power-spectral-density functions for runway 5.

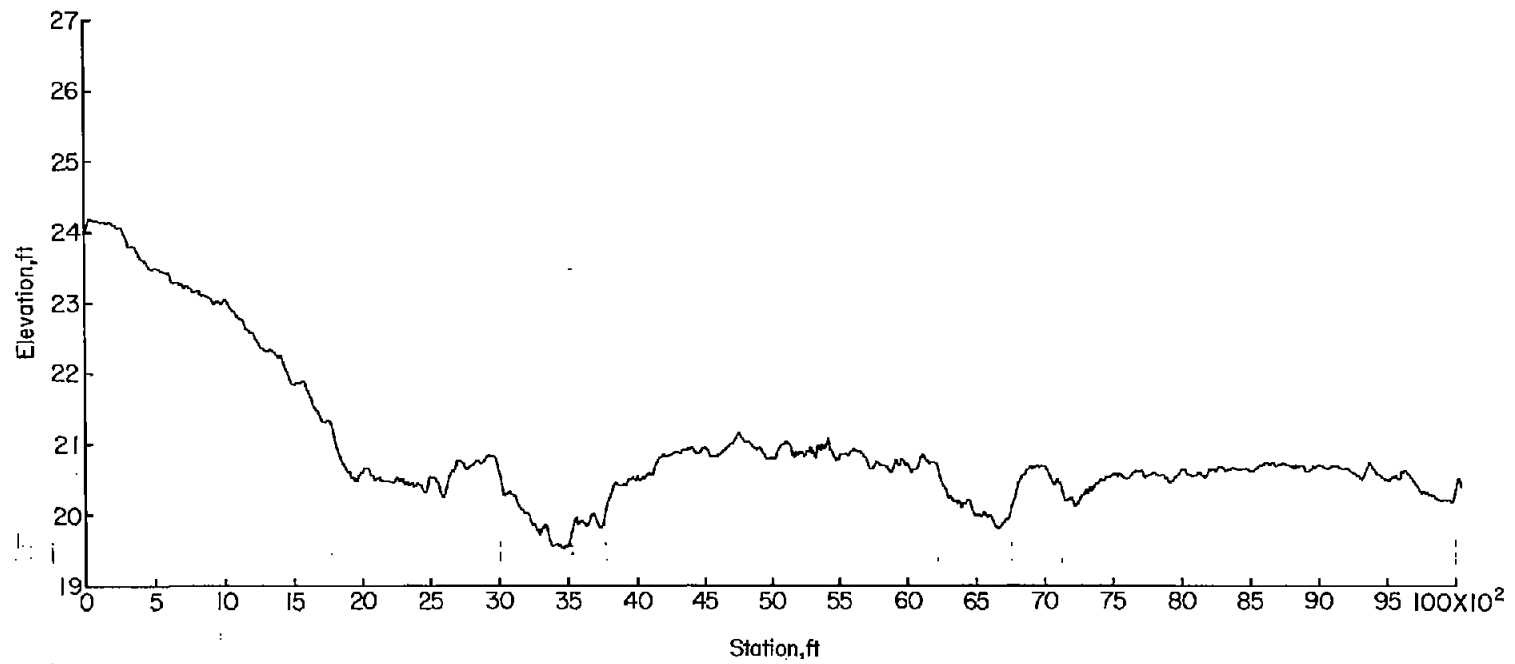


Figure 11.- Profile of runway 6.

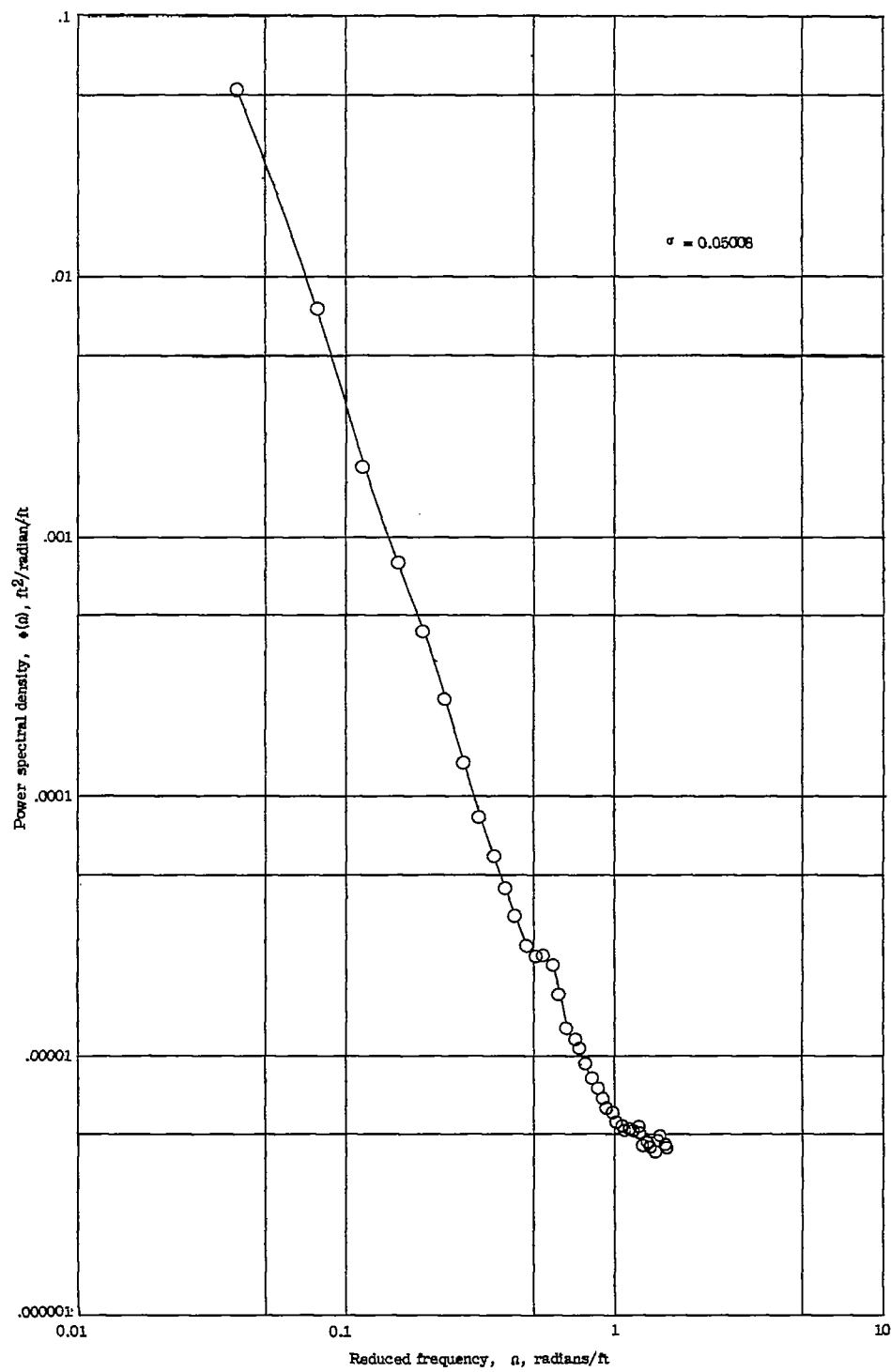


Figure 12.- Power-spectral-density functions for runway 6.

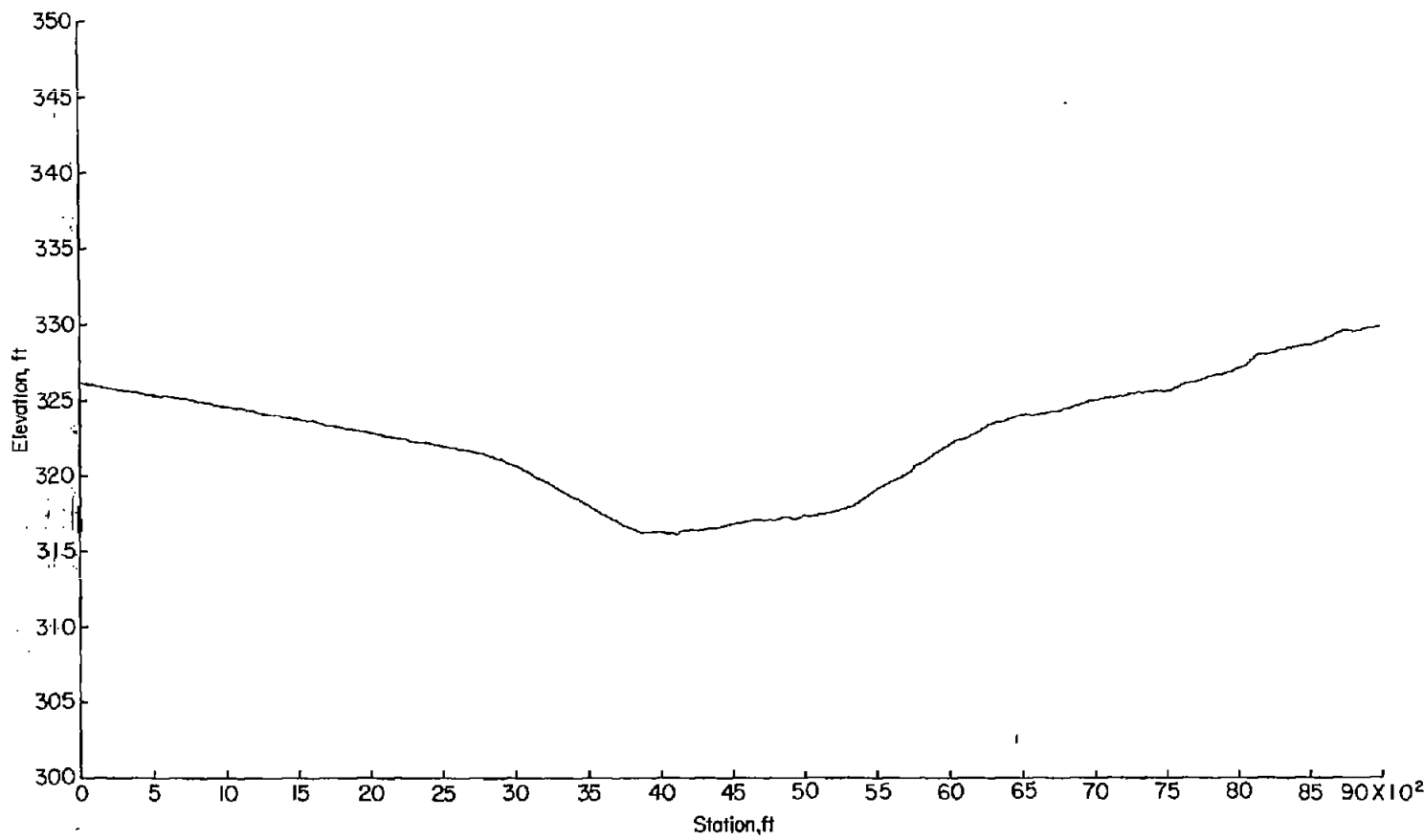


Figure 13.- Profile of runway 7.

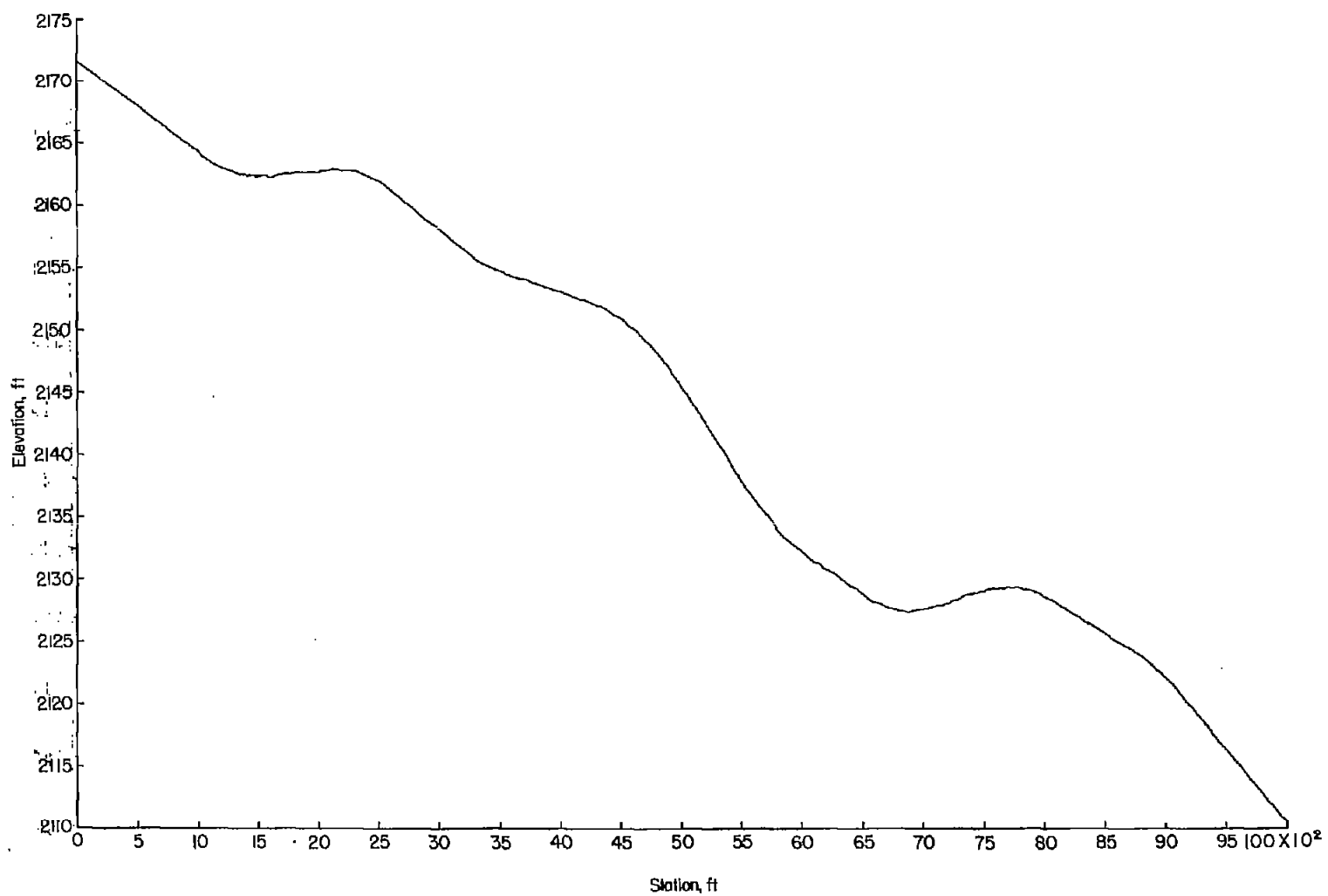


Figure 14.- Profile of runway 8.

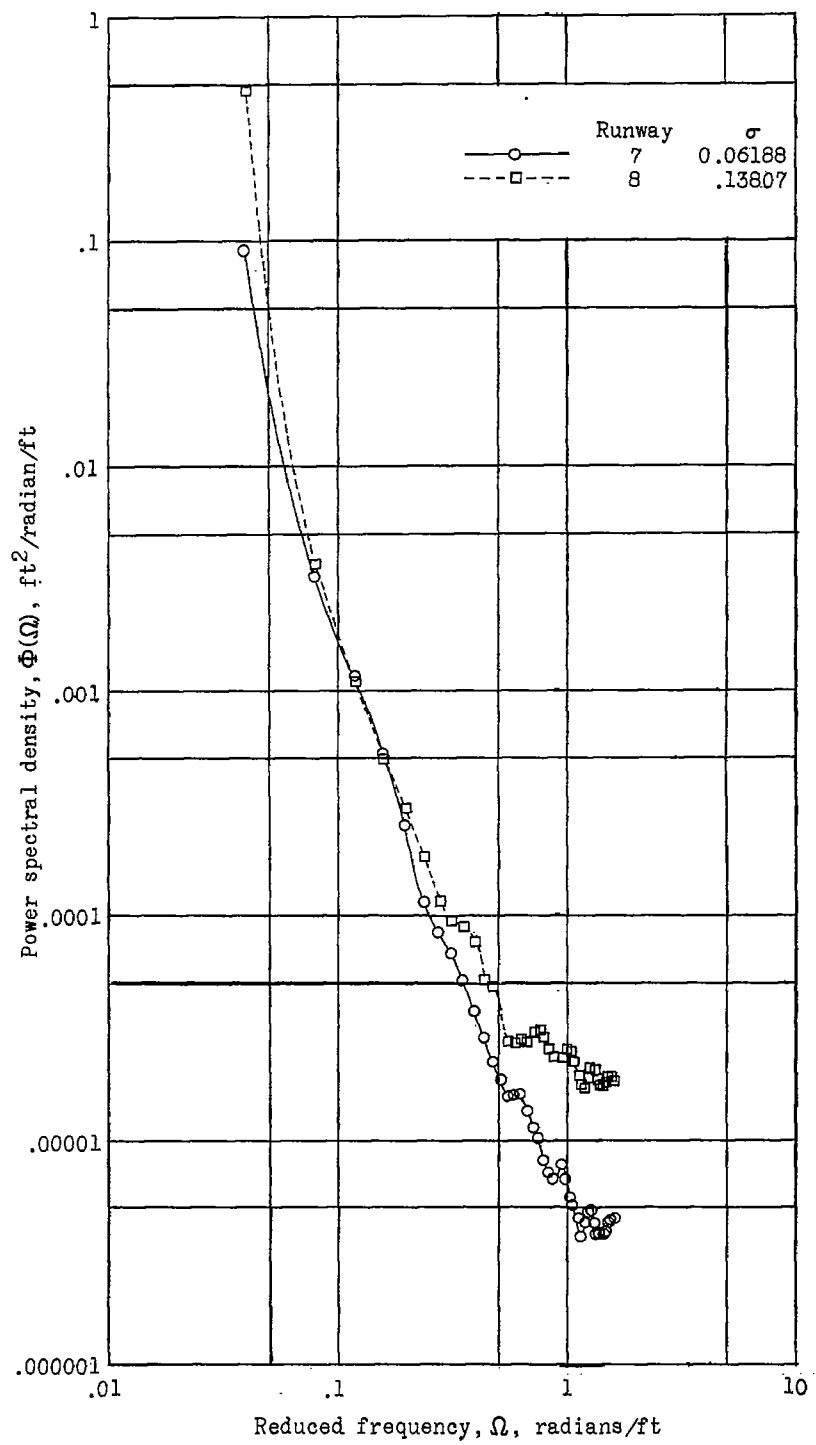


Figure 15.- Power-spectral-density functions for runways 7 and 8.

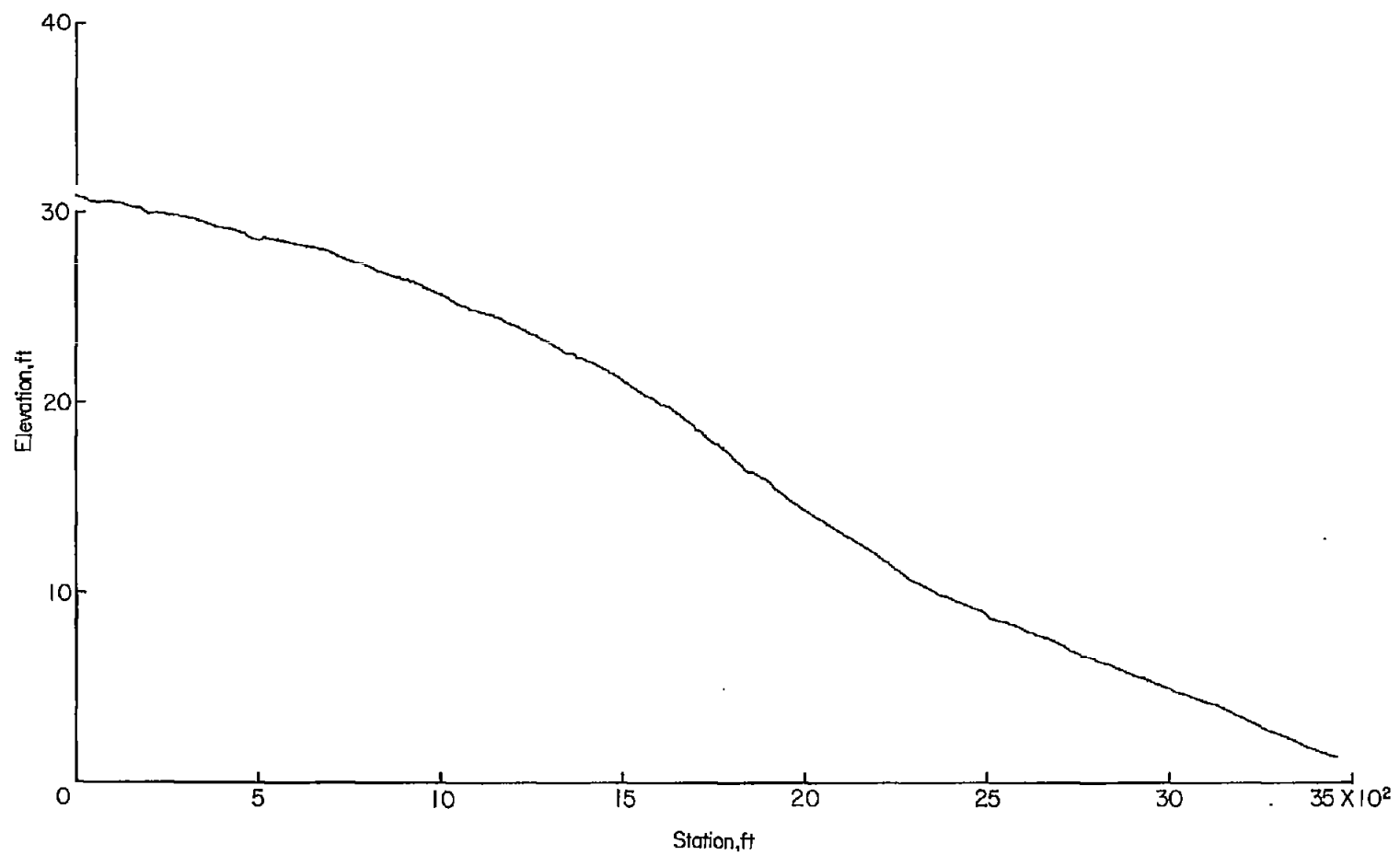


Figure 16.- Profile of runway 9.

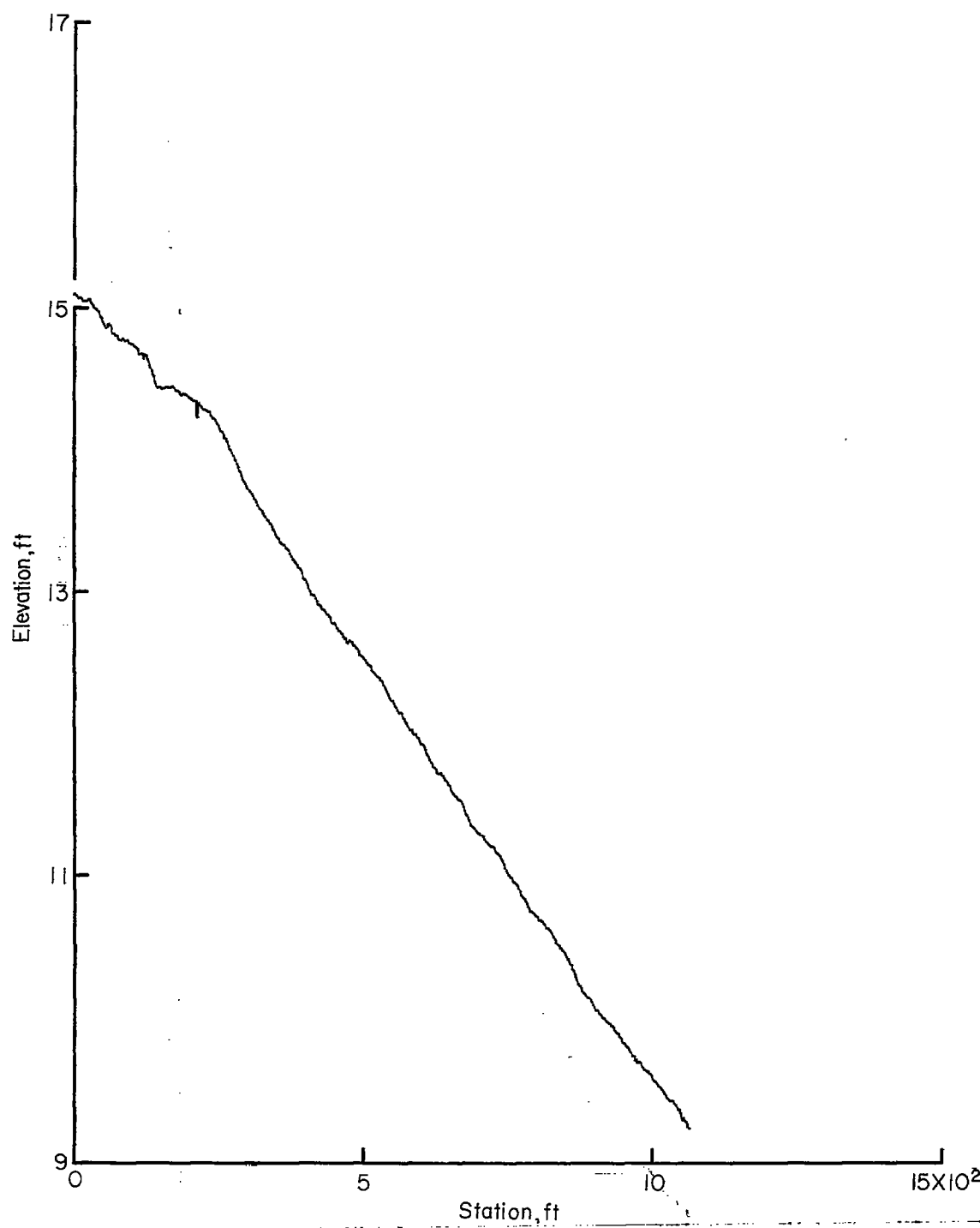


Figure 17.- Profile of runway 10-I.

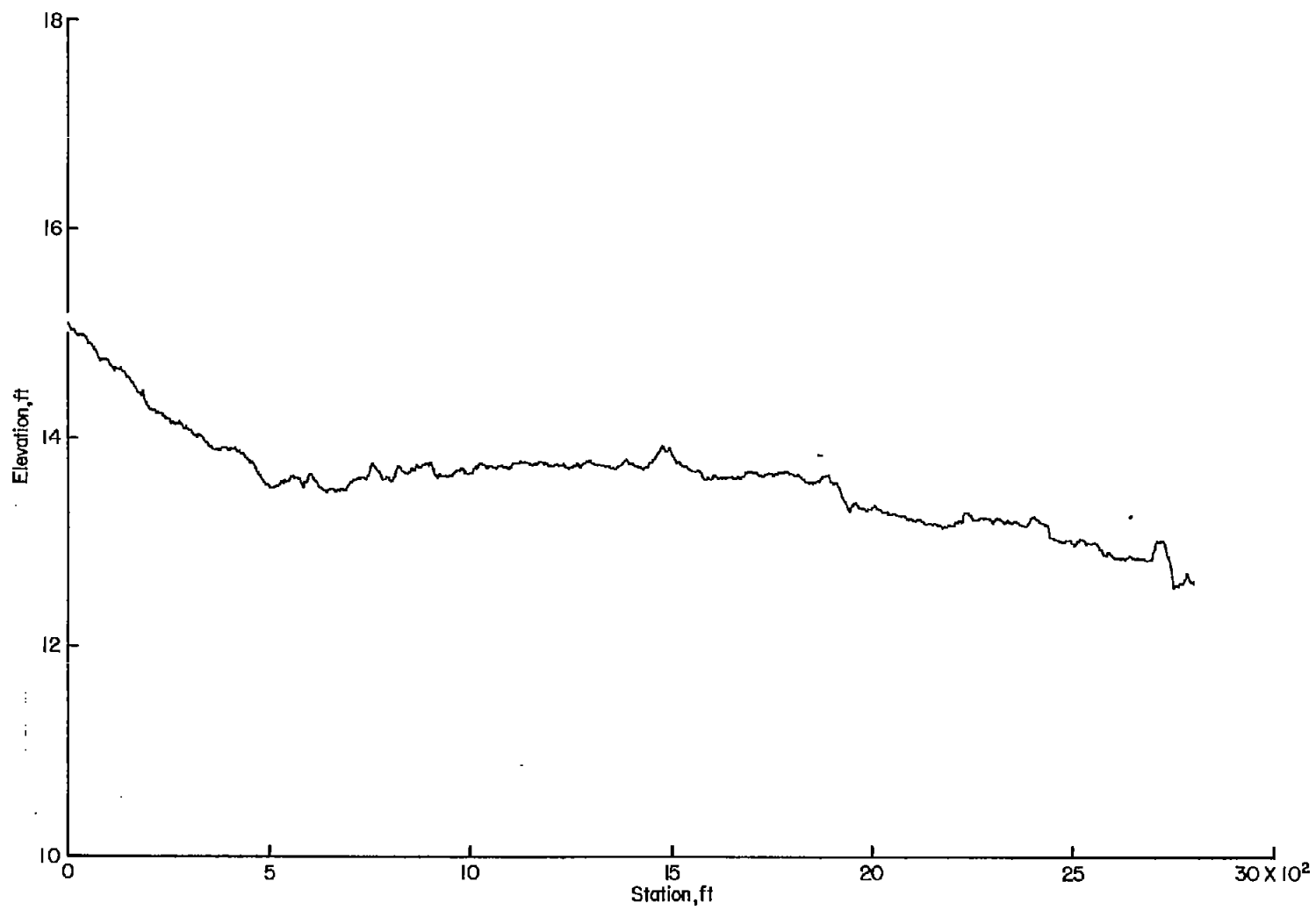


Figure 18.- Profile of runway 10-II.

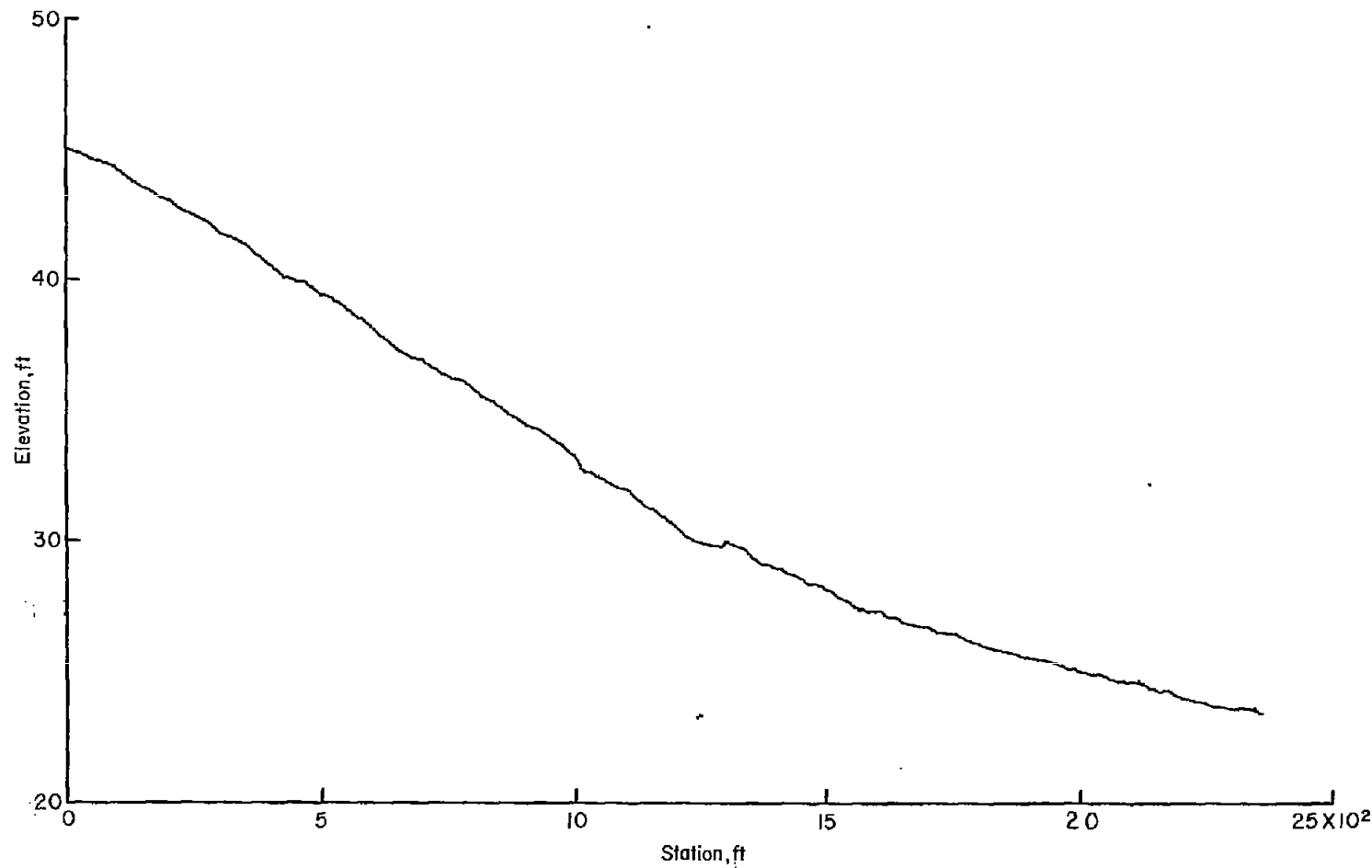


Figure 19.- Profile of runway 11.

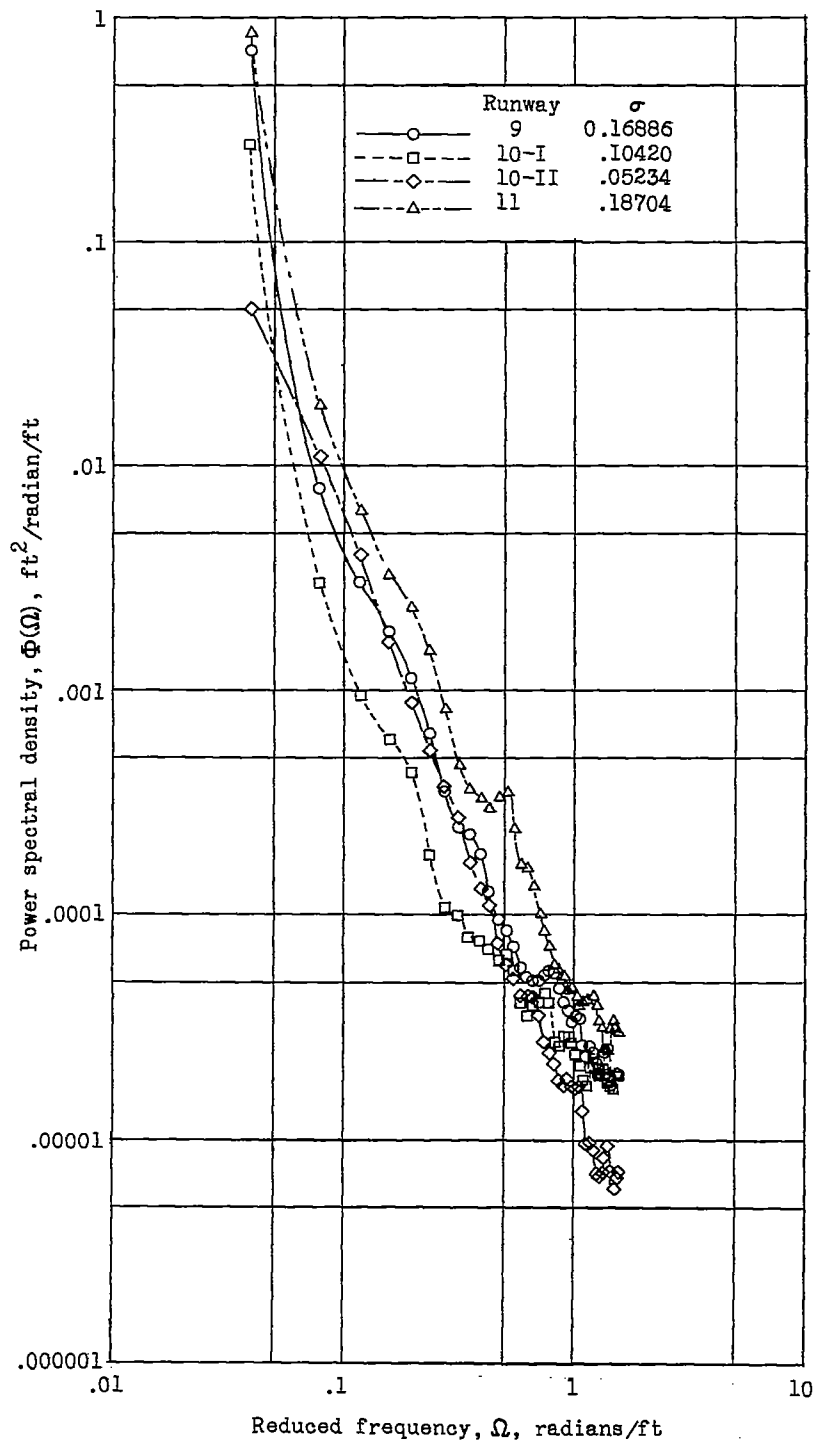


Figure 20.- Power-spectral-density functions for runways 9, 10, and 11.

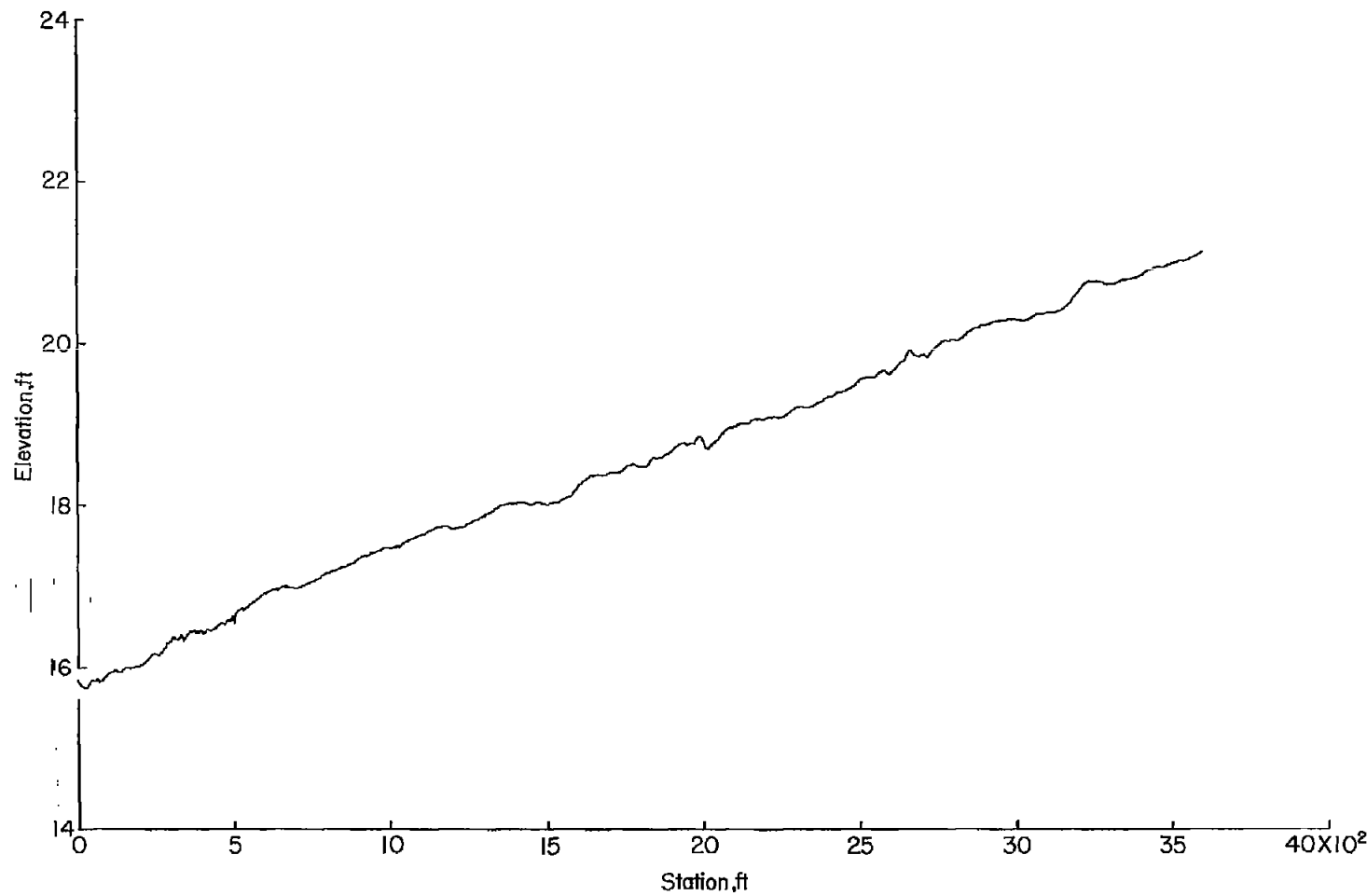


Figure 21.- Profile of runway 12.

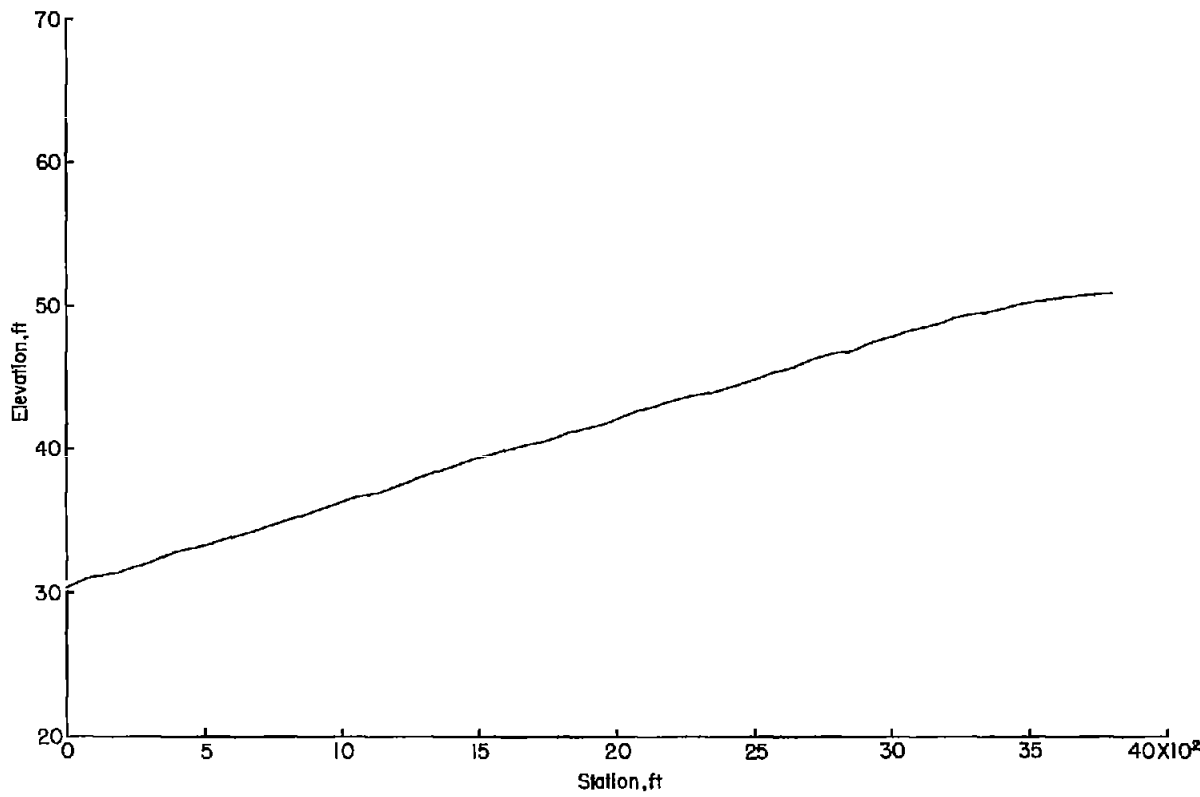


Figure 22.-- Profile of runway 13.

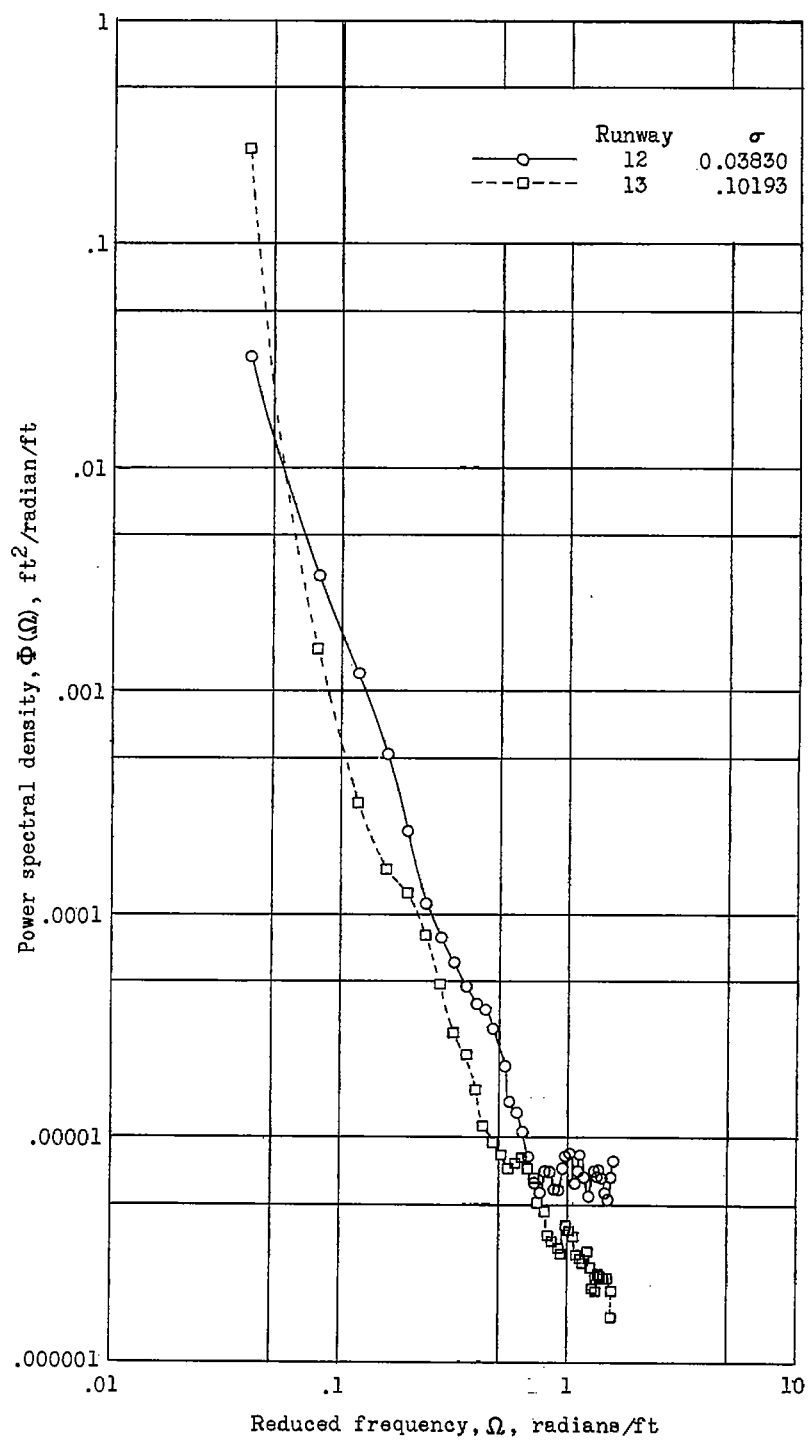


Figure 23.- Power-spectral-density functions for runways 12 and 13.

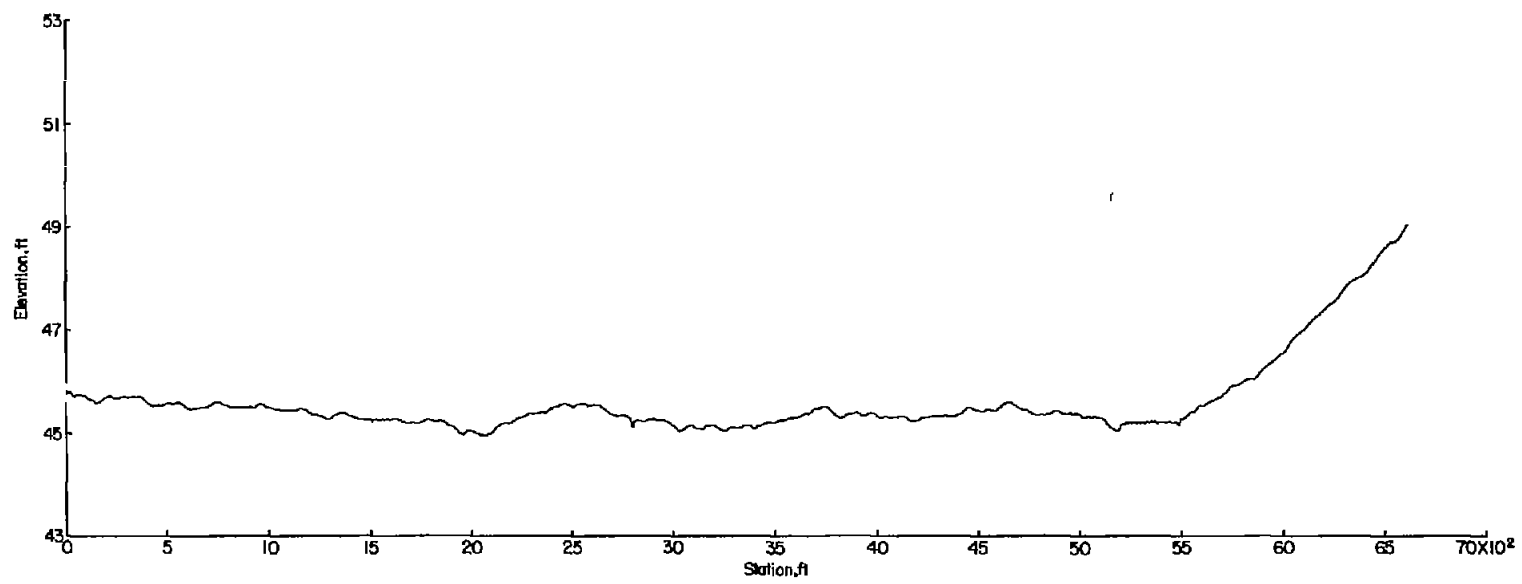


Figure 24.- Profile of runway 14.

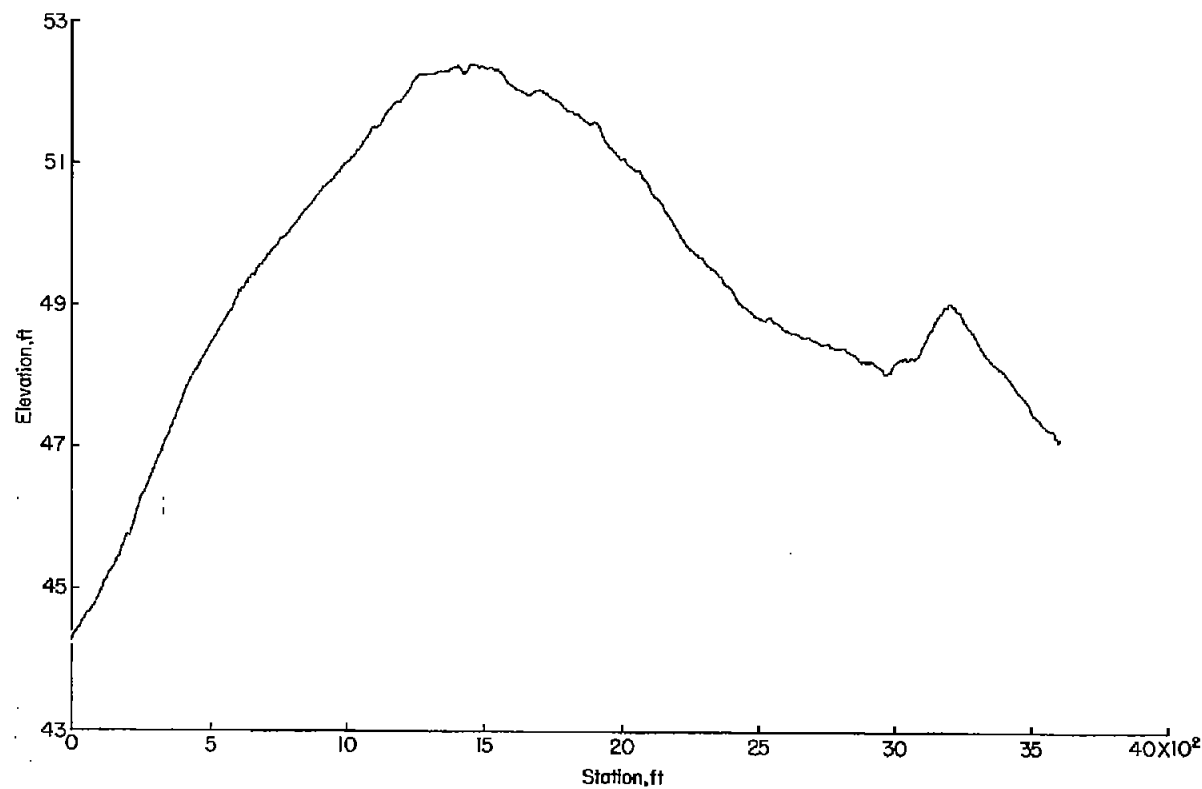


Figure 25.- Profile of runway 15.

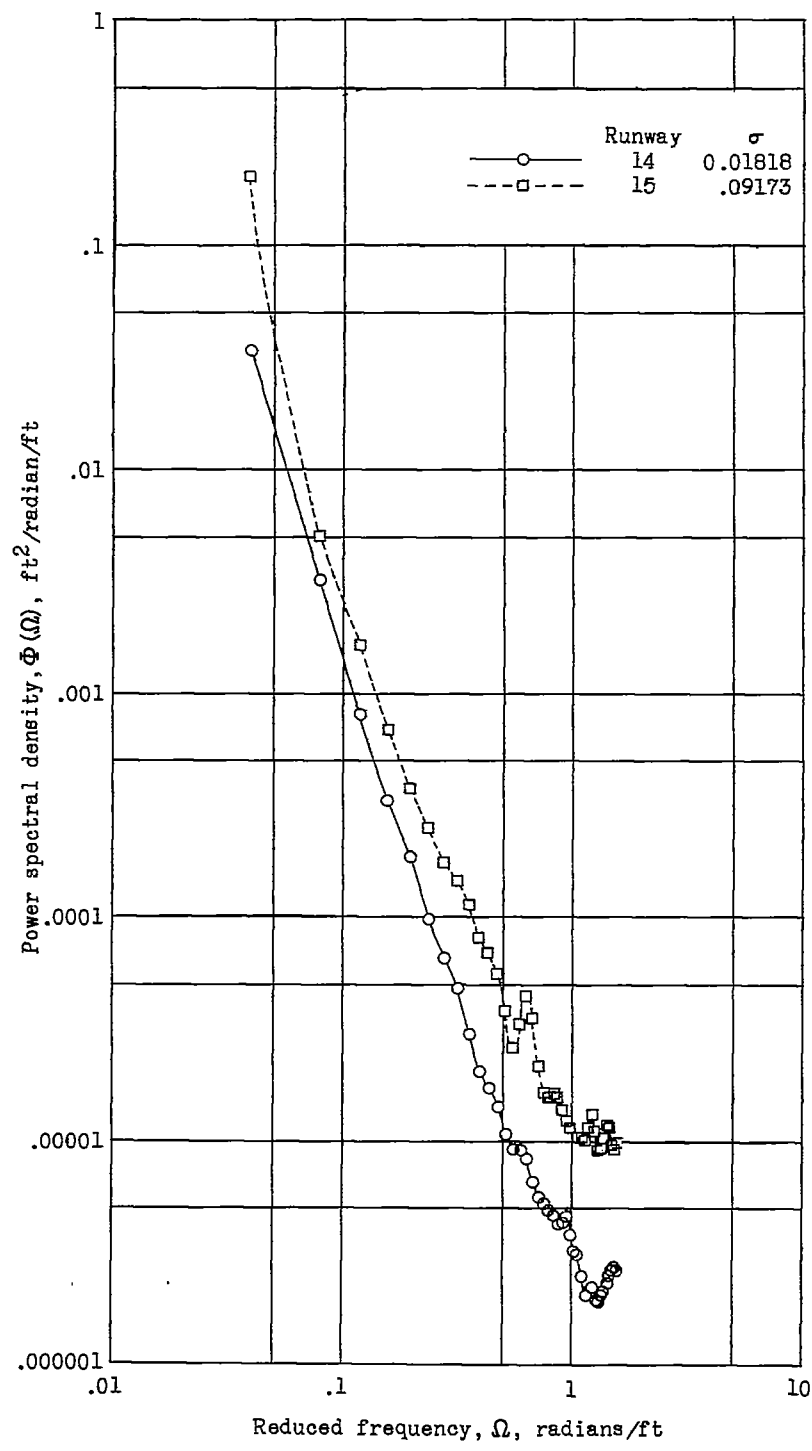


Figure 26.- Power-spectral-density functions for runways 14 and 15.

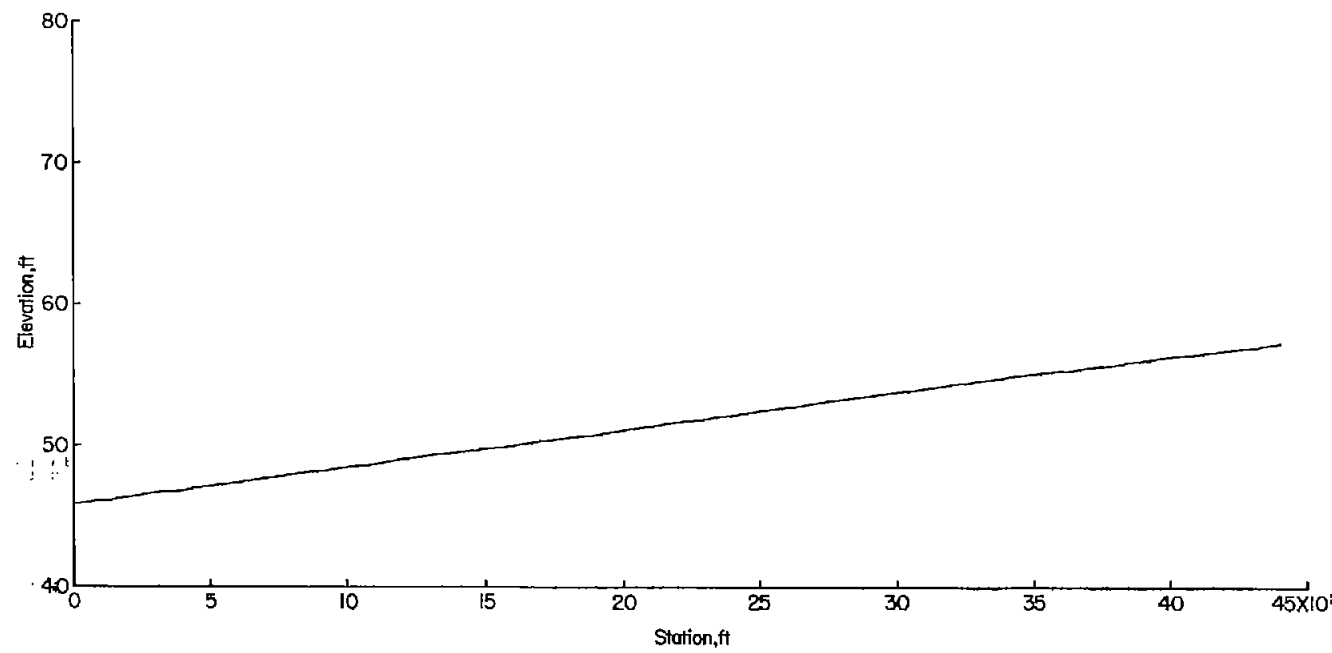


Figure 27.- Profile of runway 16.

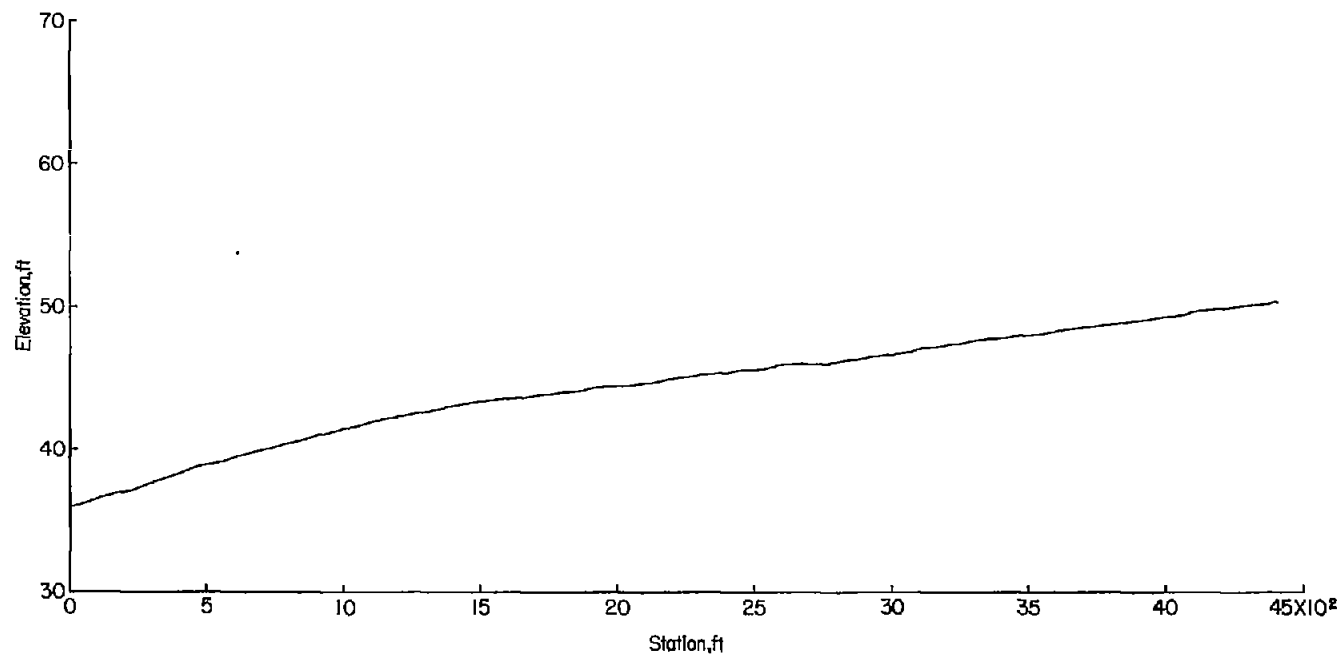


Figure 28.- Profile of runway 17.

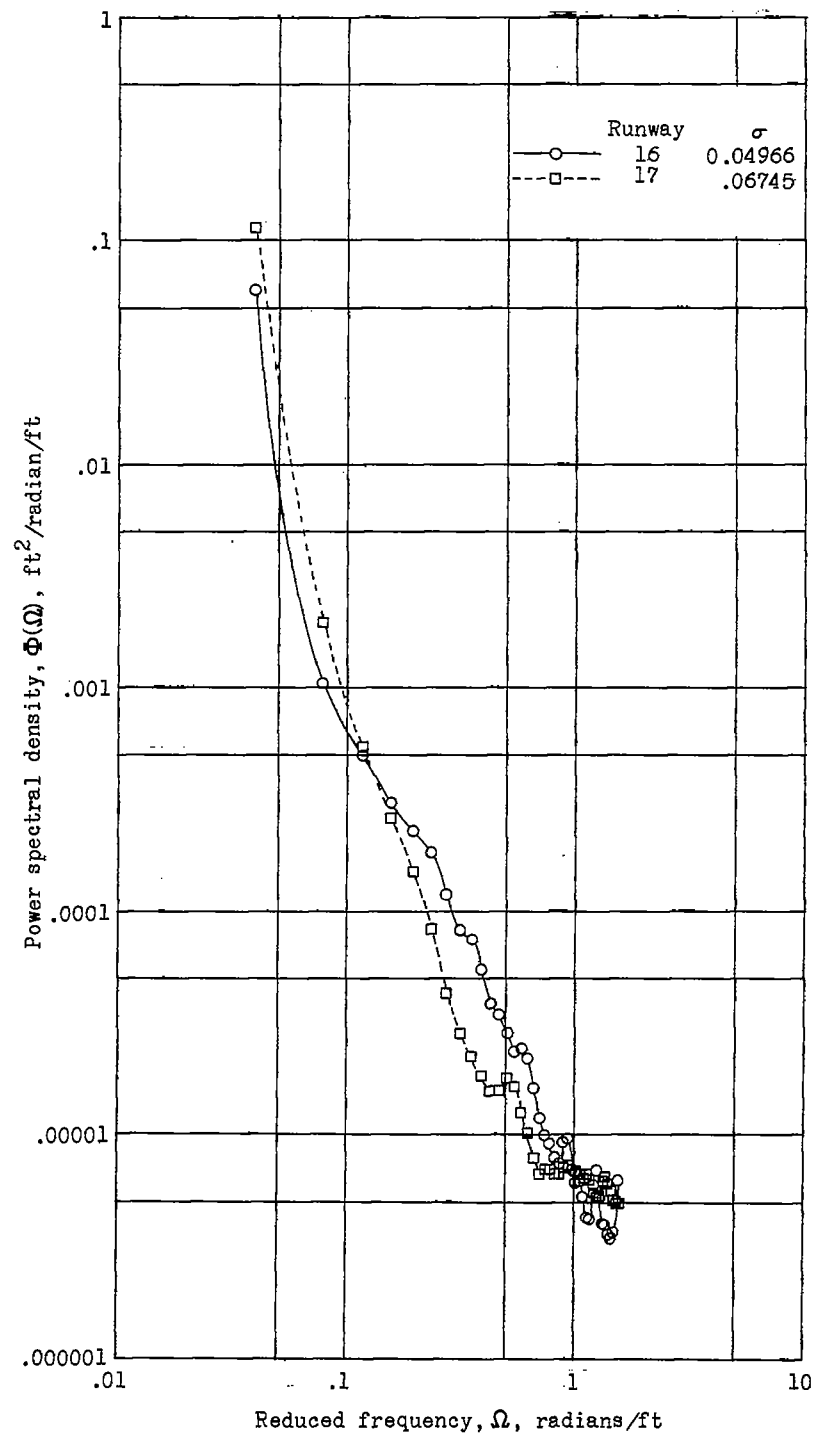


Figure 29.- Power-spectral-density functions for runways 16 and 17.

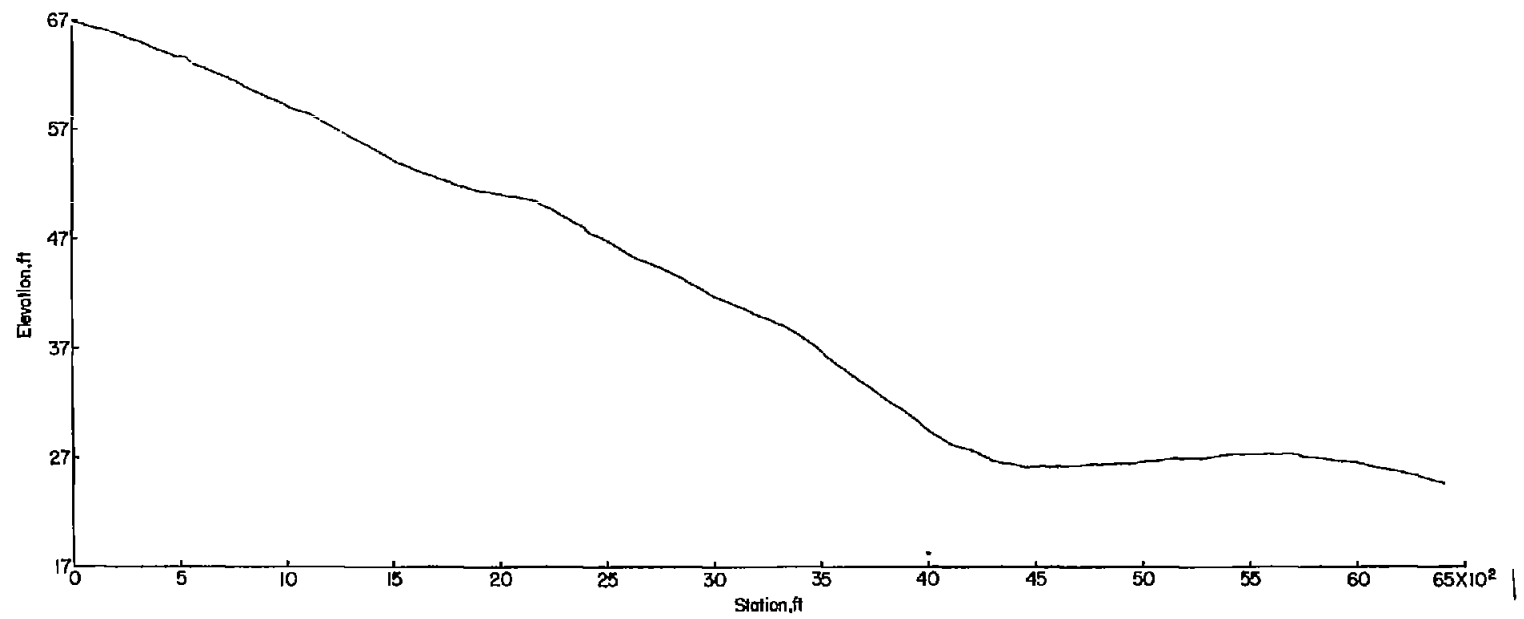


Figure 30.- Profile of runway 18.

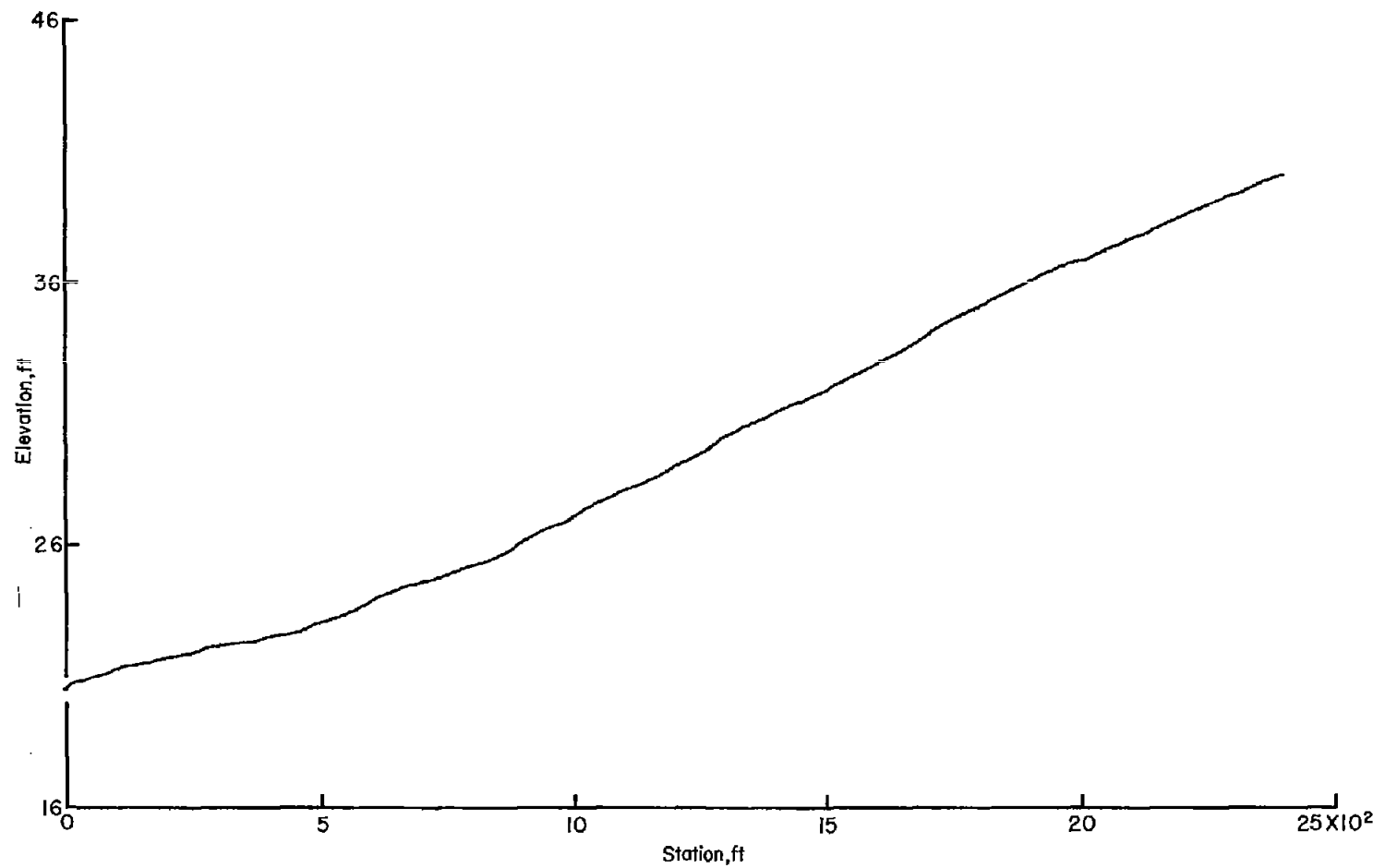


Figure 31.- Profile of runway 19.

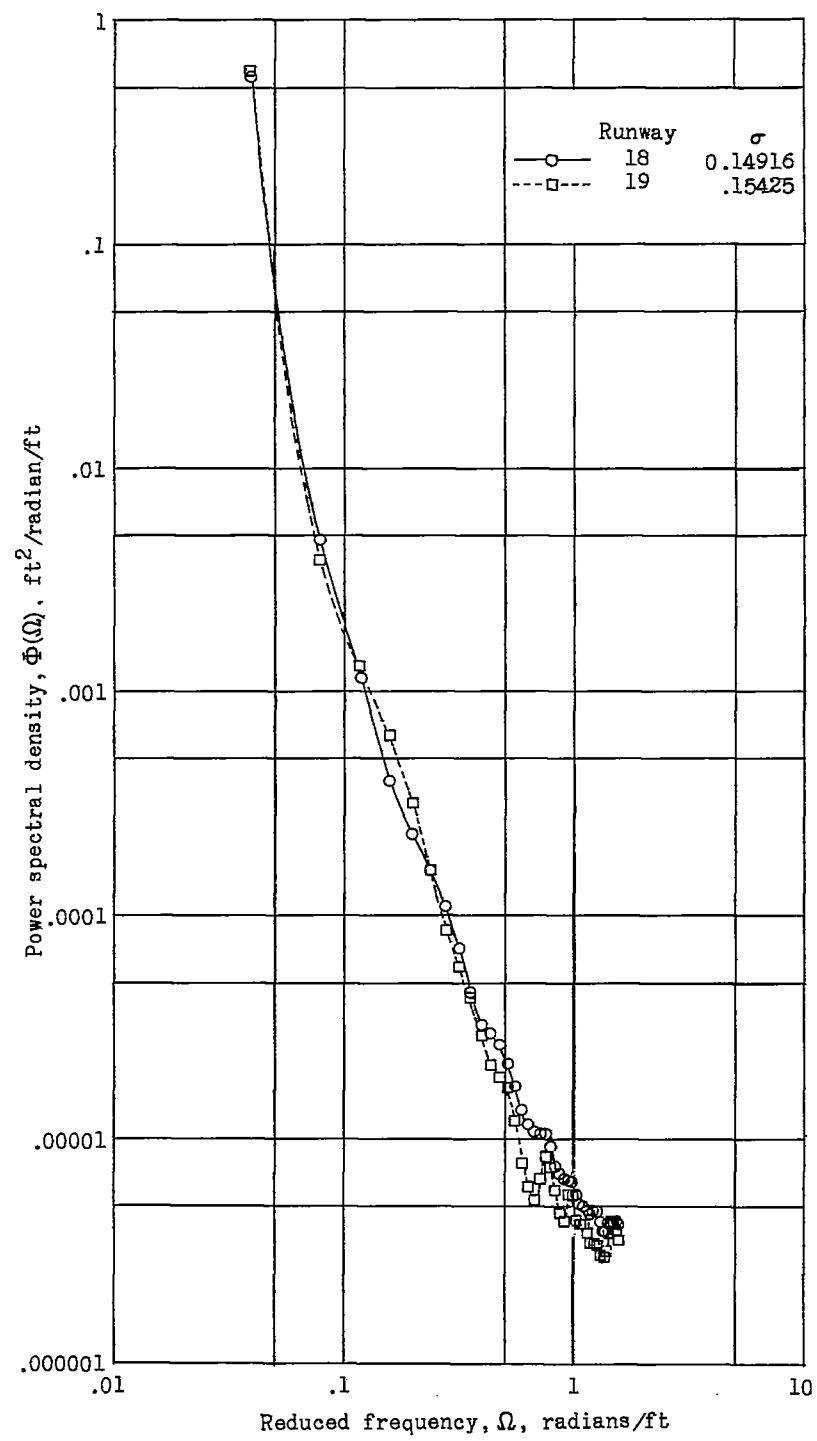


Figure 32.- Power-spectral-density functions for runways 18 and 19.

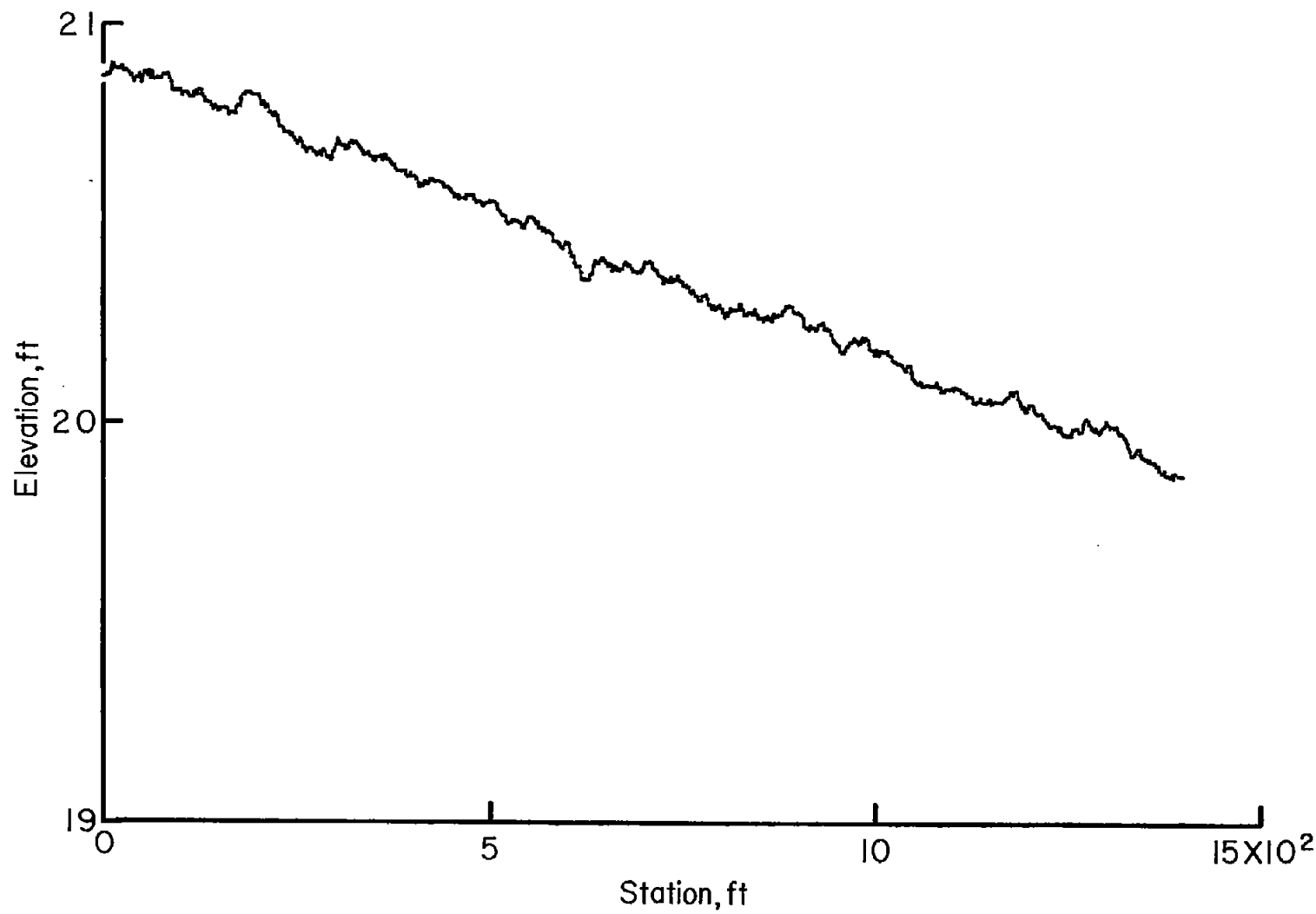


Figure 33.- Profile of runway 20.

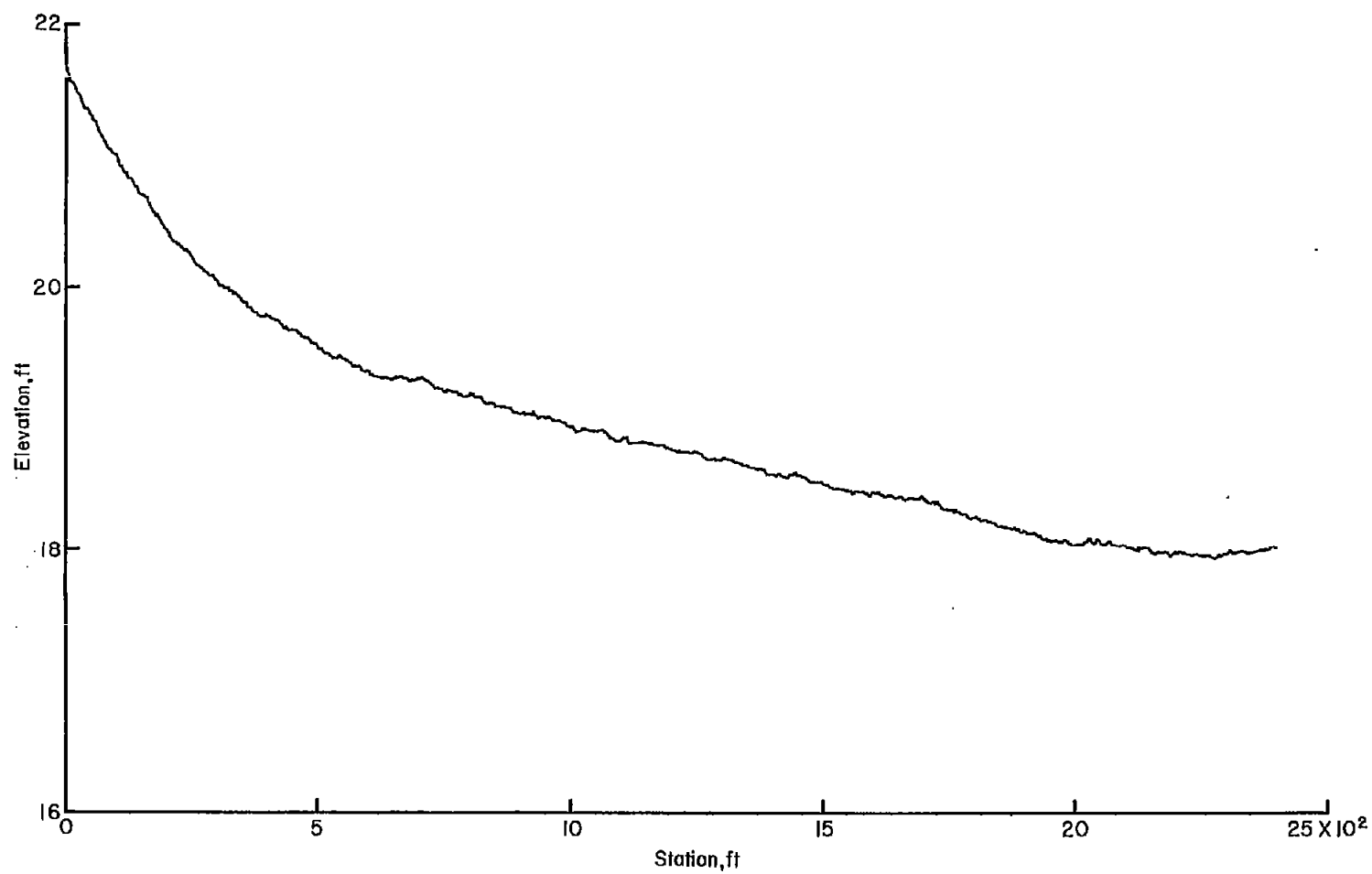


Figure 34.- Profile of runway 21.

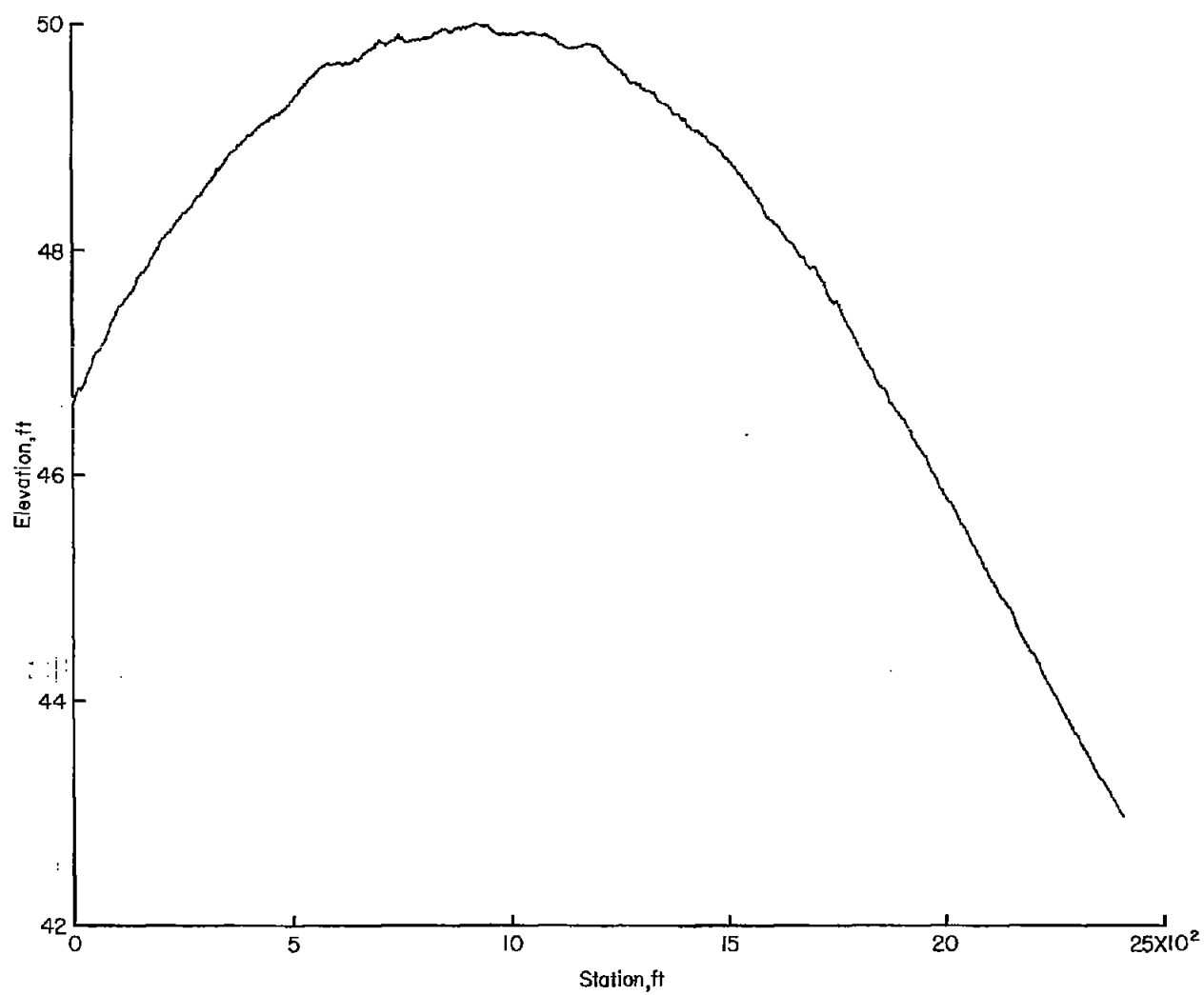


Figure 35.- Profile of runway 22-I.

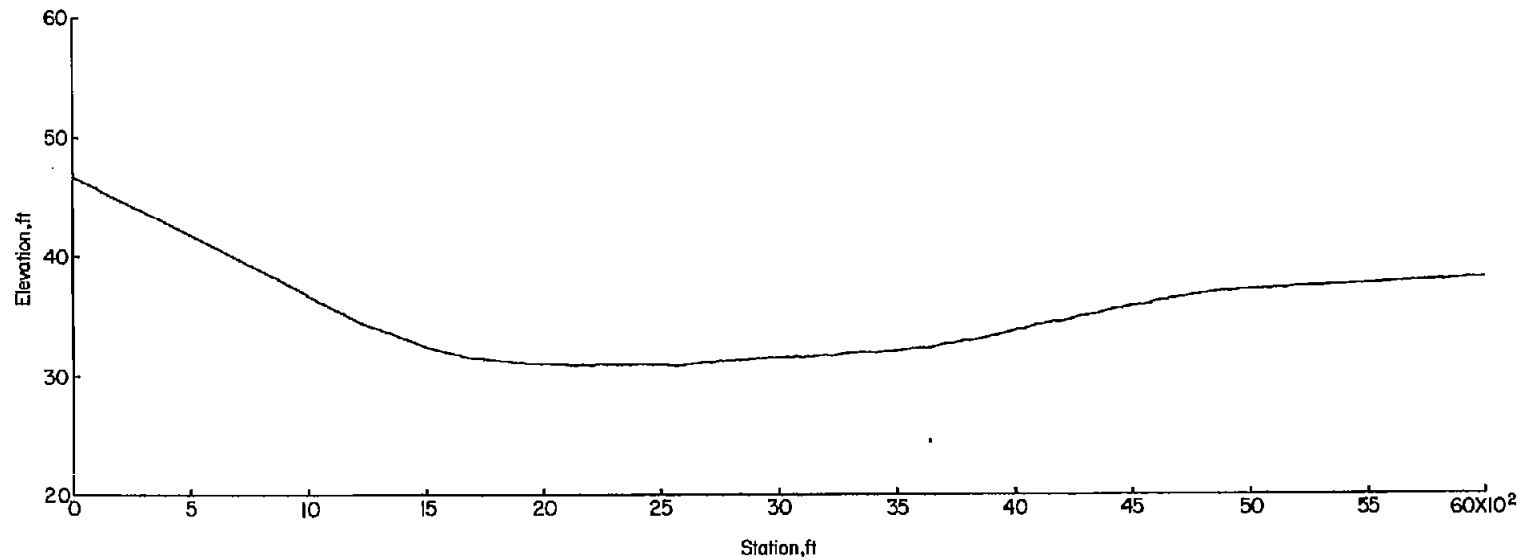


Figure 36.- Profile of runway 22-II.

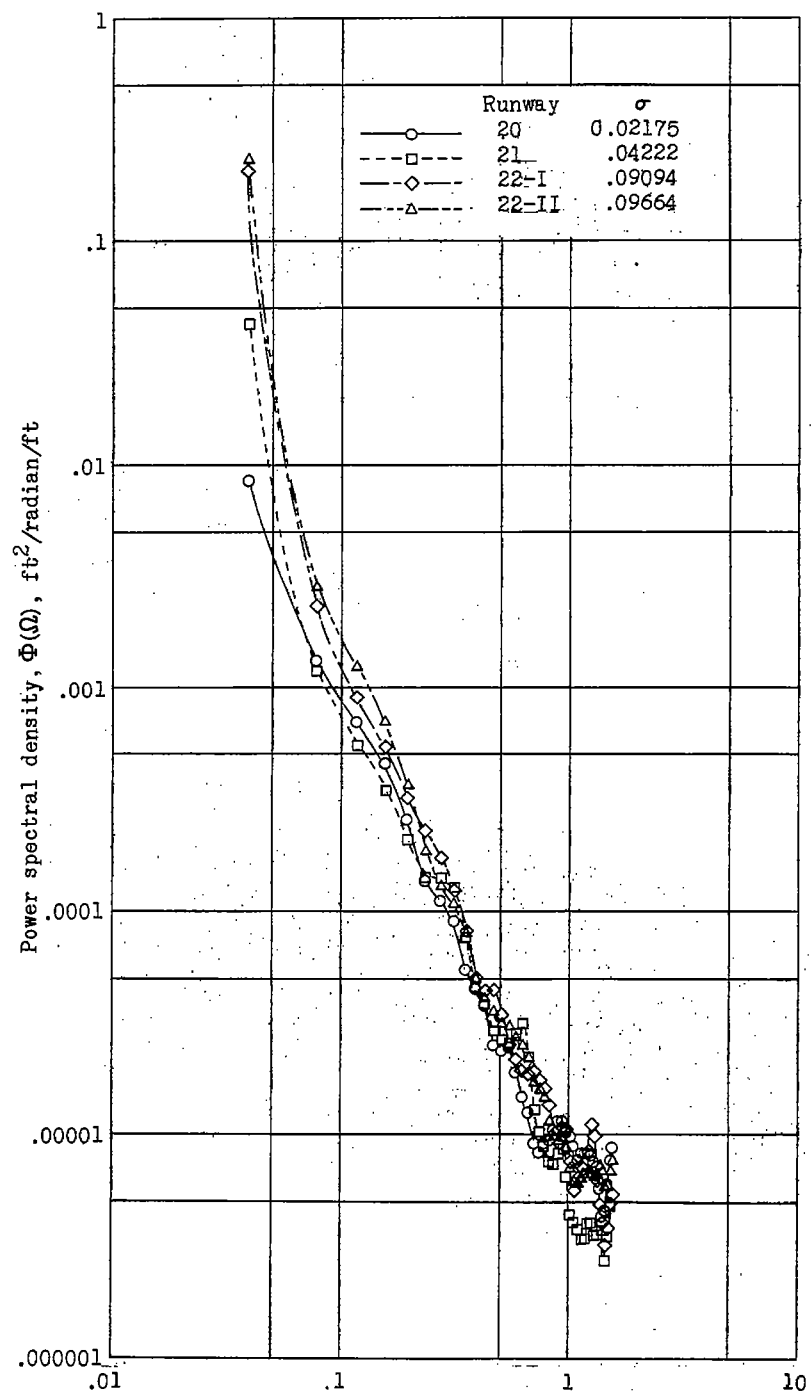


Figure 37.- Power-spectral-density functions for runways 20, 21, and 22.

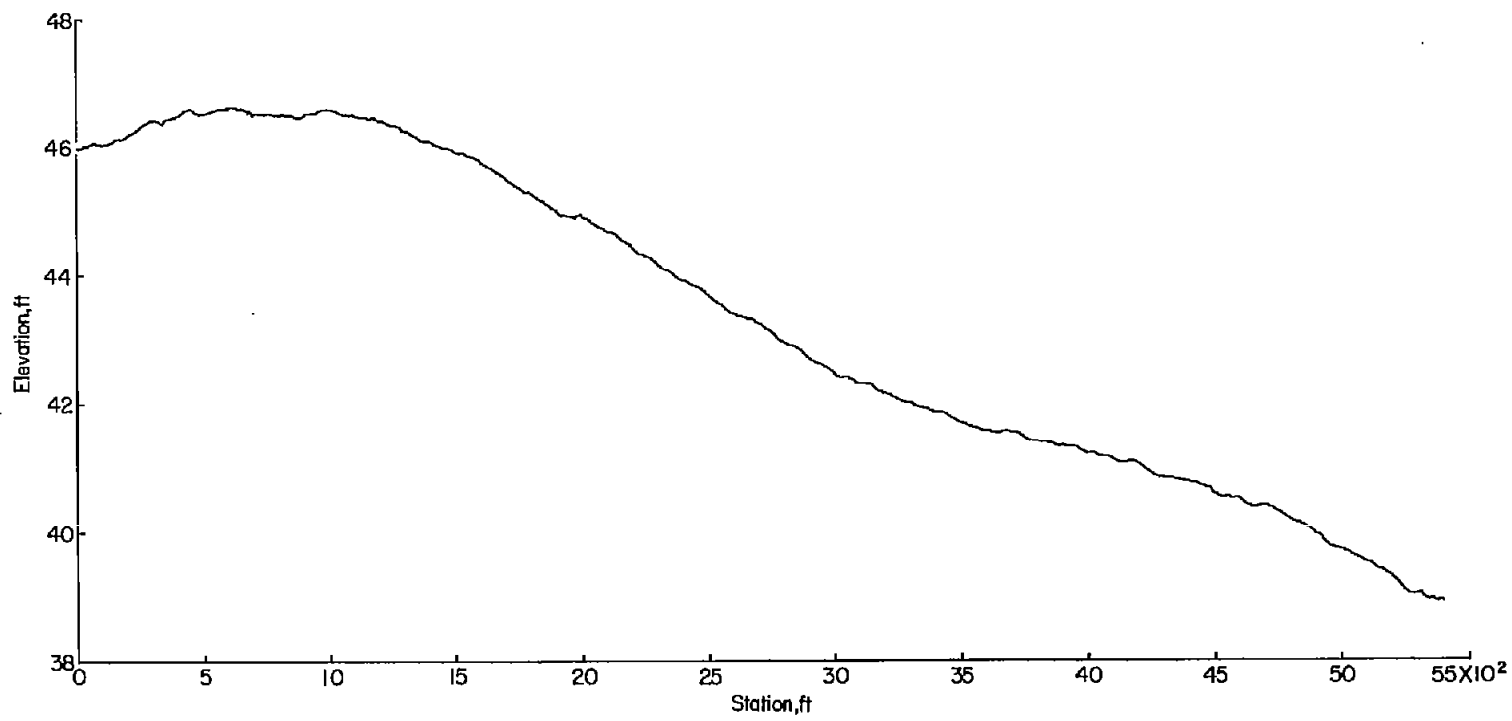


Figure 38.- Profile of runway 23.

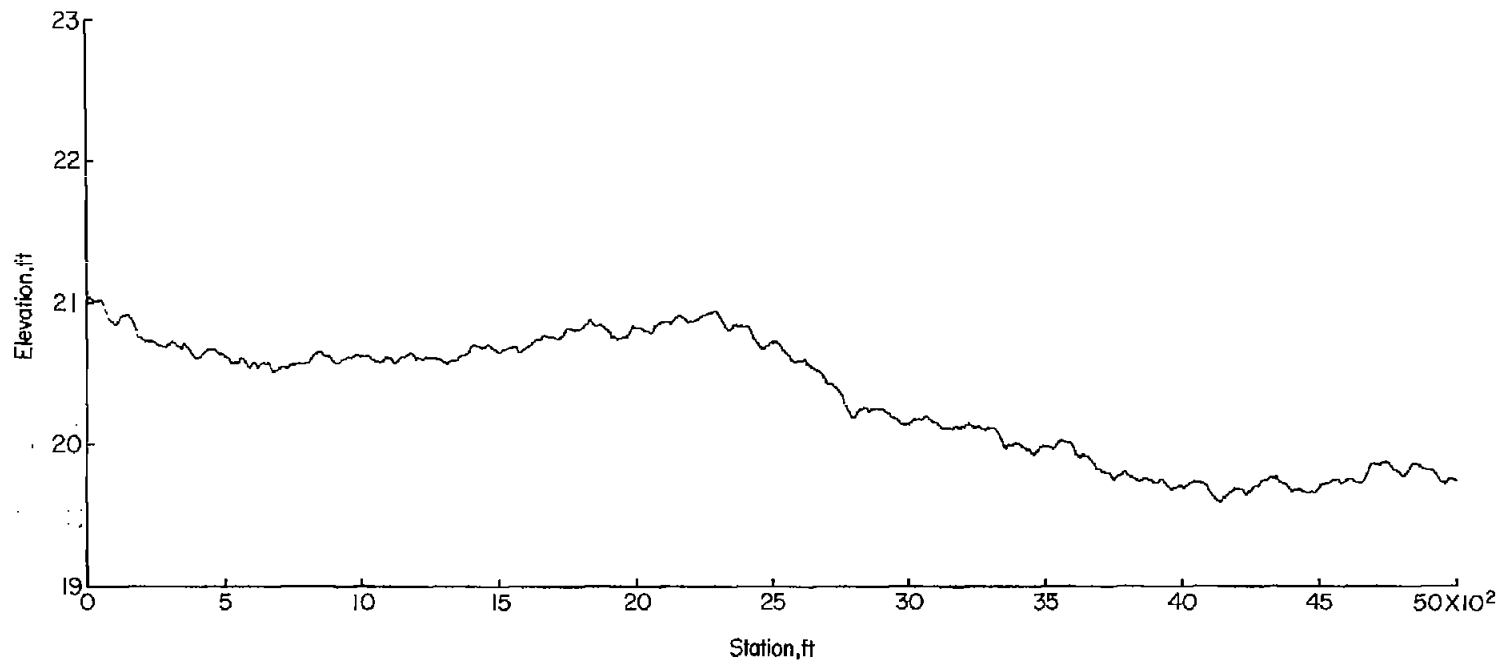


Figure 39.- Profile of runway 24.

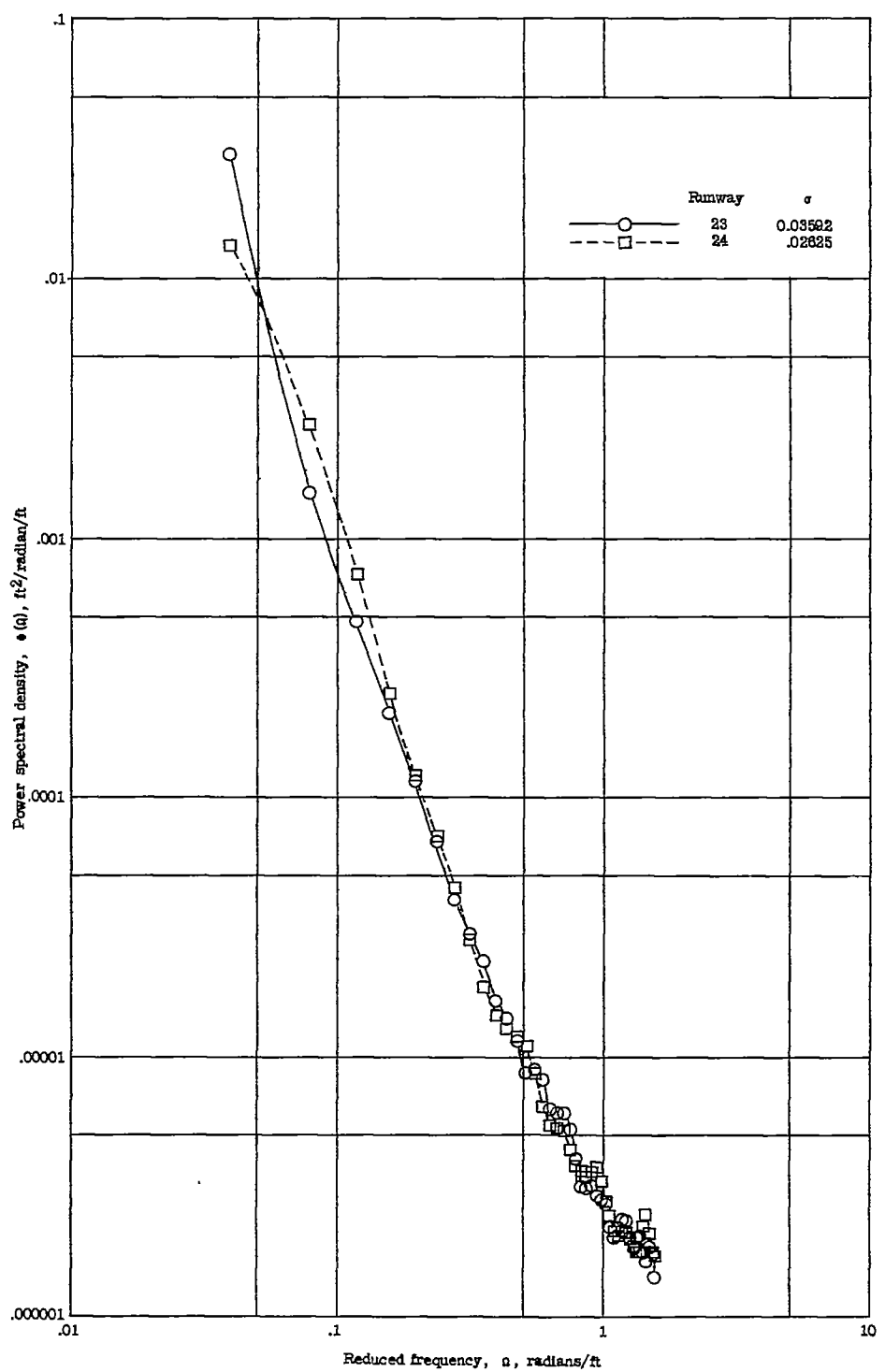


Figure 40.- Power-spectral-density functions for runways 23 and 24.

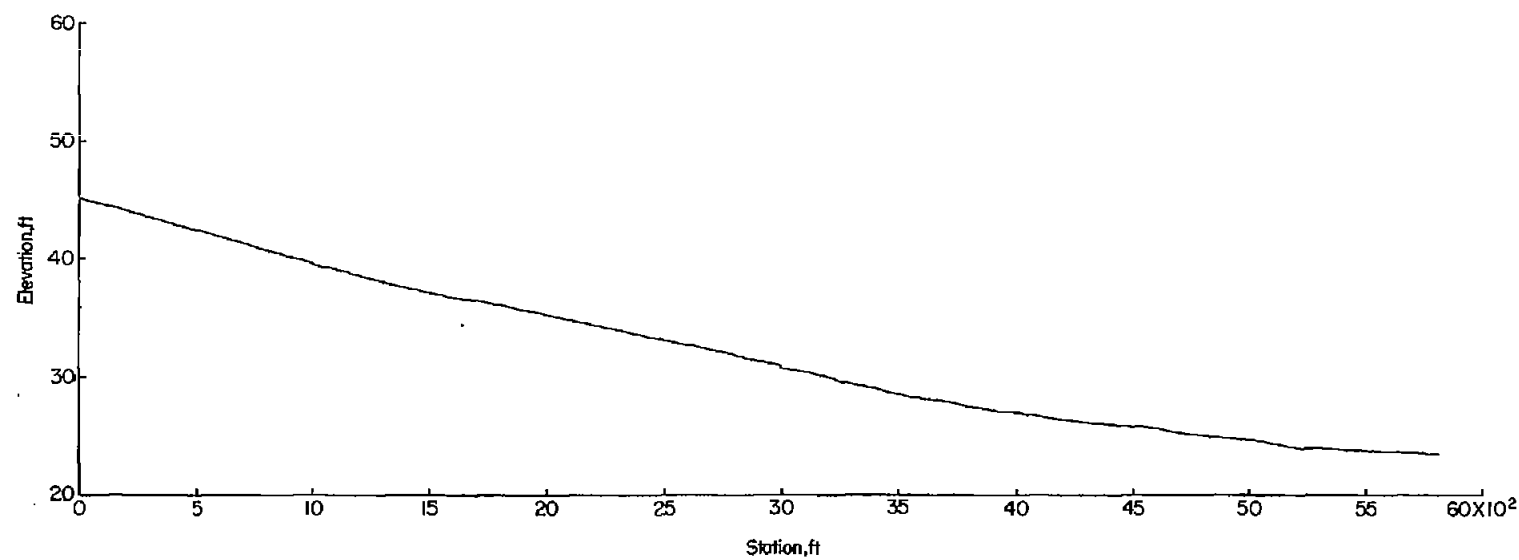


Figure 41.- Profile of runway 25.

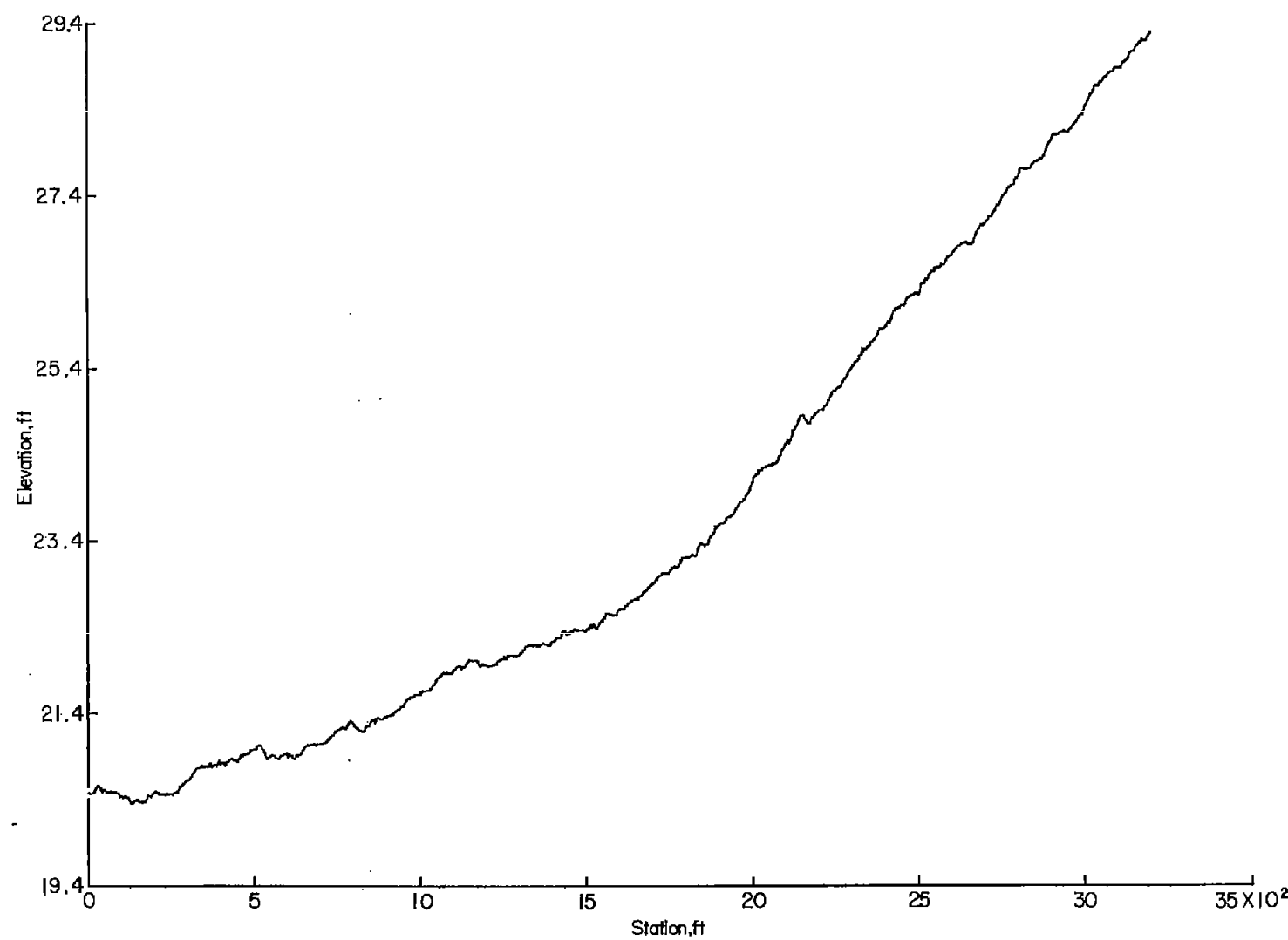


Figure 42.- Profile of runway 26.

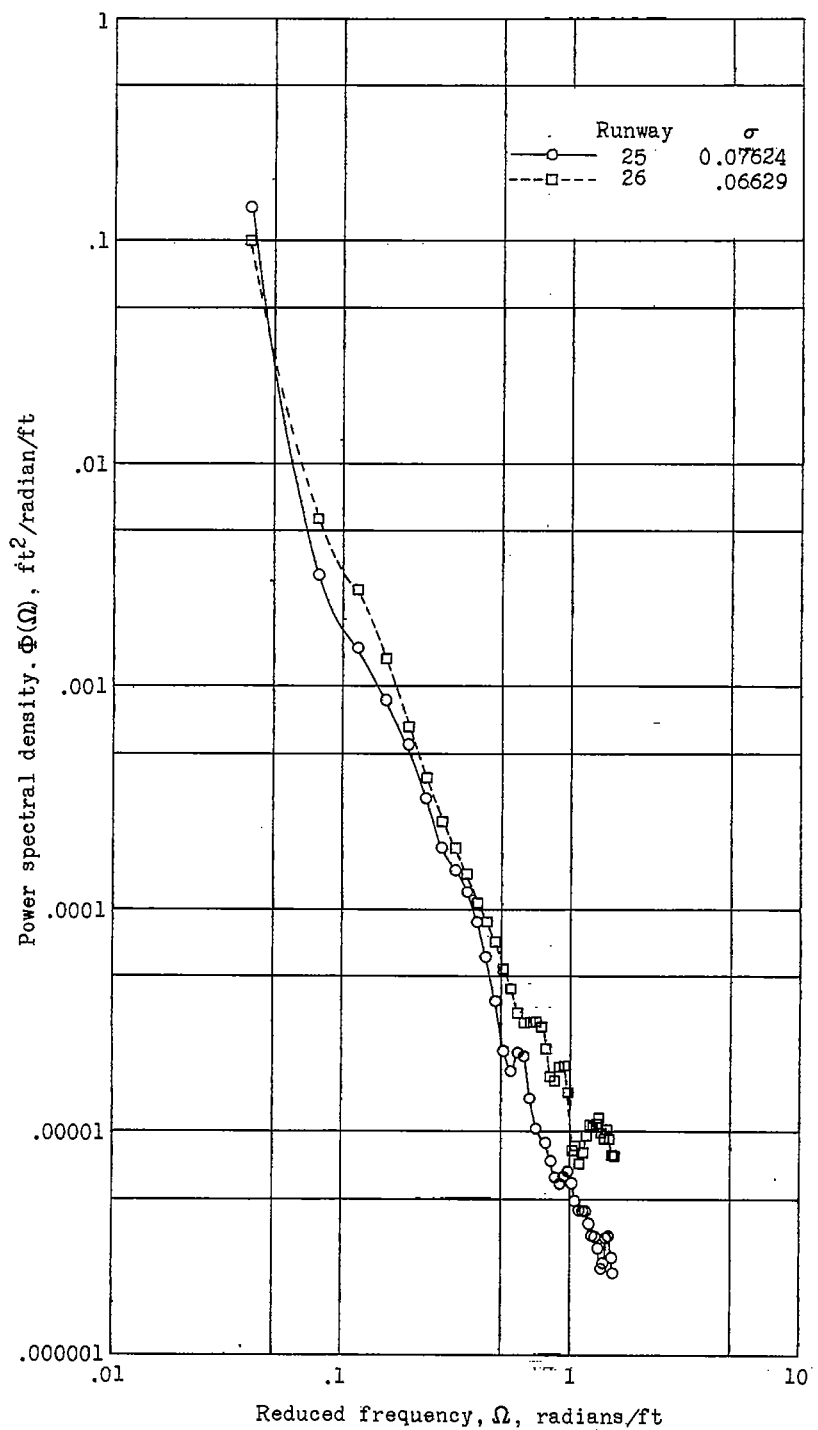


Figure 43.- Power-spectral-density functions for runways 25 and 26.

2
NACA TN 4303

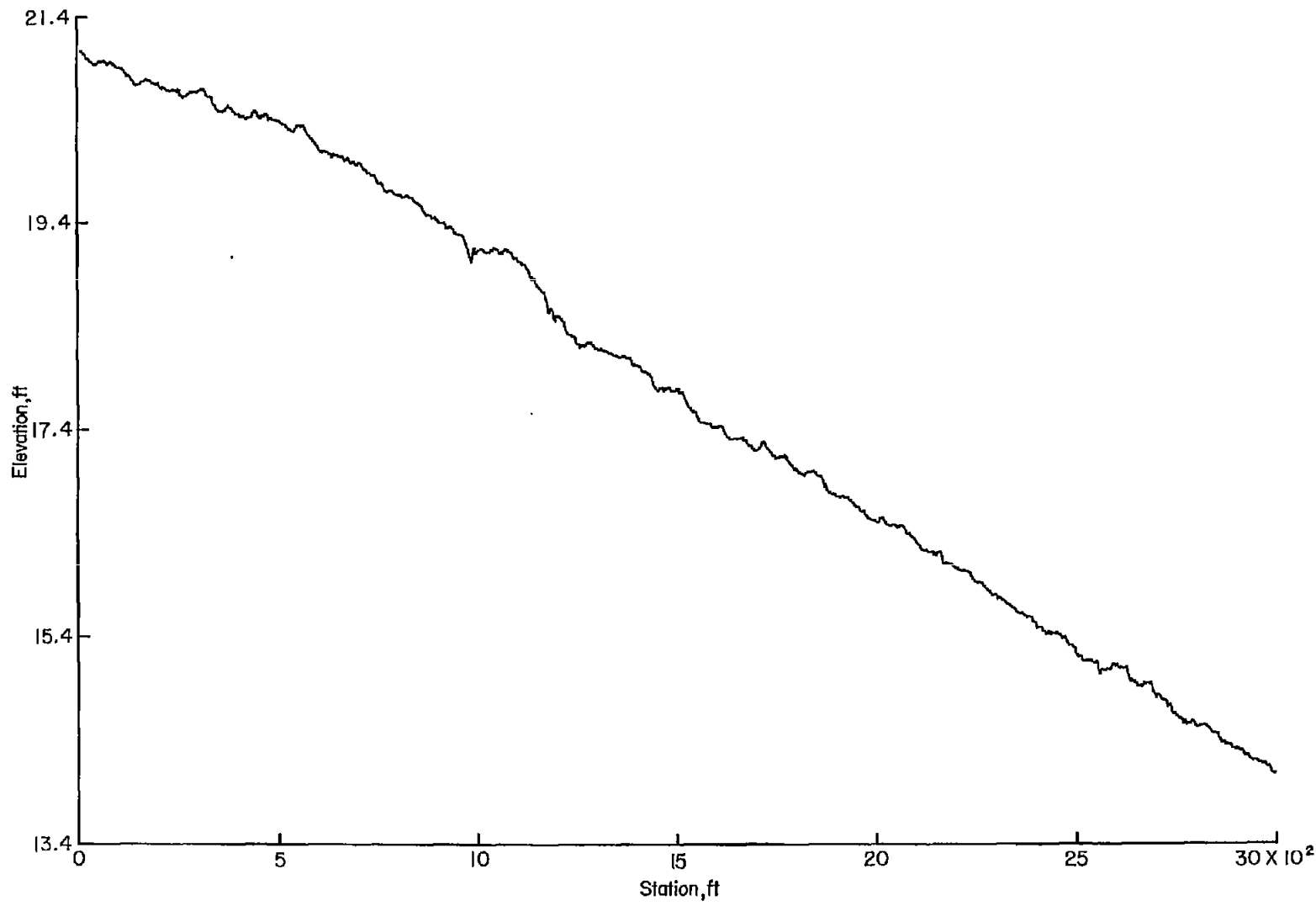


Figure 44.- Profile of runway 27.
64

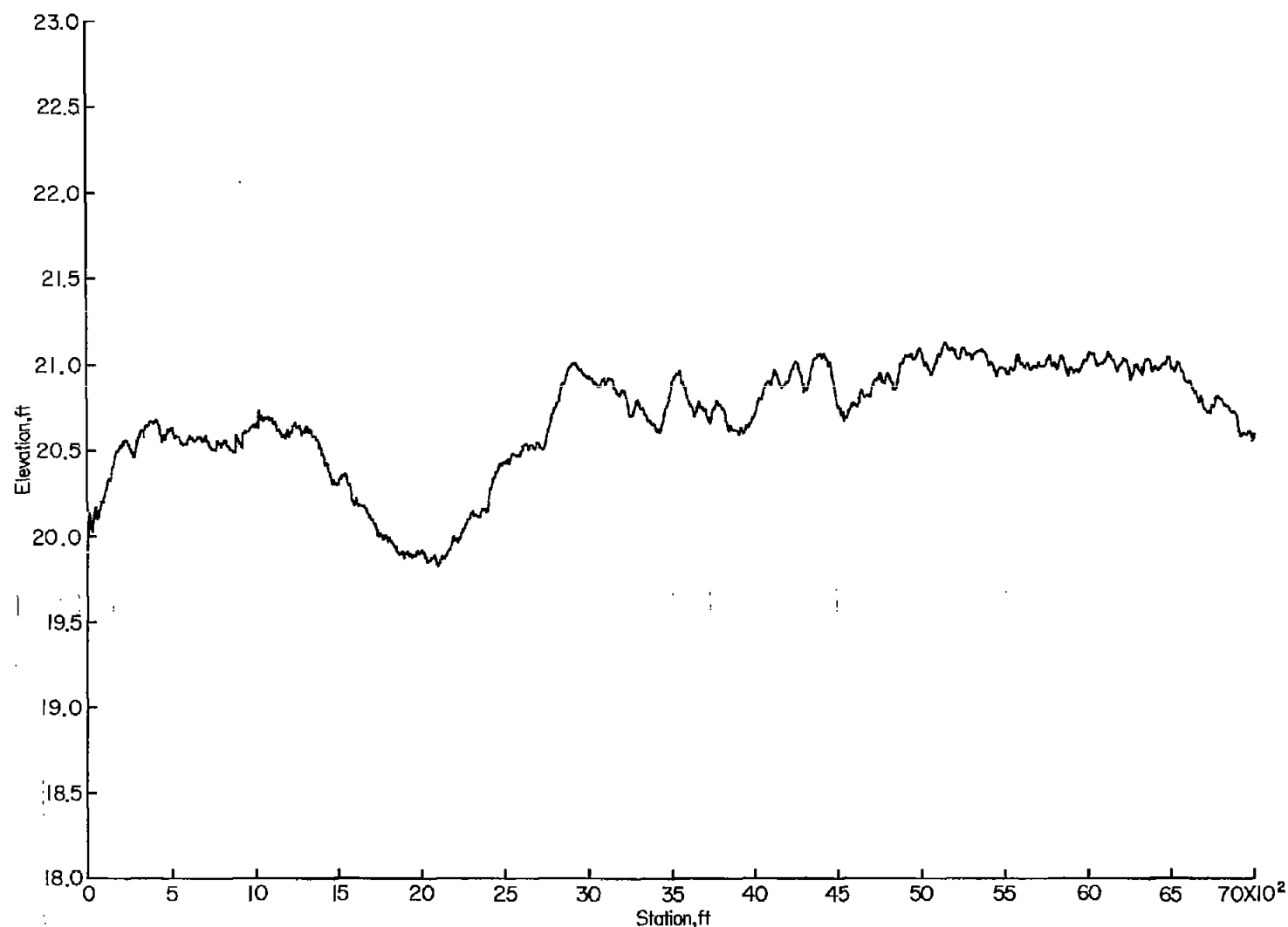


Figure 45.- Profile of runway 28.

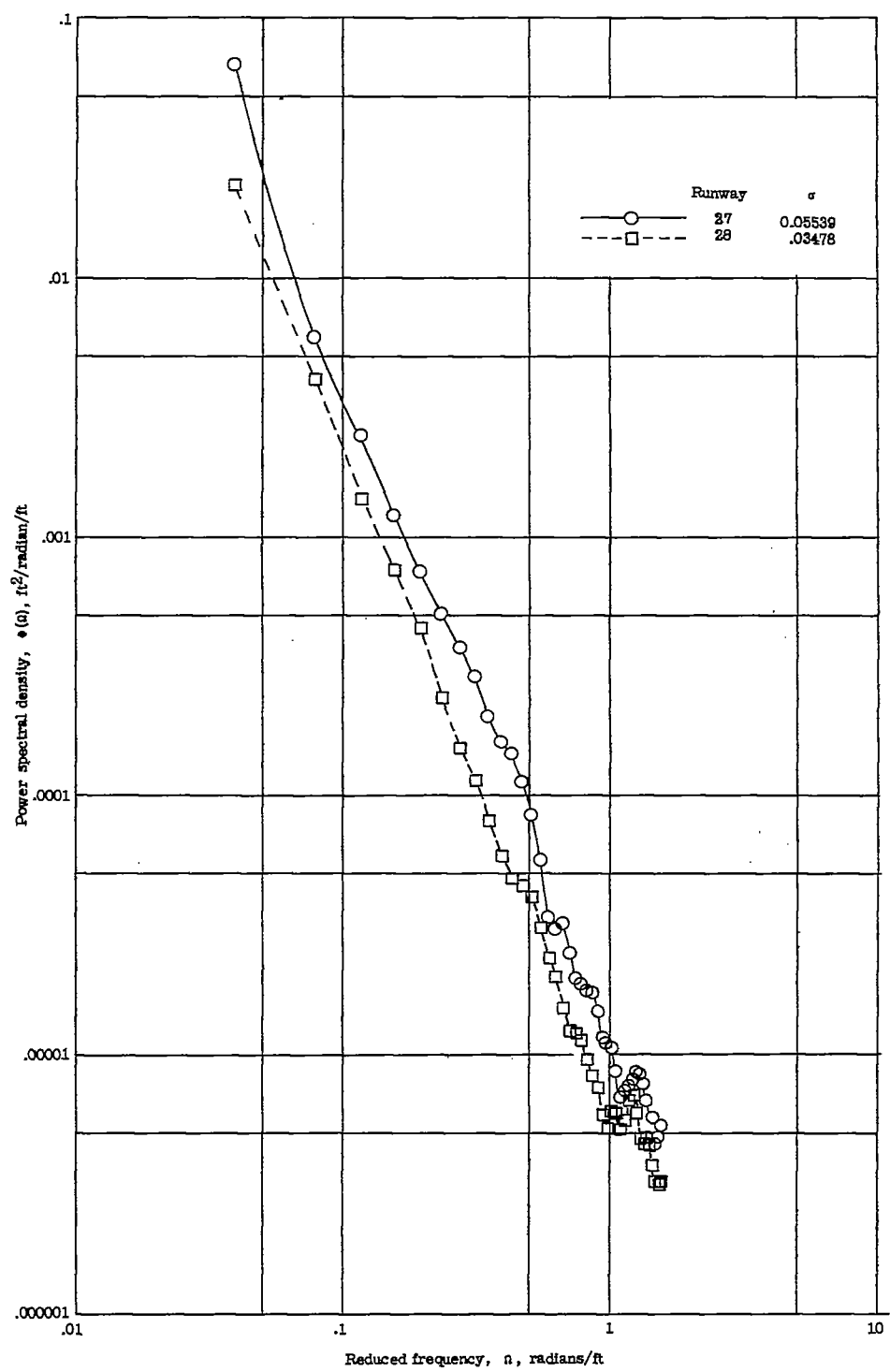


Figure 46.- Power-spectral-density functions for runways 27 and 28.

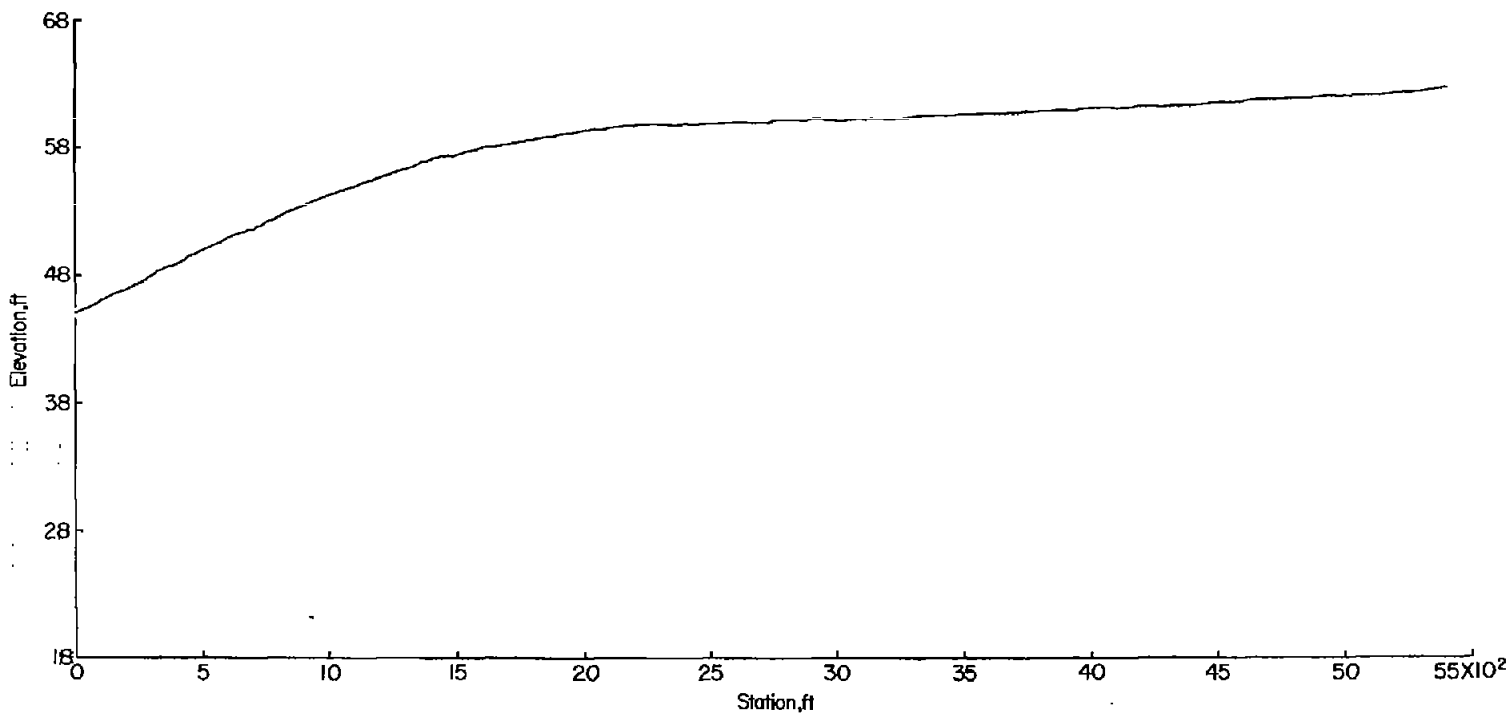


Figure 47.- Profile of runway 29.

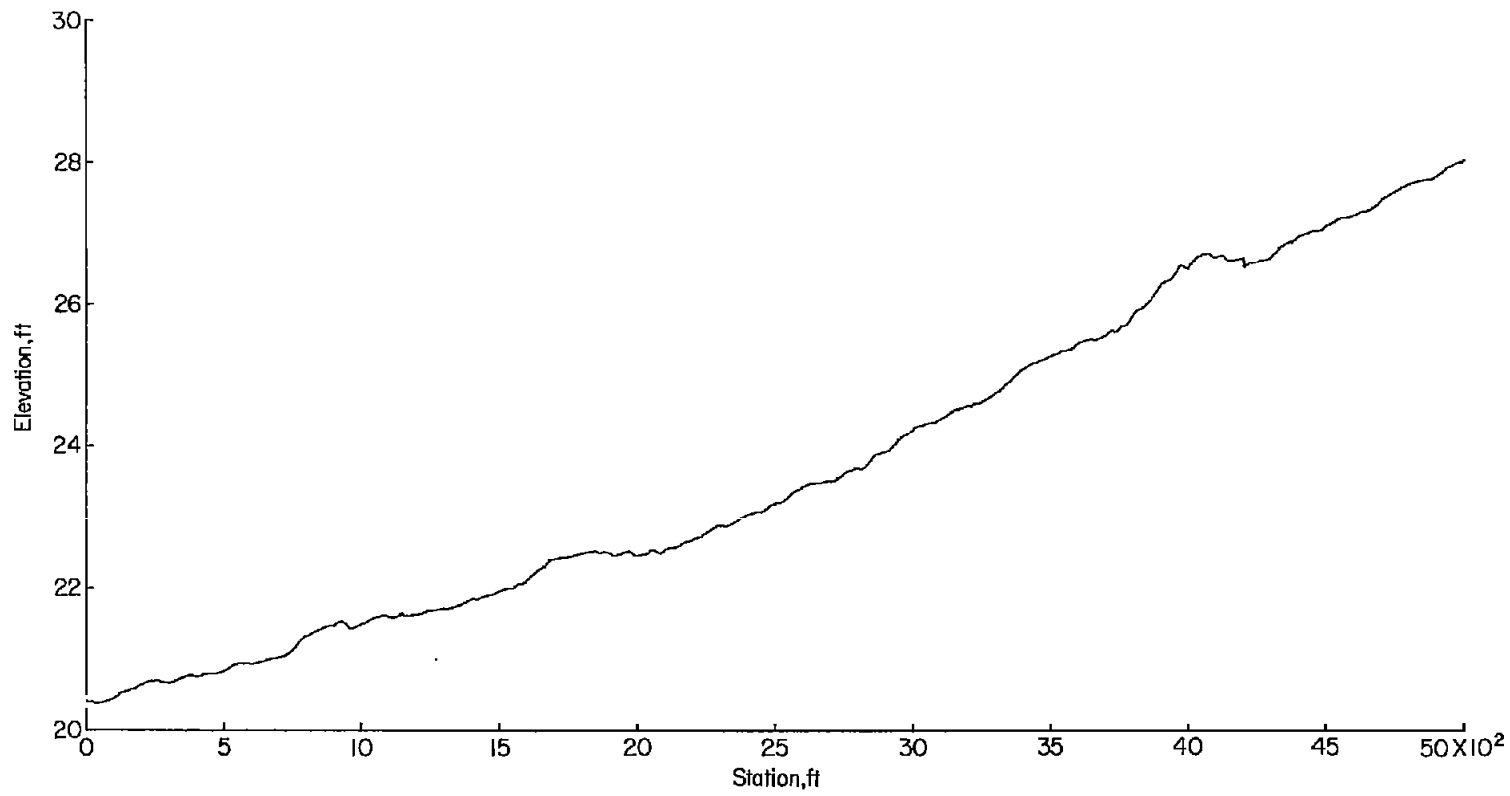


Figure 48.- Profile of runway 30.

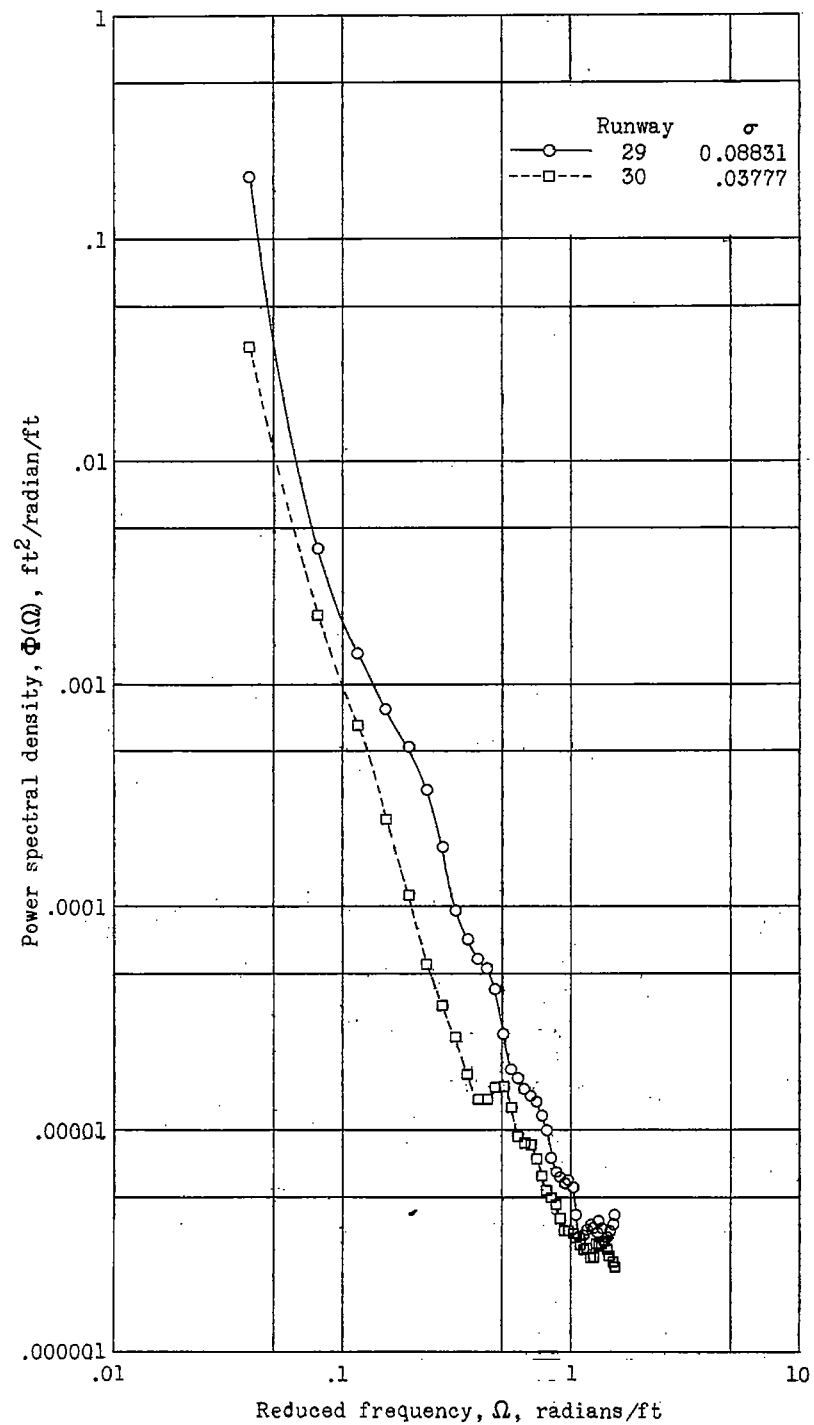


Figure 49.- Power-spectral-density functions for runways 29 and 30.

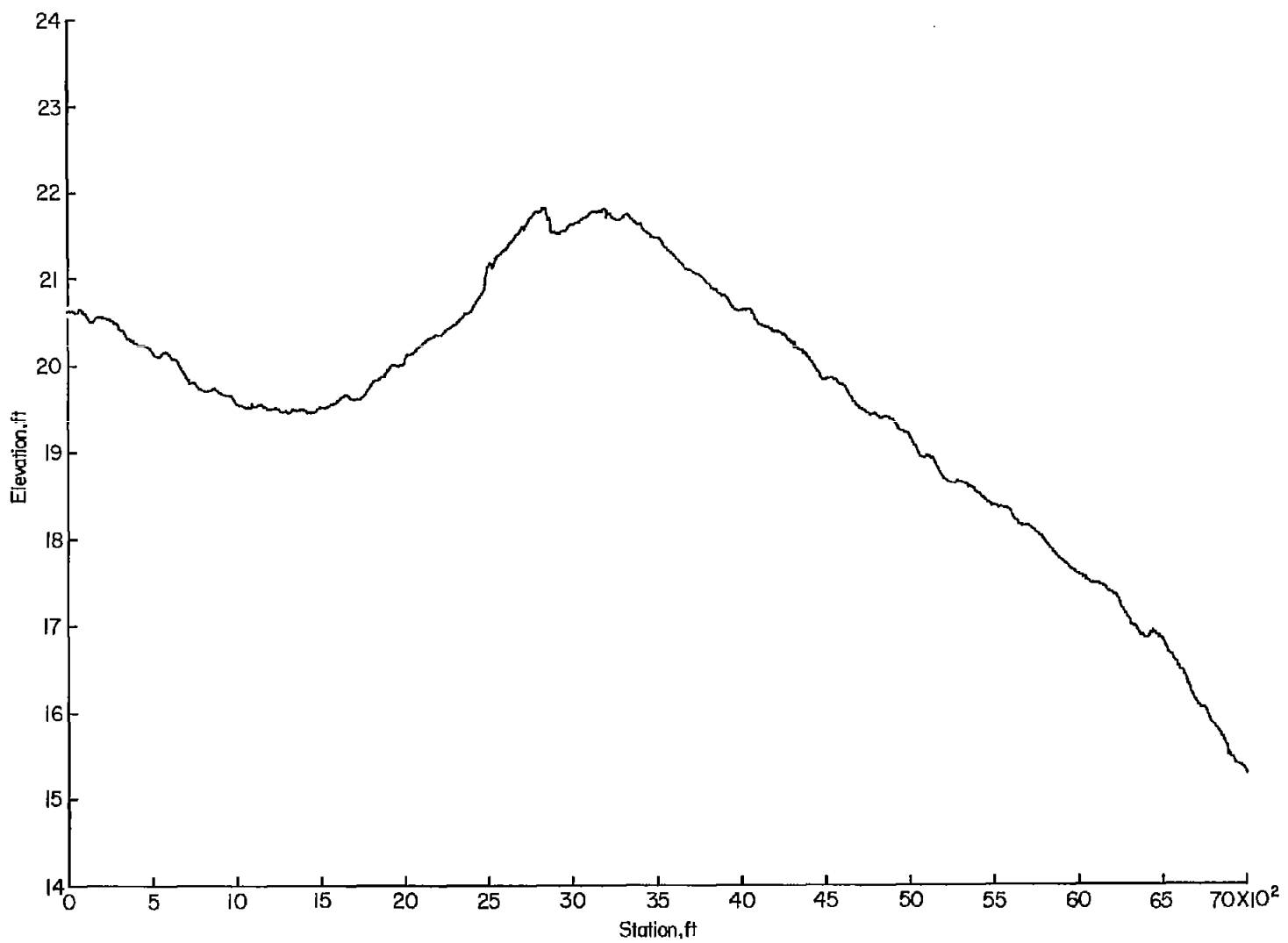


Figure 50.- Profile of runway 31.

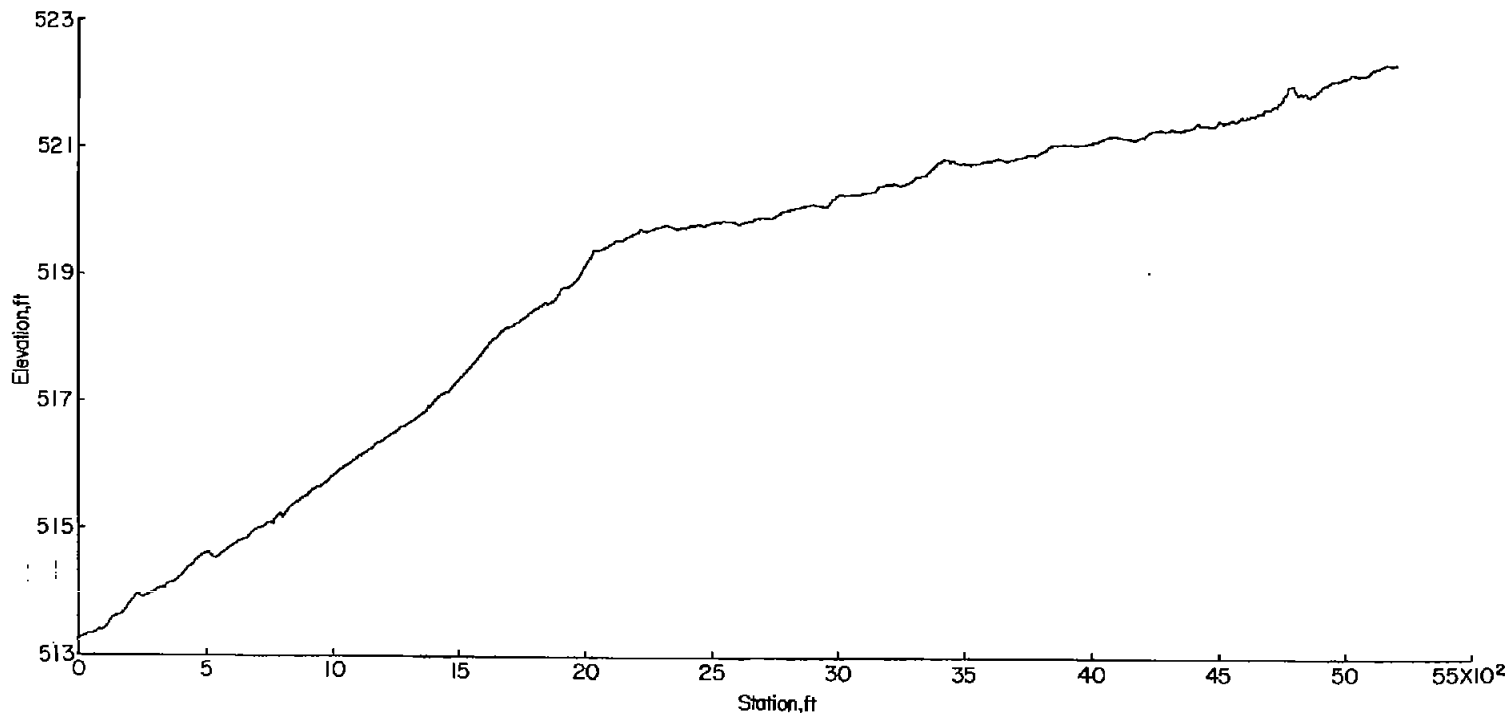


Figure 51.-- Profile of runway 32.

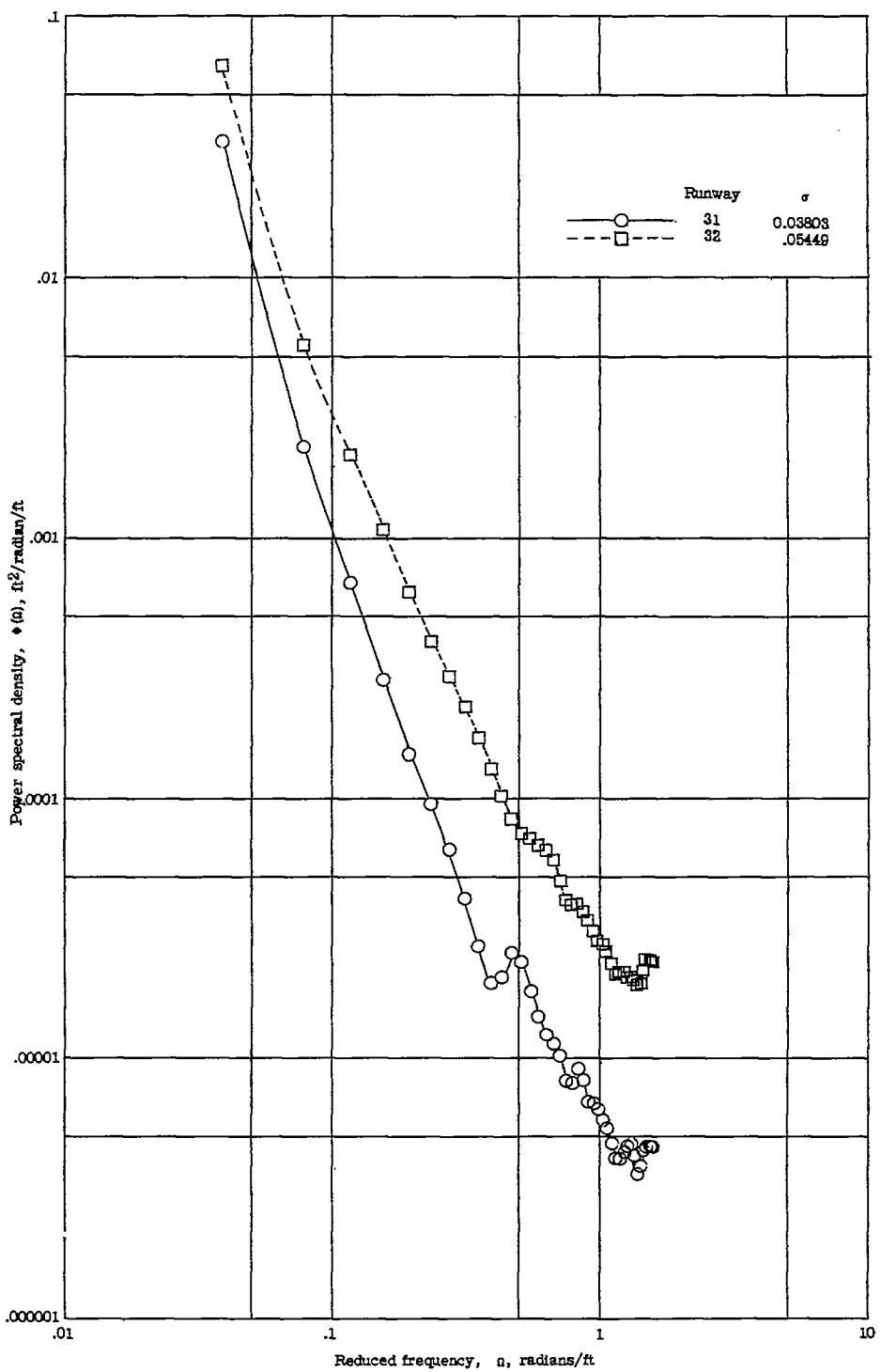
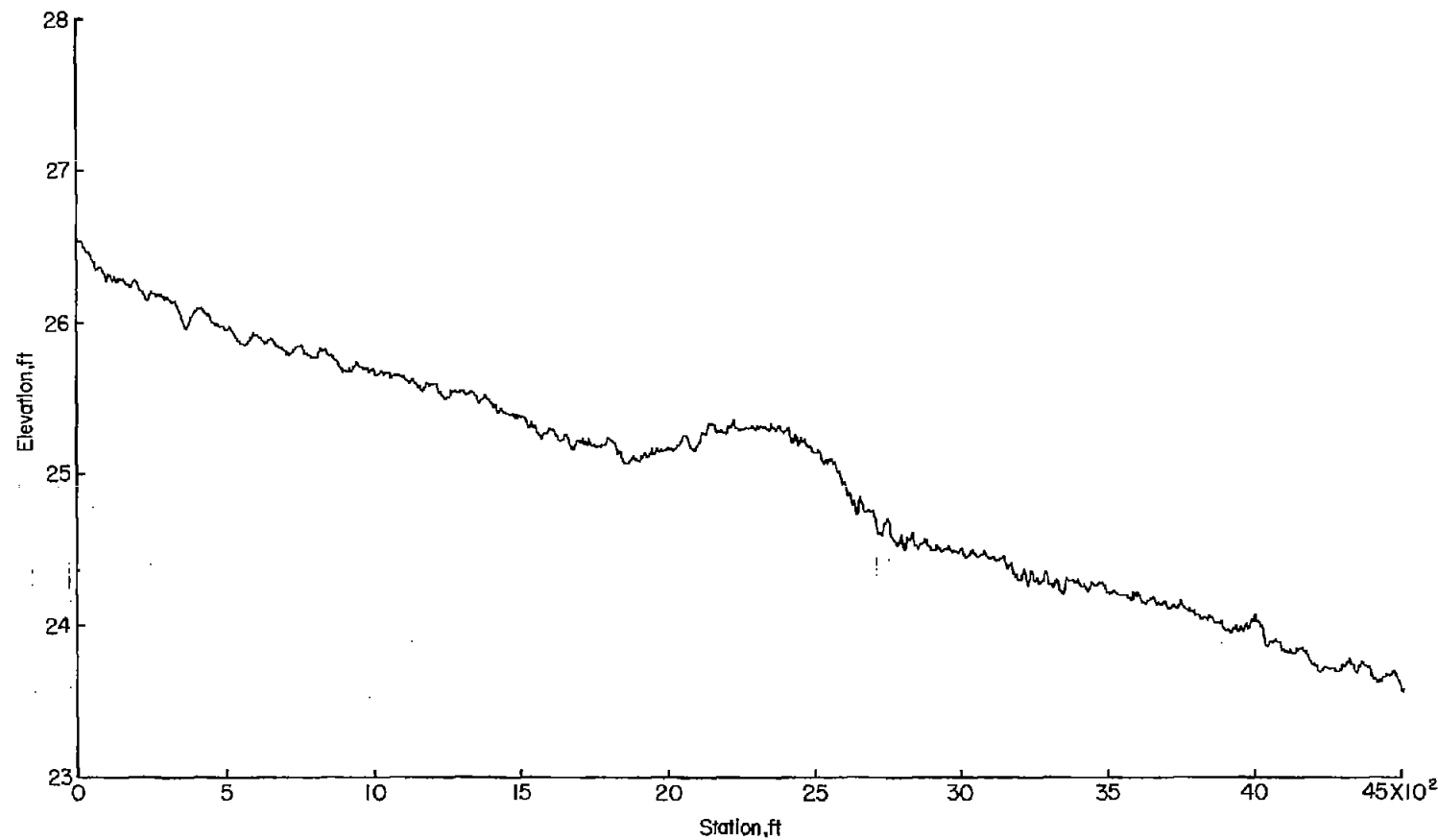
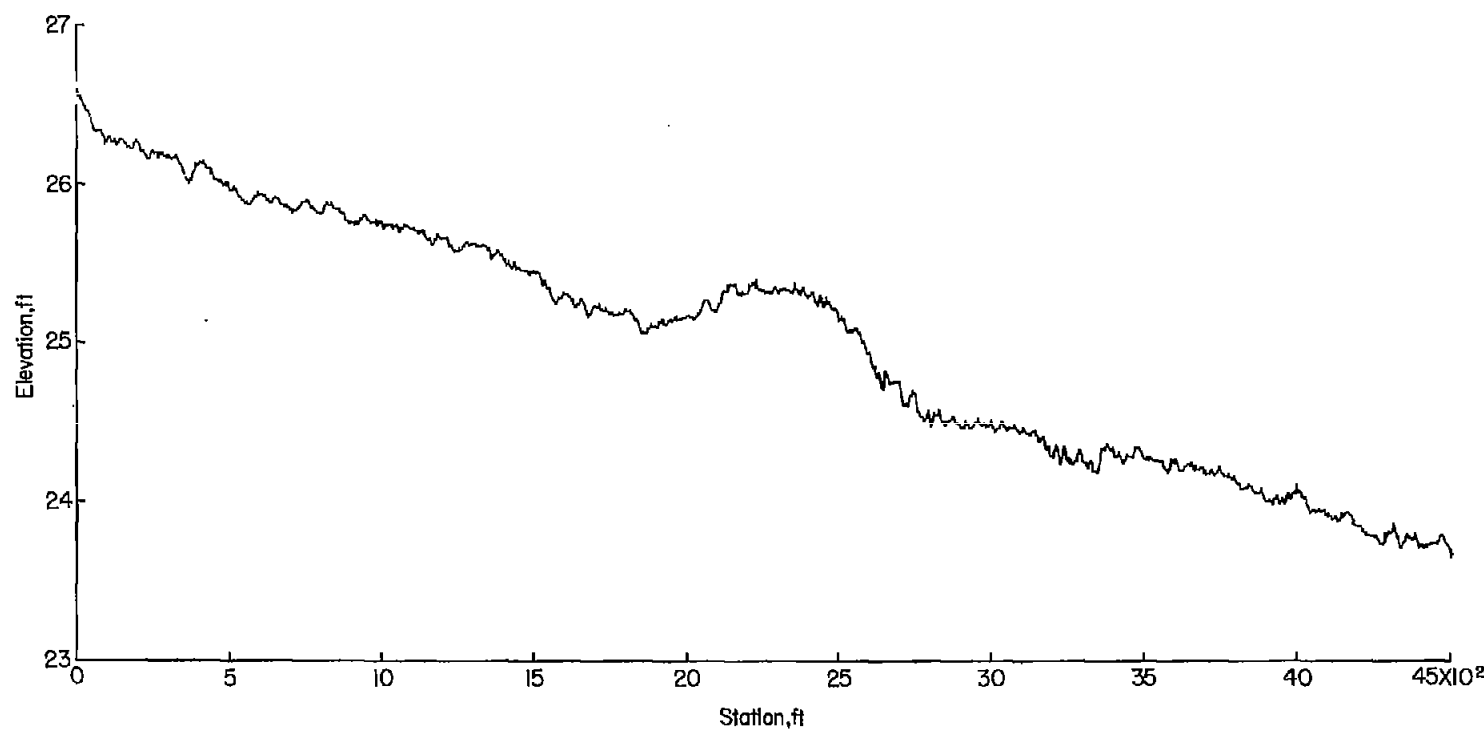


Figure 52.- Power-spectral-density functions for runways 31 and 32.



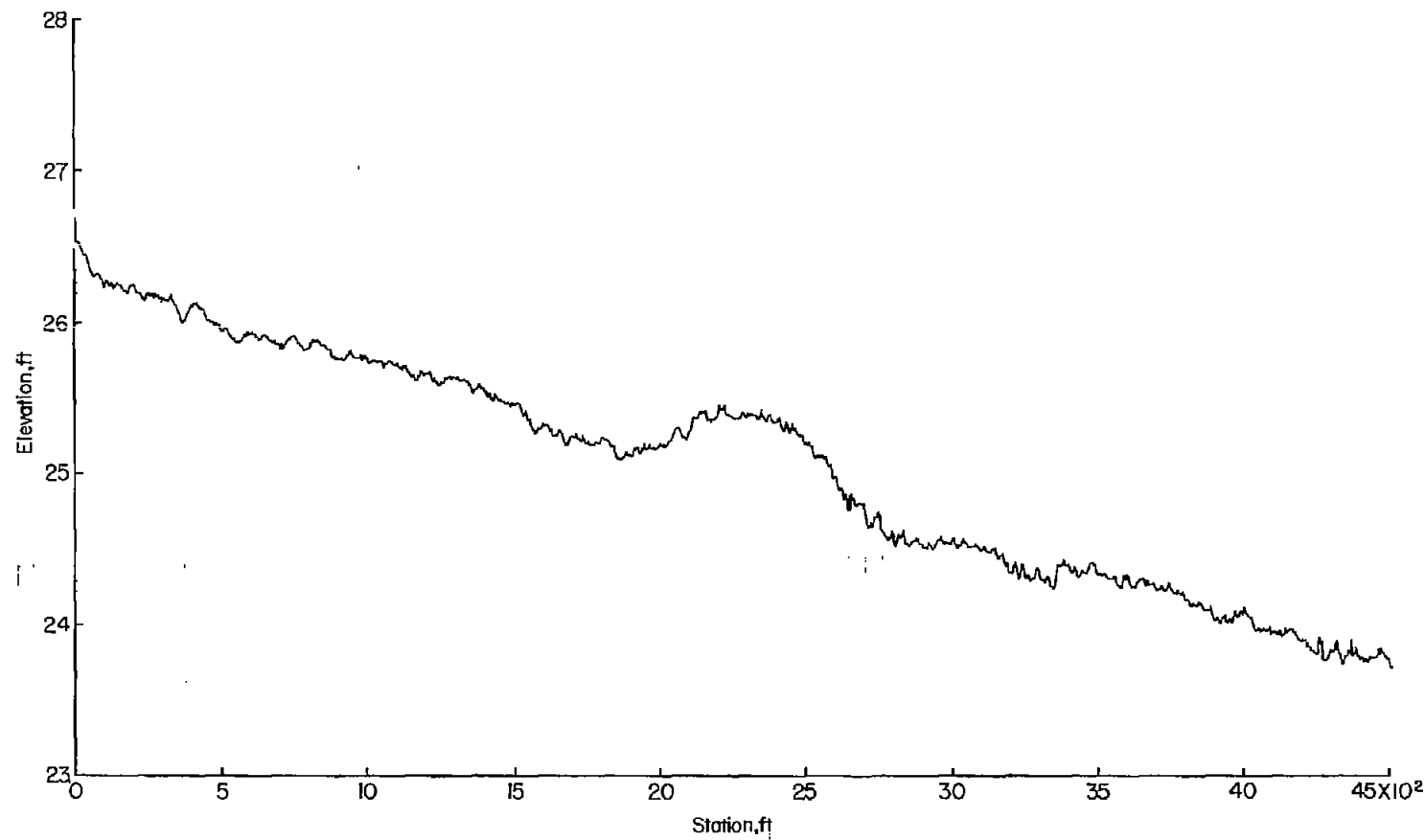
(a) December 1956.

Figure 53.- Profiles of runway 33.



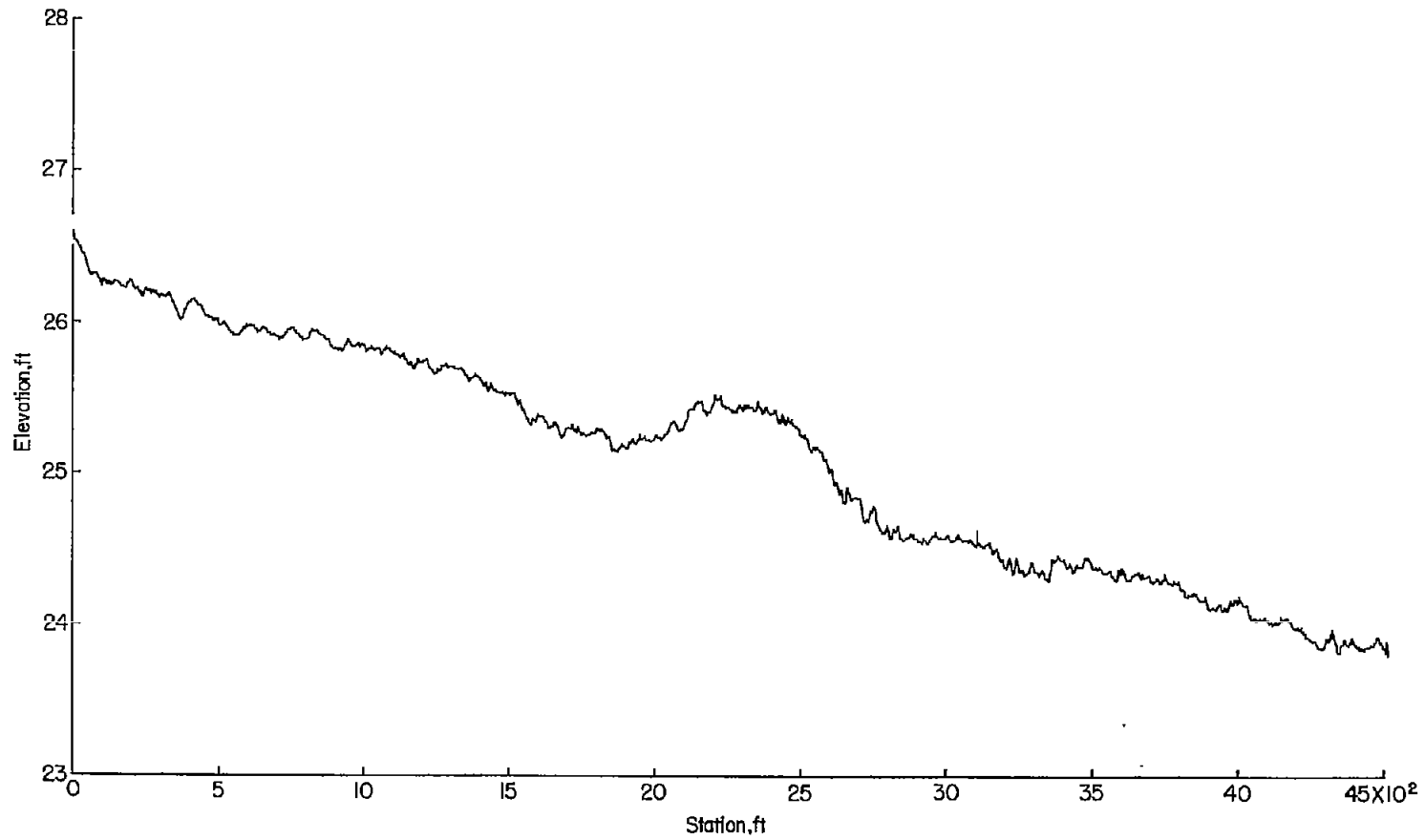
(b) January 1957.

Figure 53.- Continued.



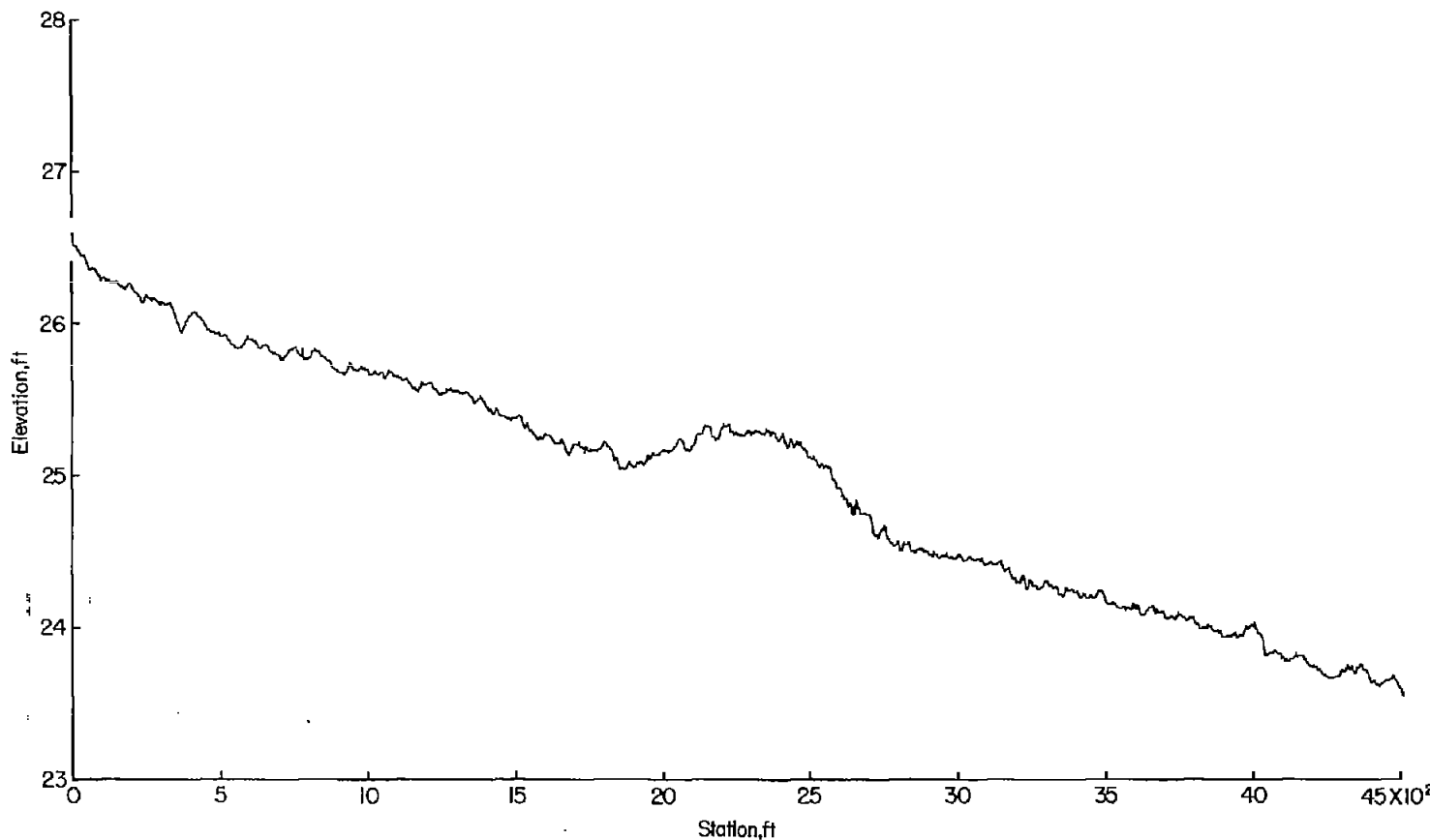
(c) February 1957.

Figure 53.- Continued.



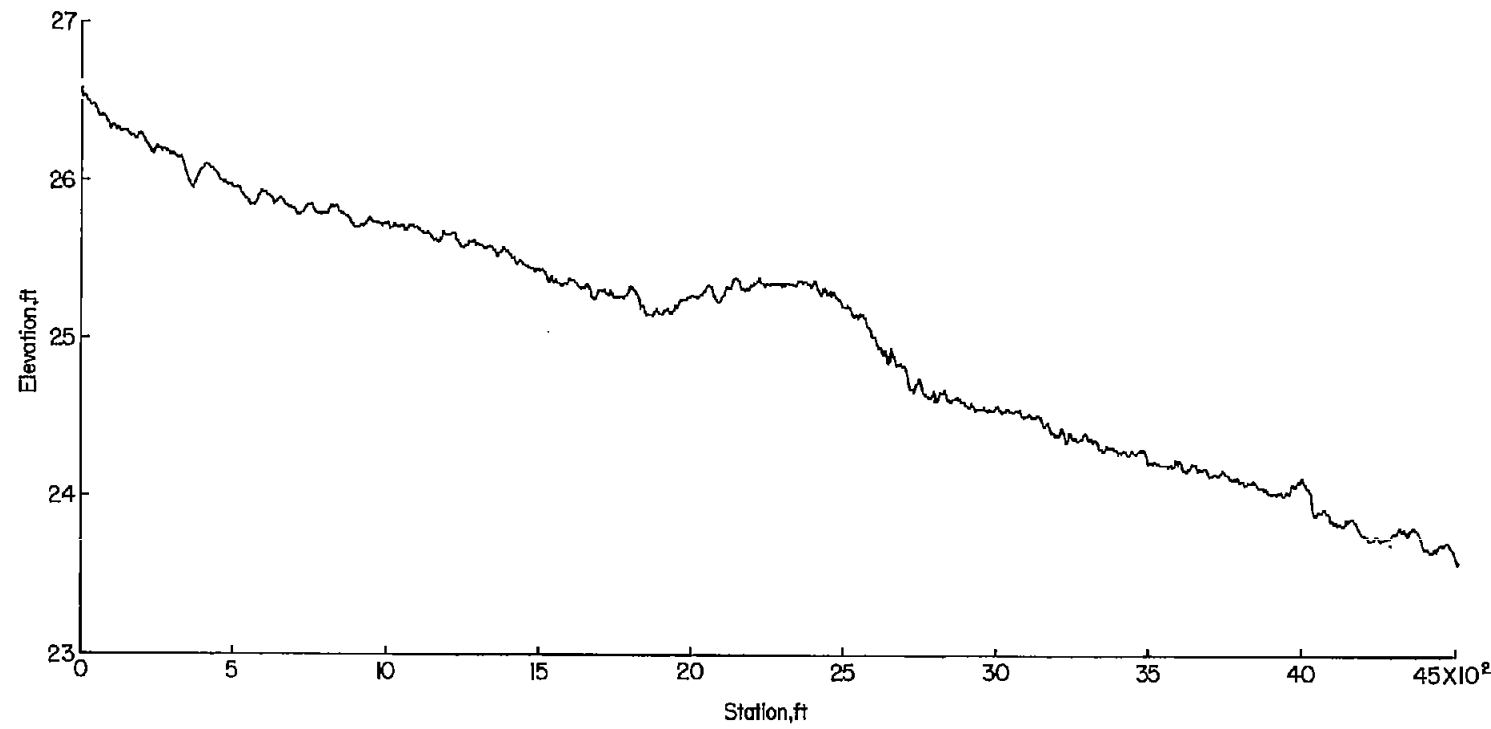
(d) March 1957.

Figure 53.- Continued.



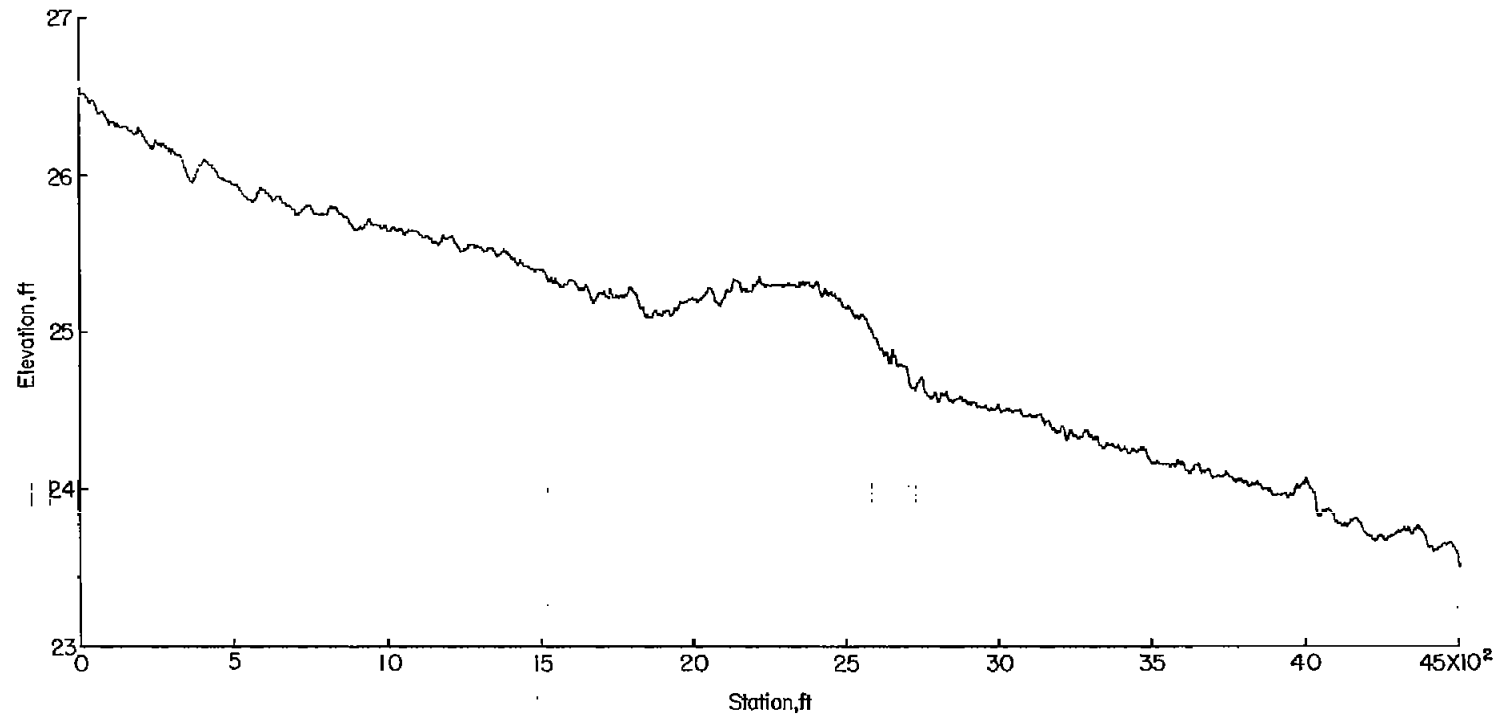
(e) April 1957.

Figure 53.- Continued.



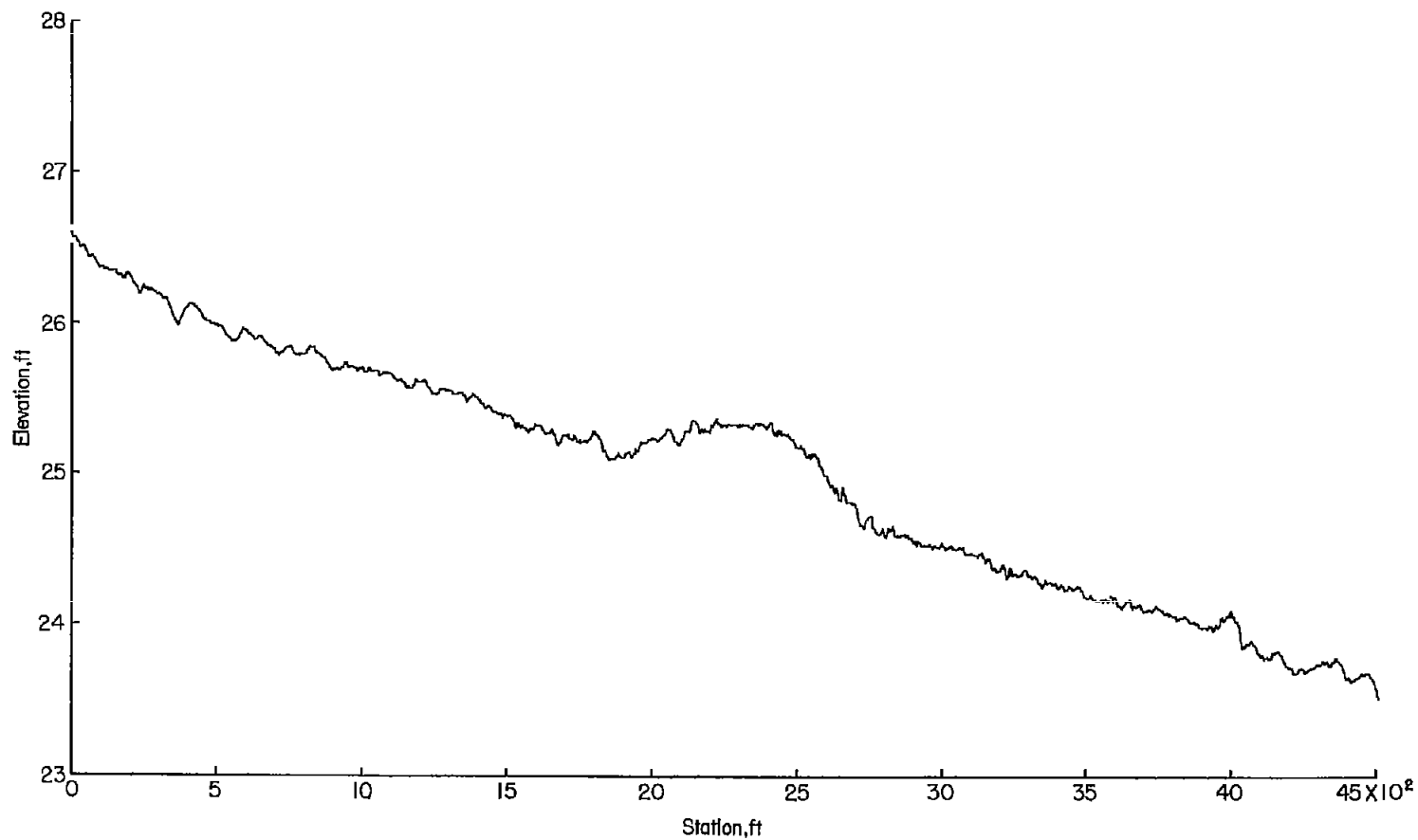
(f) May 1957.

Figure 53.- Continued.



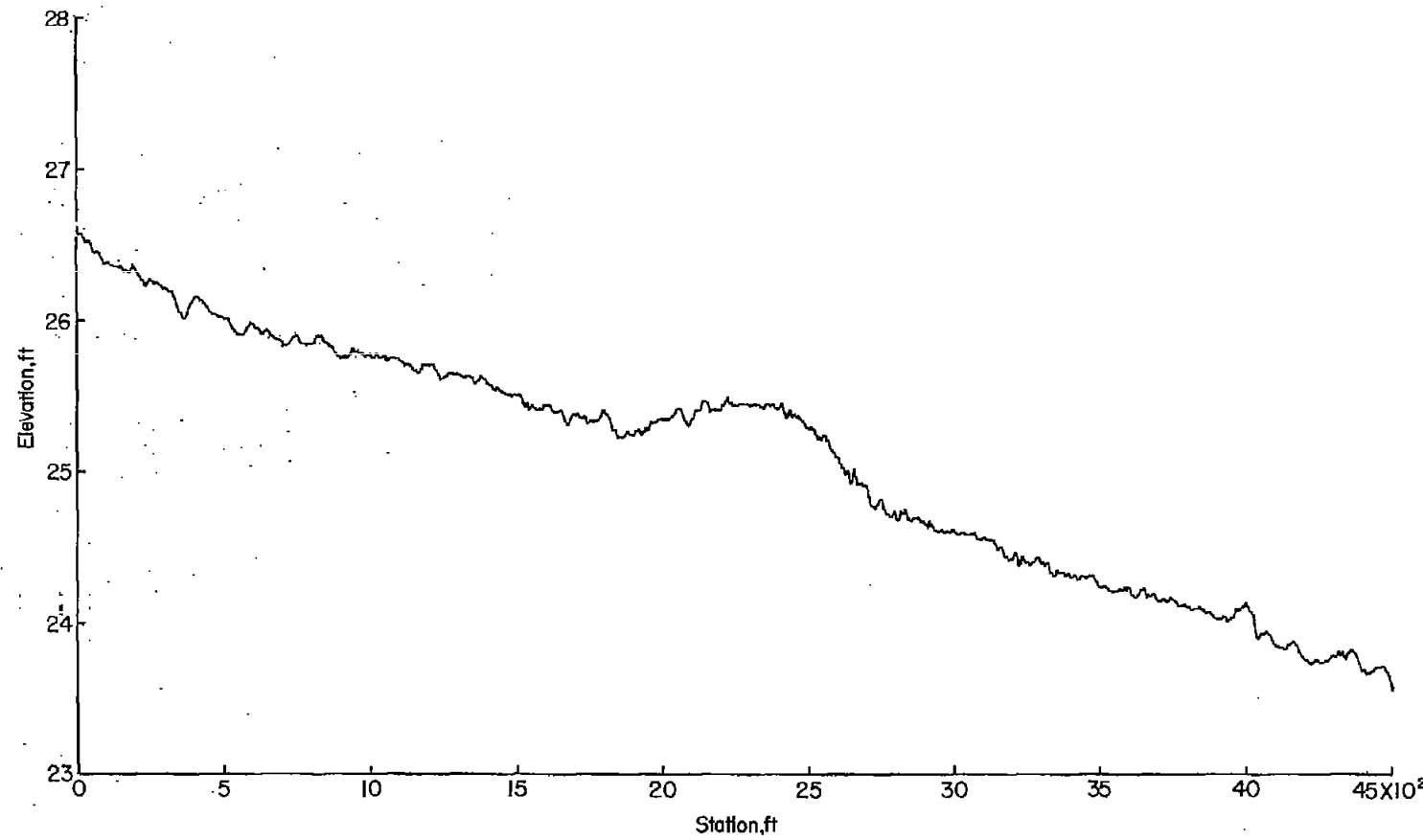
(g) June 1957.

Figure 53.- Continued.



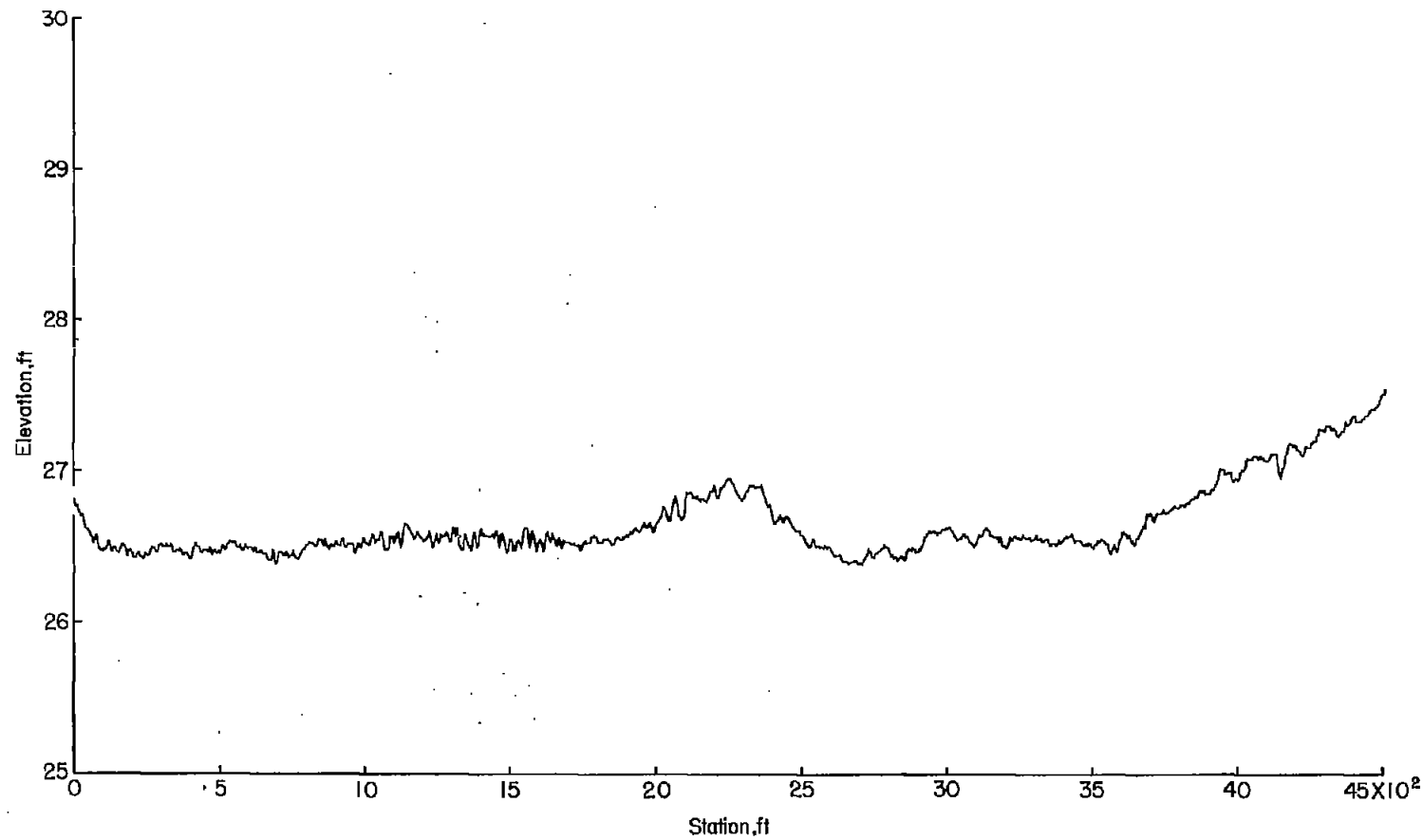
(h) July 1957.

Figure 53.- Continued.



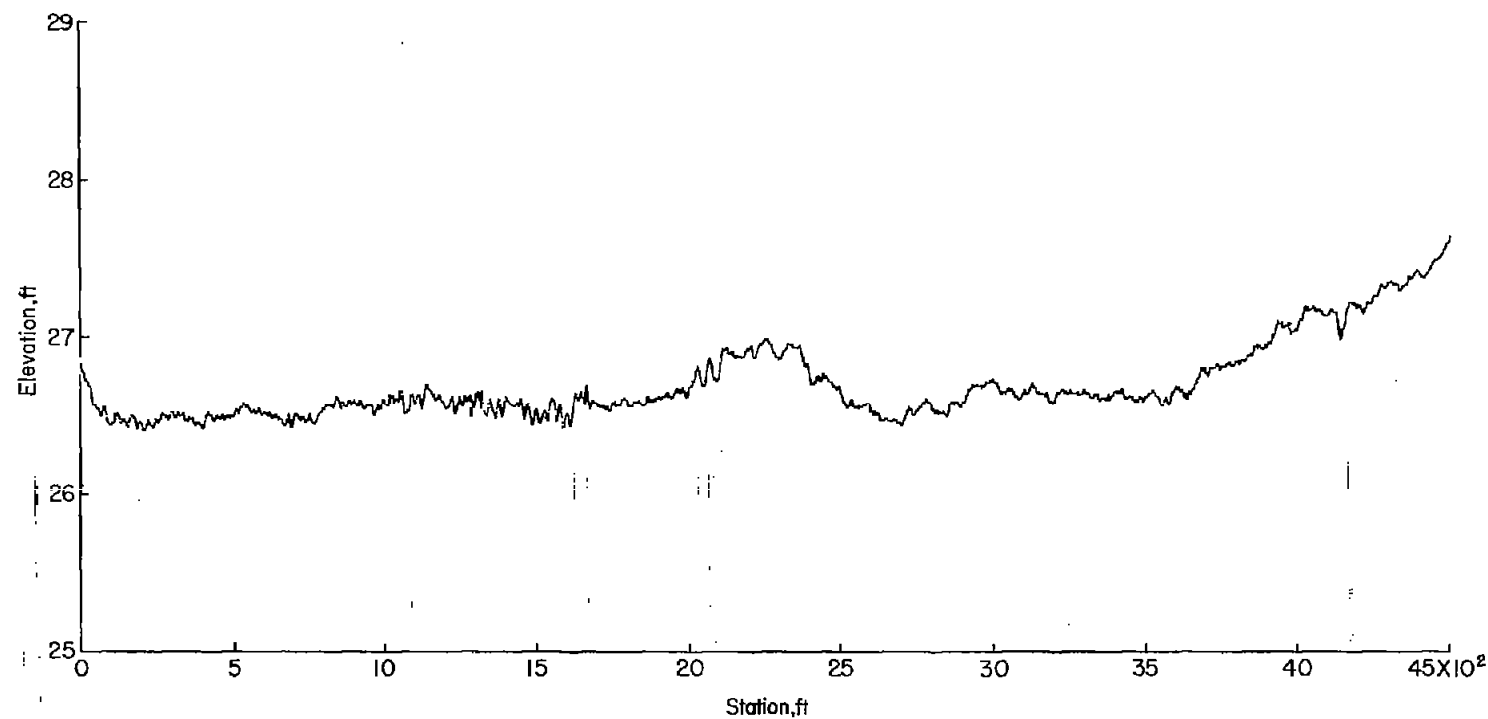
(i) August 1957.

Figure 53.- Concluded.



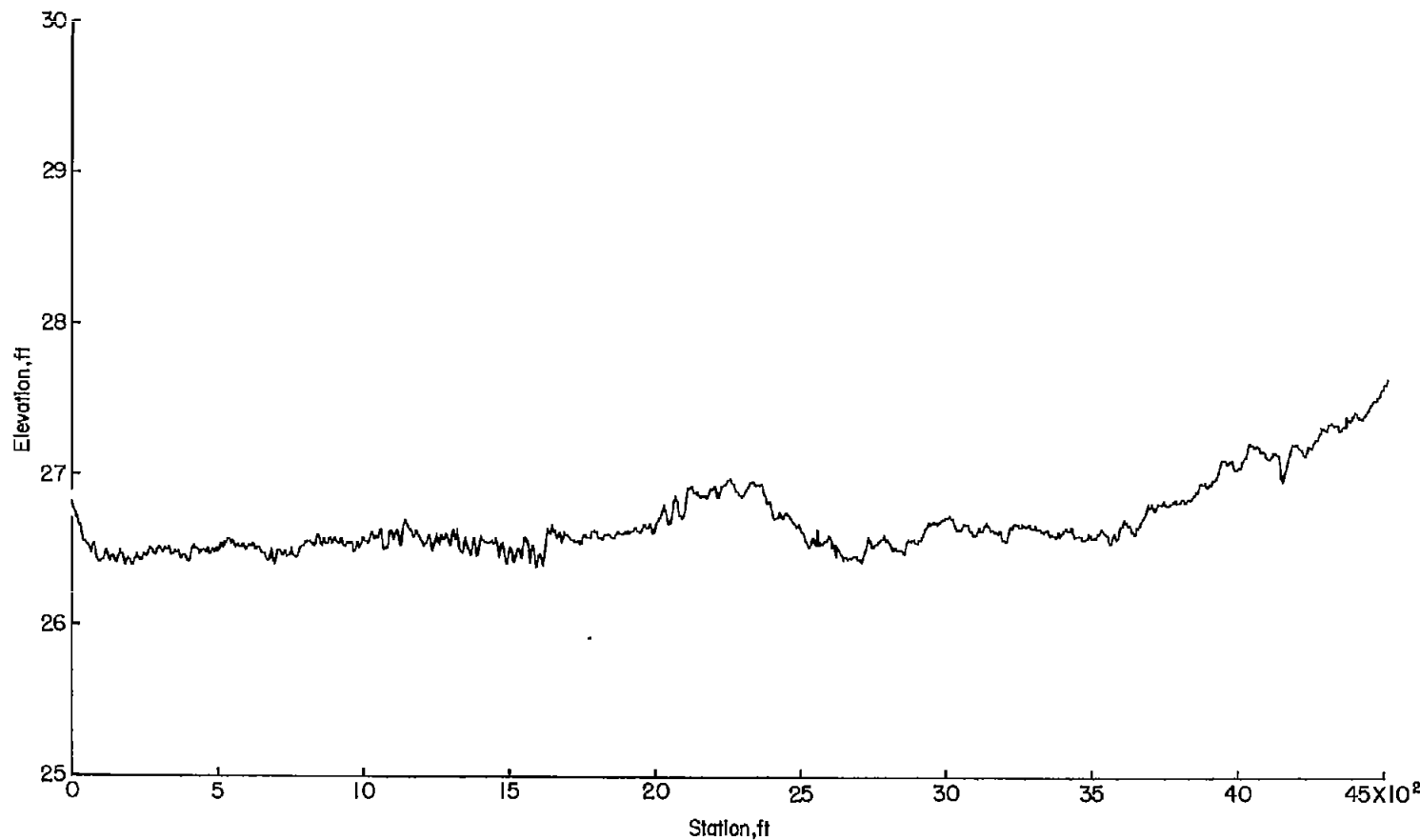
(a) December 1956.

Figure 54.- Profiles of runway 34.



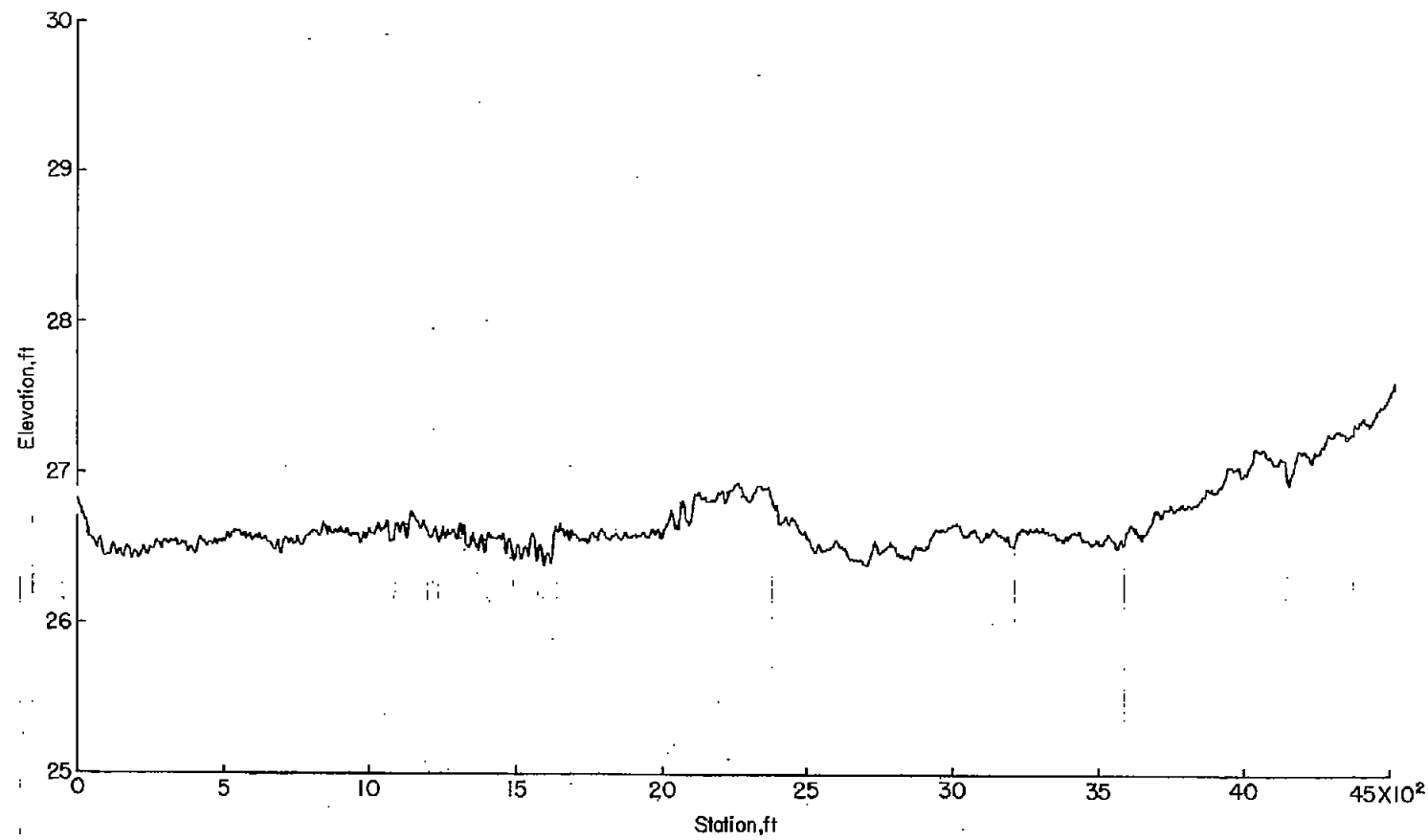
(b) January 1957.

Figure 54.- Continued.



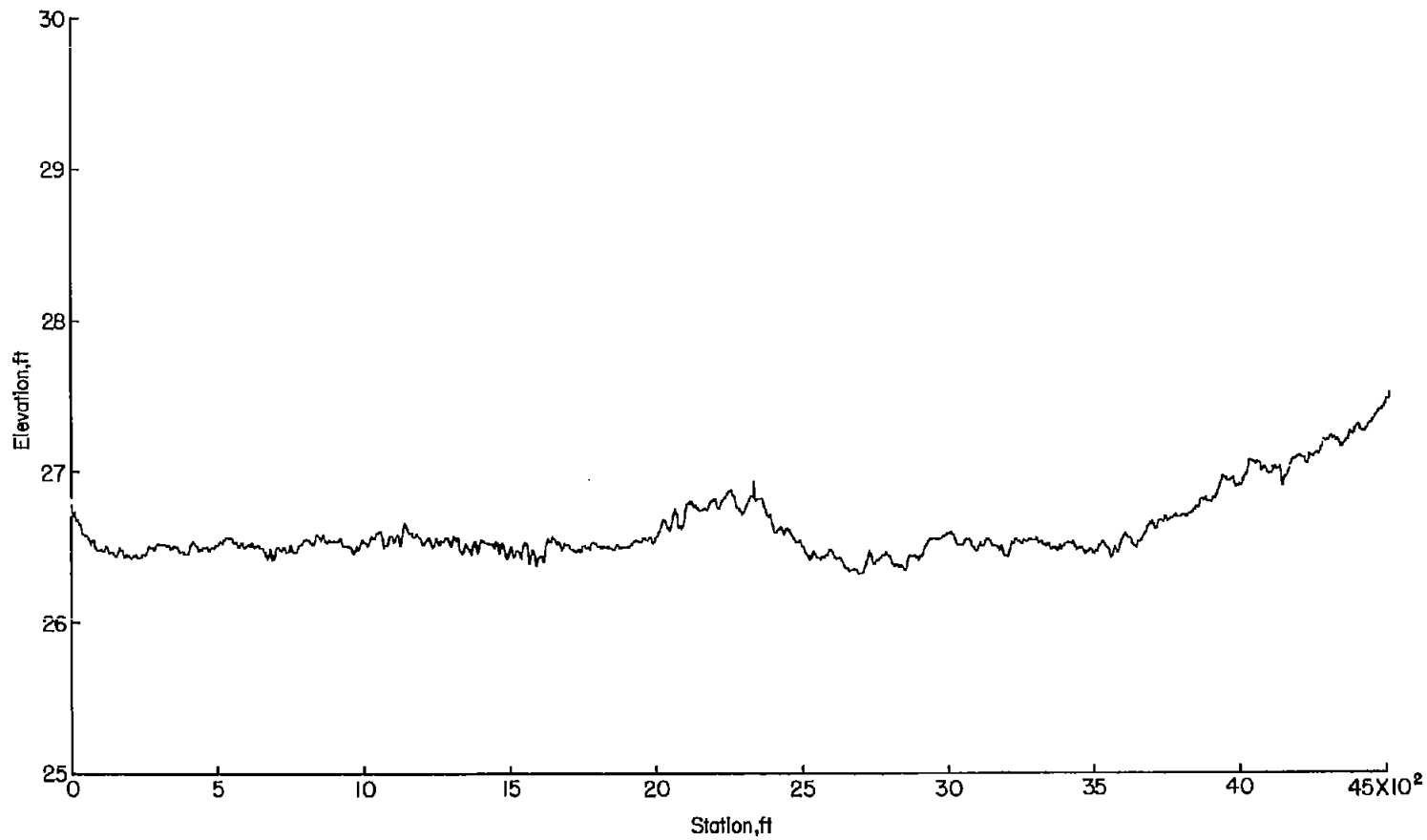
(c) February 1957.

Figure 54.- Continued.



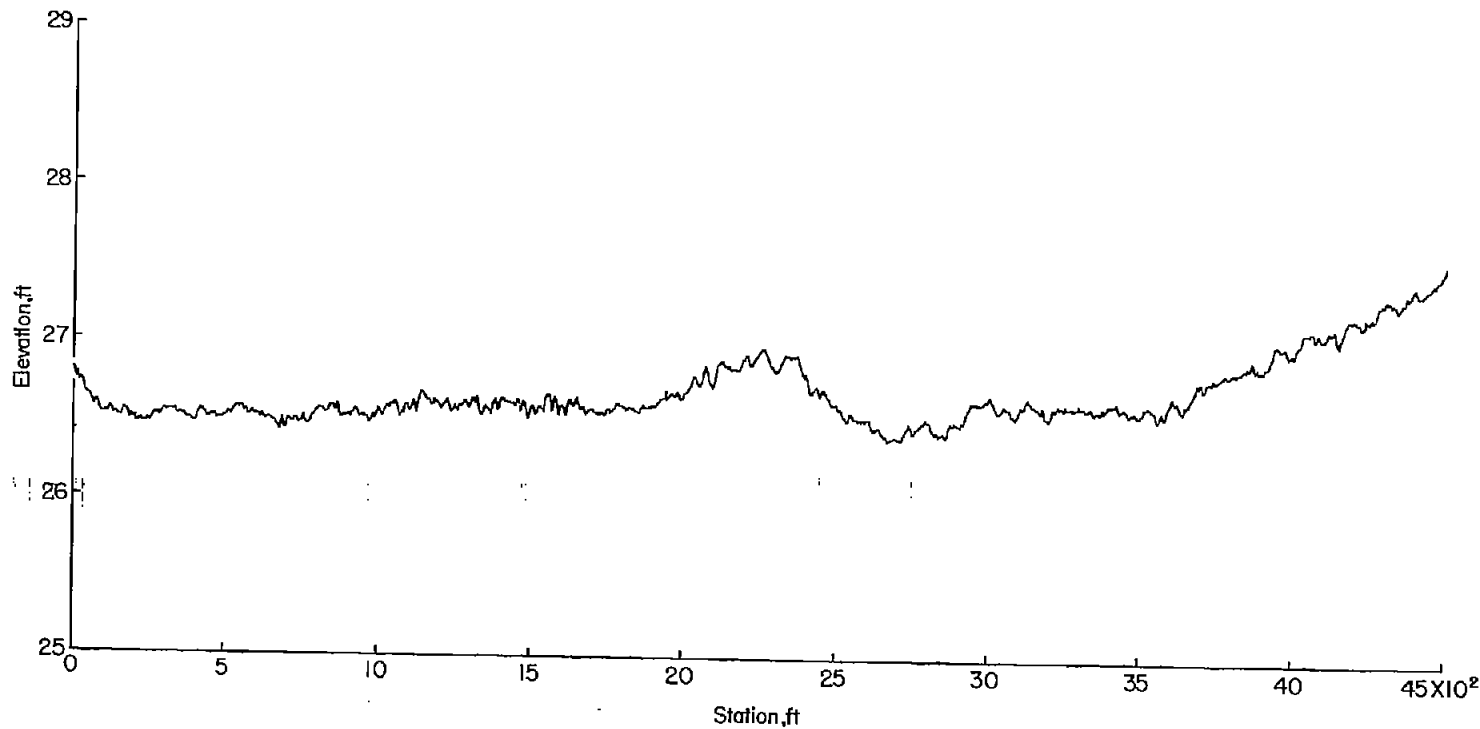
(d) March 1957.

Figure 54.- Continued.



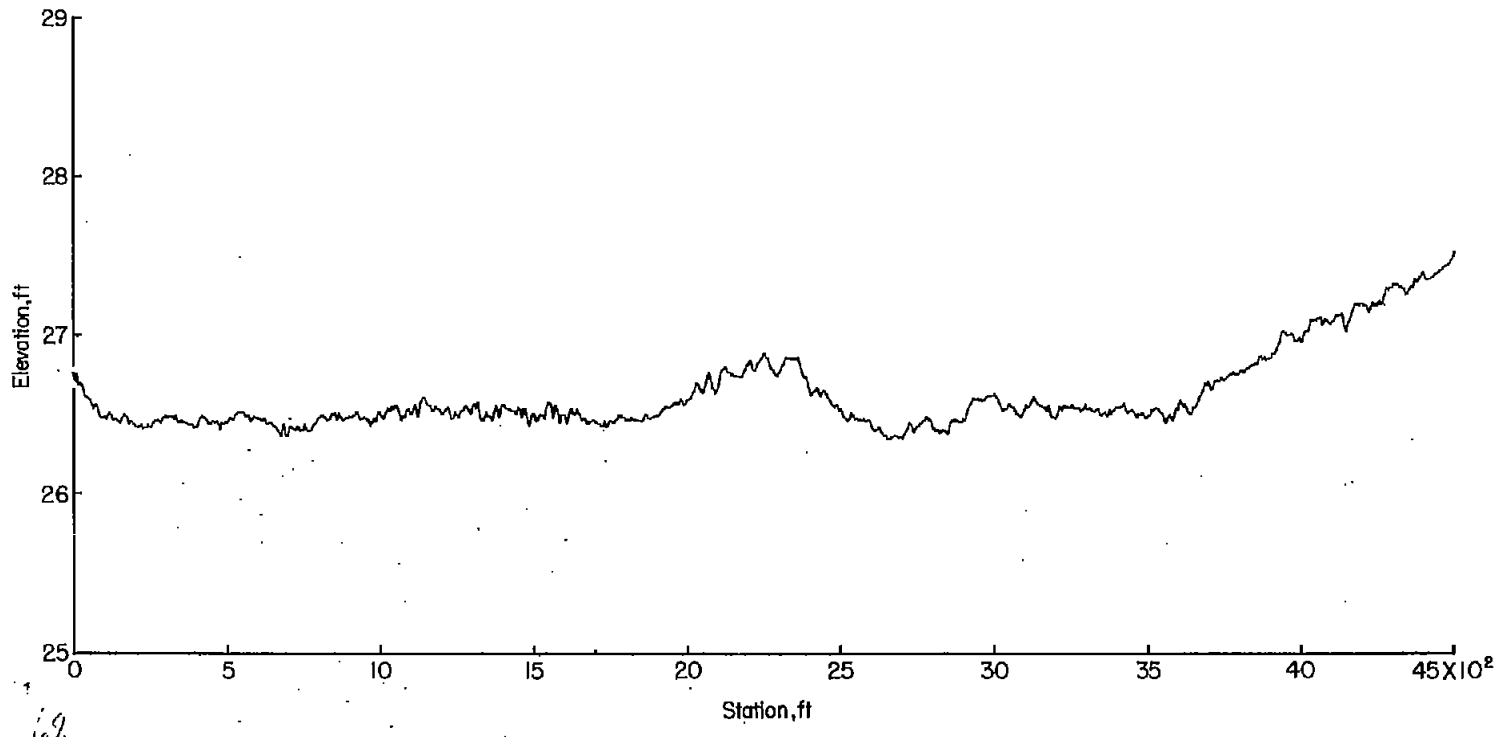
(e) April 1957.

Figure 54.- Continued.



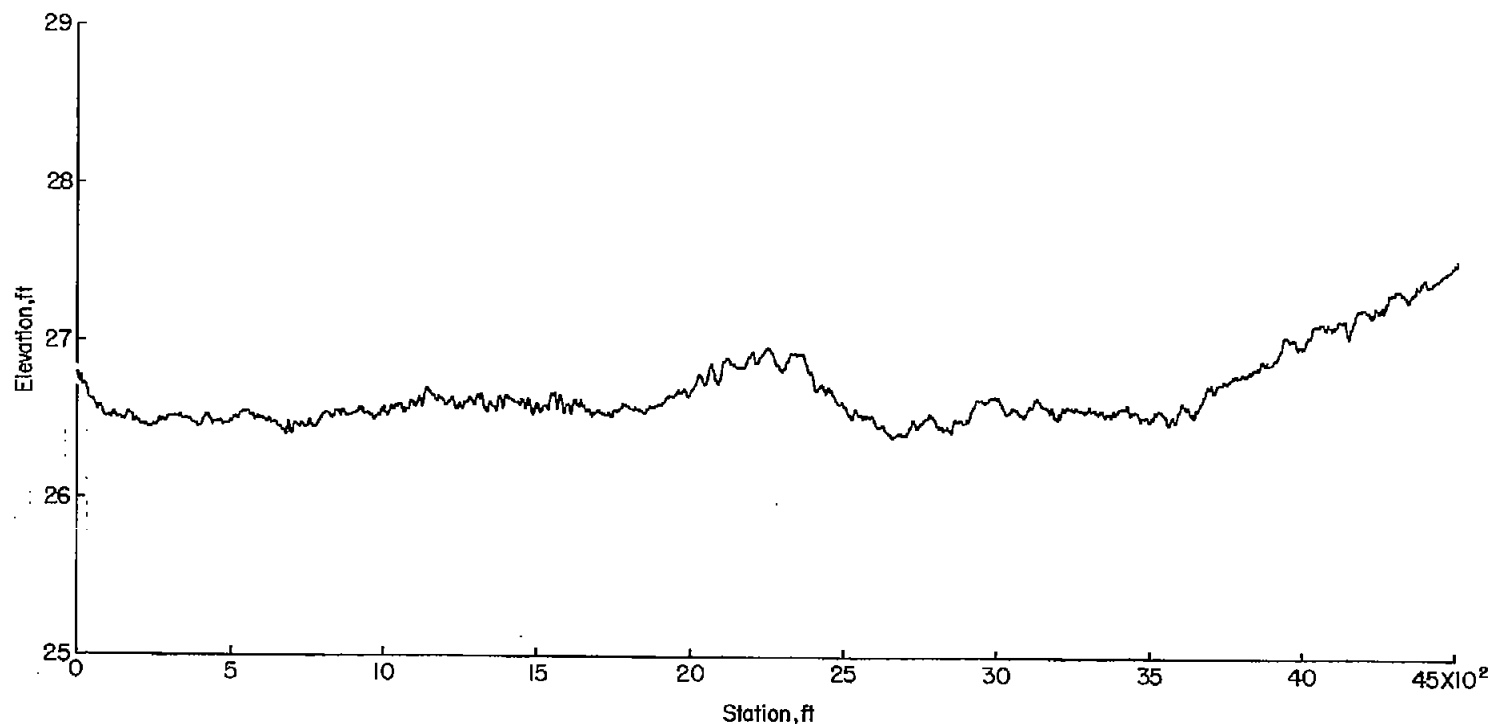
(f) May 1957.

Figure 54.- Continued.



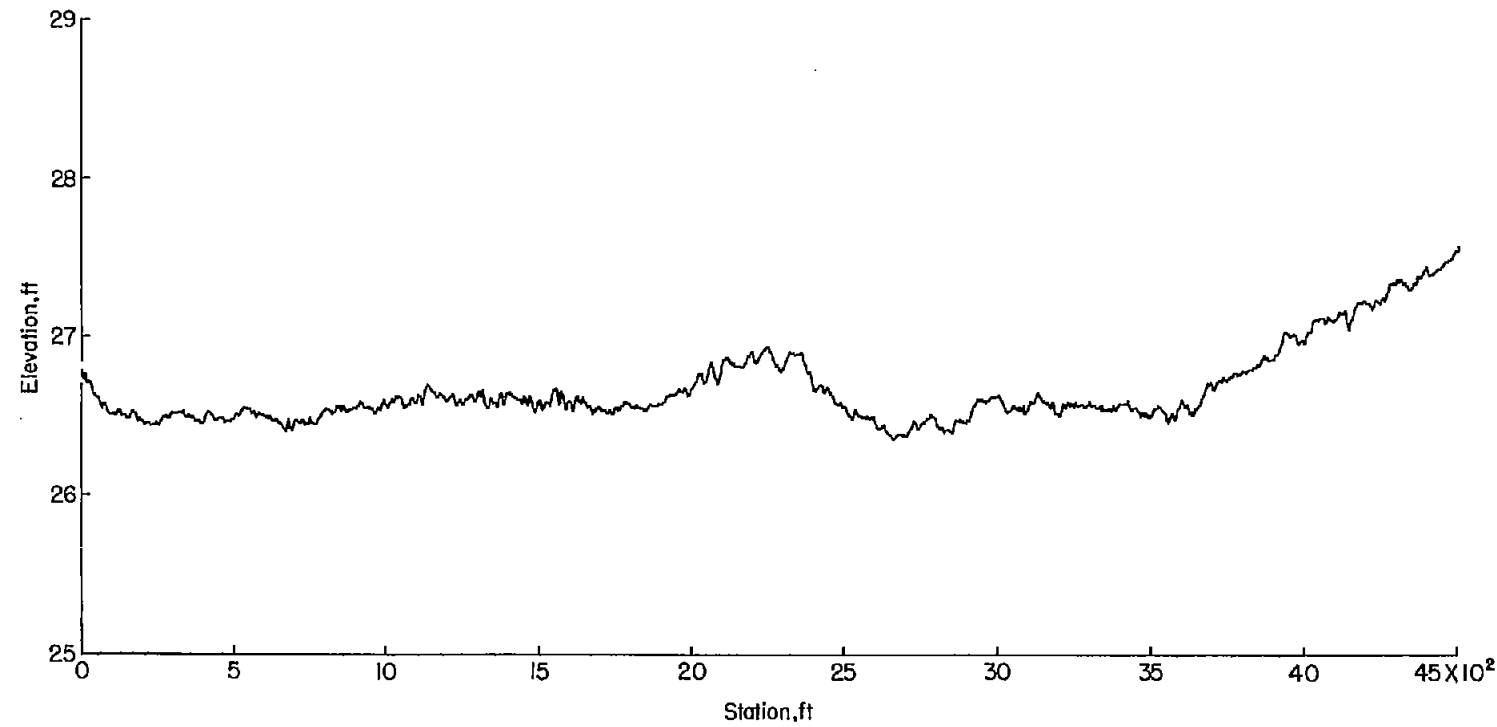
(g) June 1957.

Figure 54.-- Continued.



(h) July 1957.

Figure 54.- Continued.



(i) August 1957.

Figure 54.- Concluded.

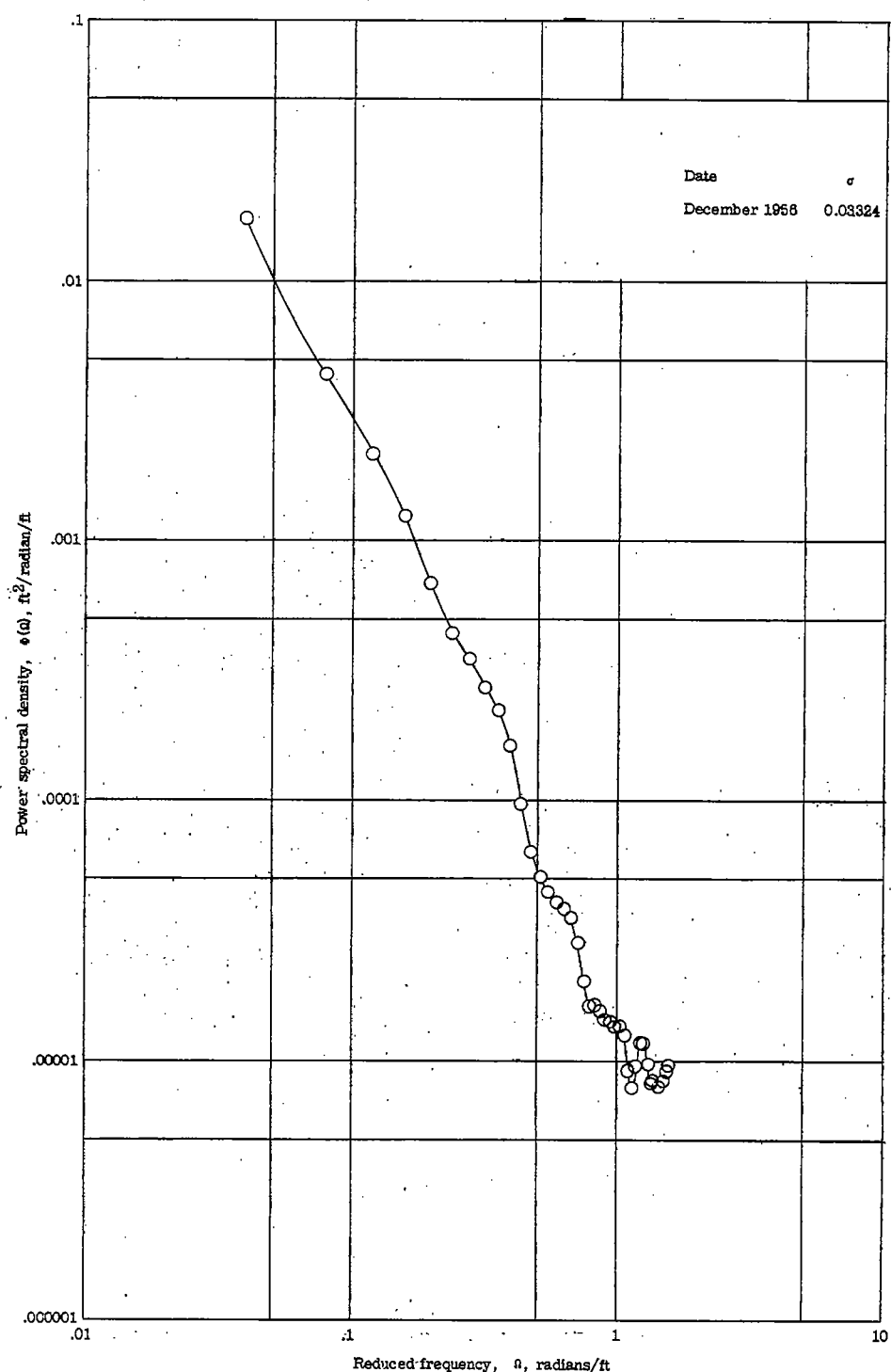


Figure 55.- Power-spectral-density functions for runway 33.

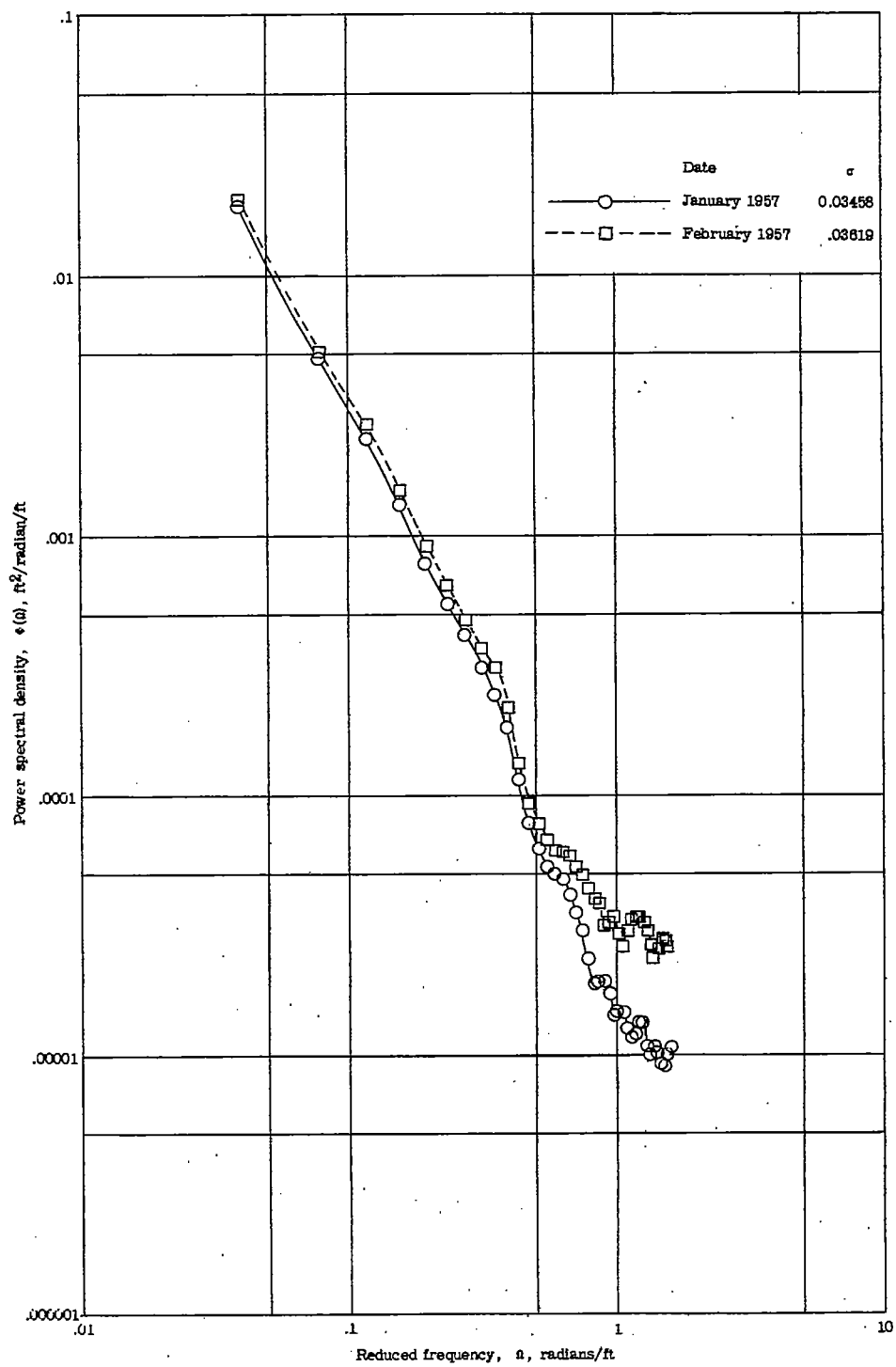


Figure 55.- Continued.

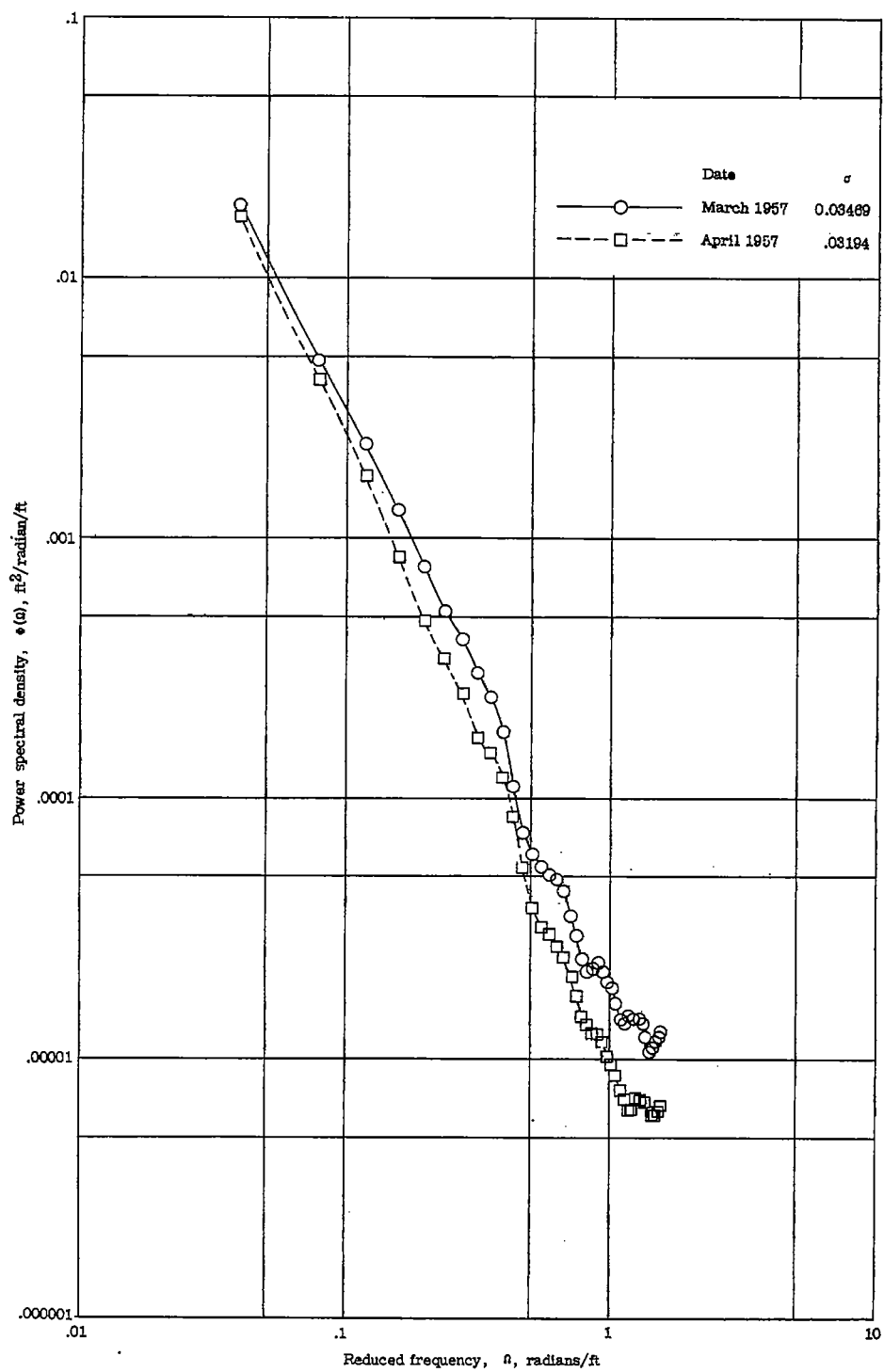


Figure 55.- Continued.

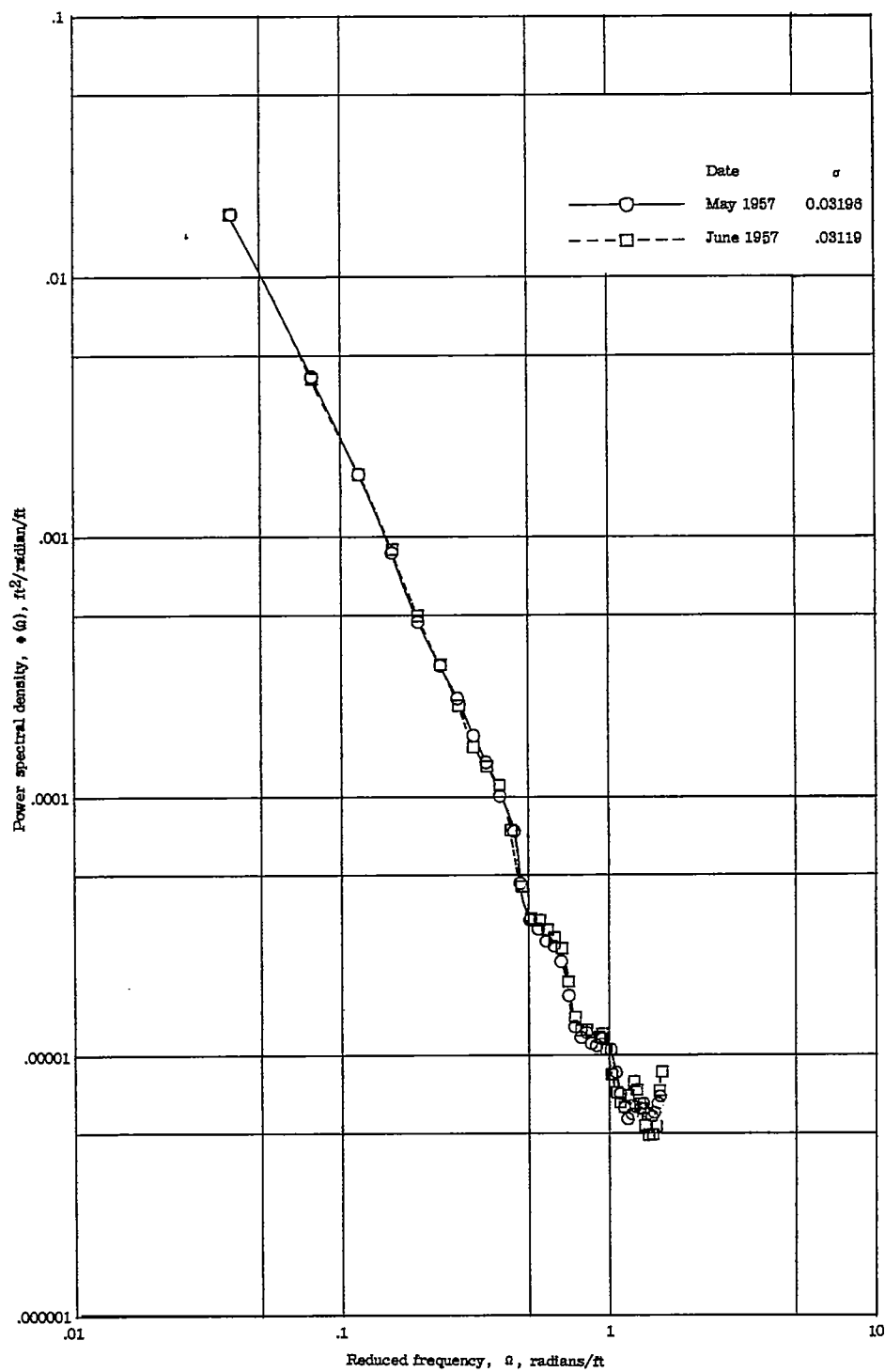


Figure 55.- Continued.

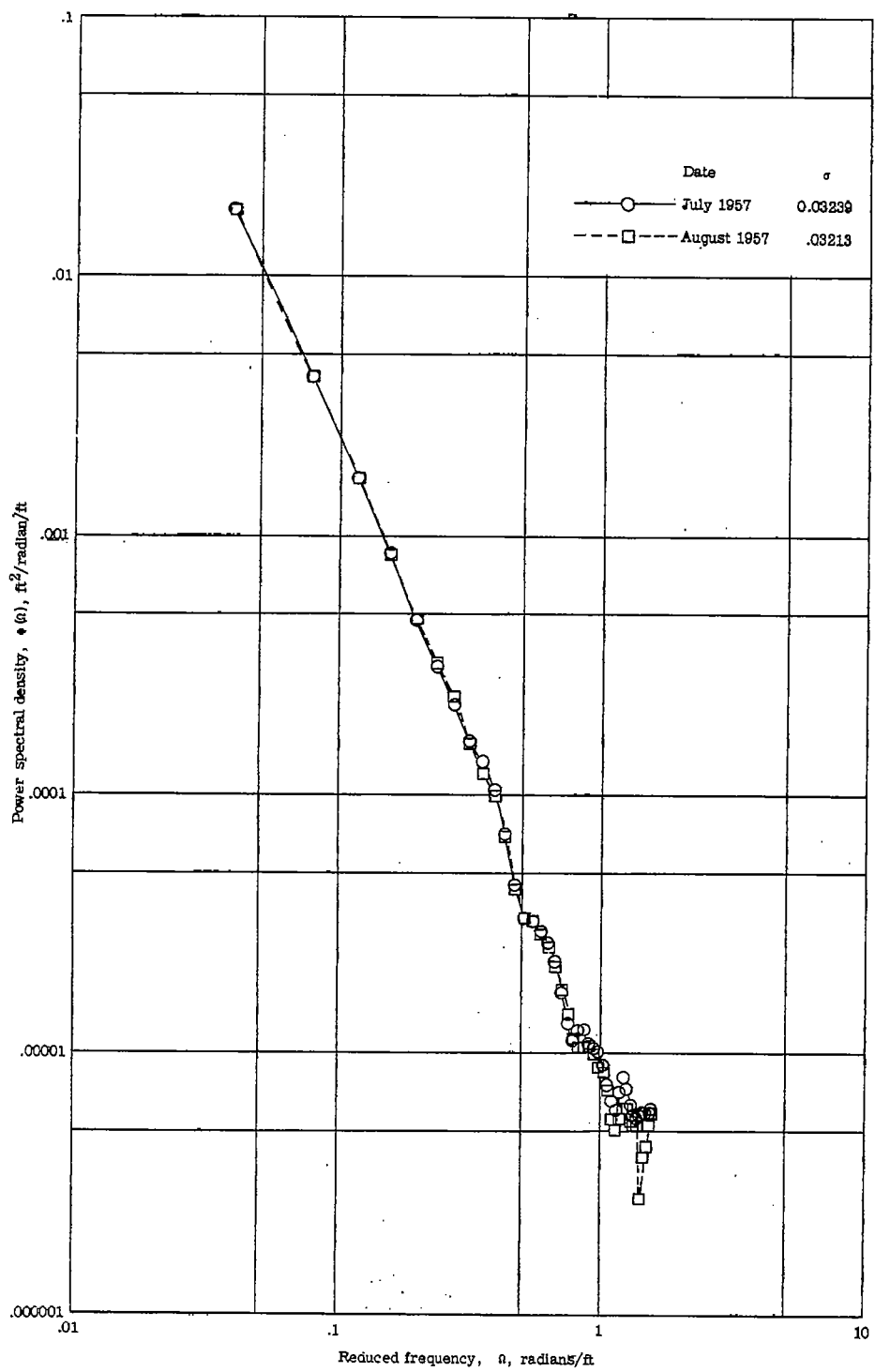


Figure 55.- Concluded.

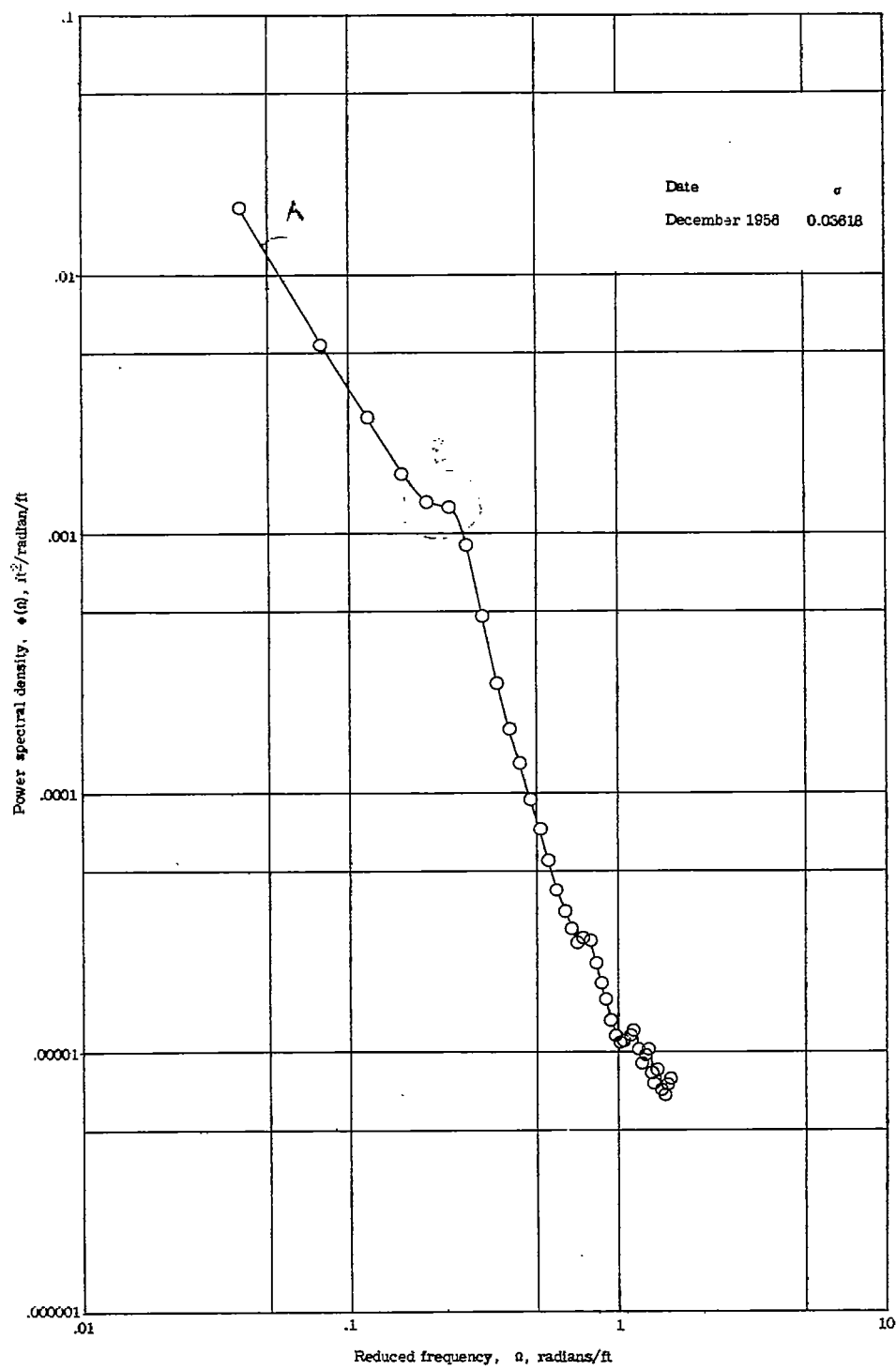


Figure 56.- Power-spectral-density functions for runway 34.

$$\begin{aligned} A: \Delta &= \frac{2\pi}{n} = .3 \\ \lambda &= \frac{2\pi}{.3} = 21' \\ \nu &= 90 \text{ ft} = 133 \frac{\text{ft}}{\text{sec}} \\ f &= \frac{\nu}{\lambda} = \frac{133}{21} = 6.3 \text{ Hz} \end{aligned}$$

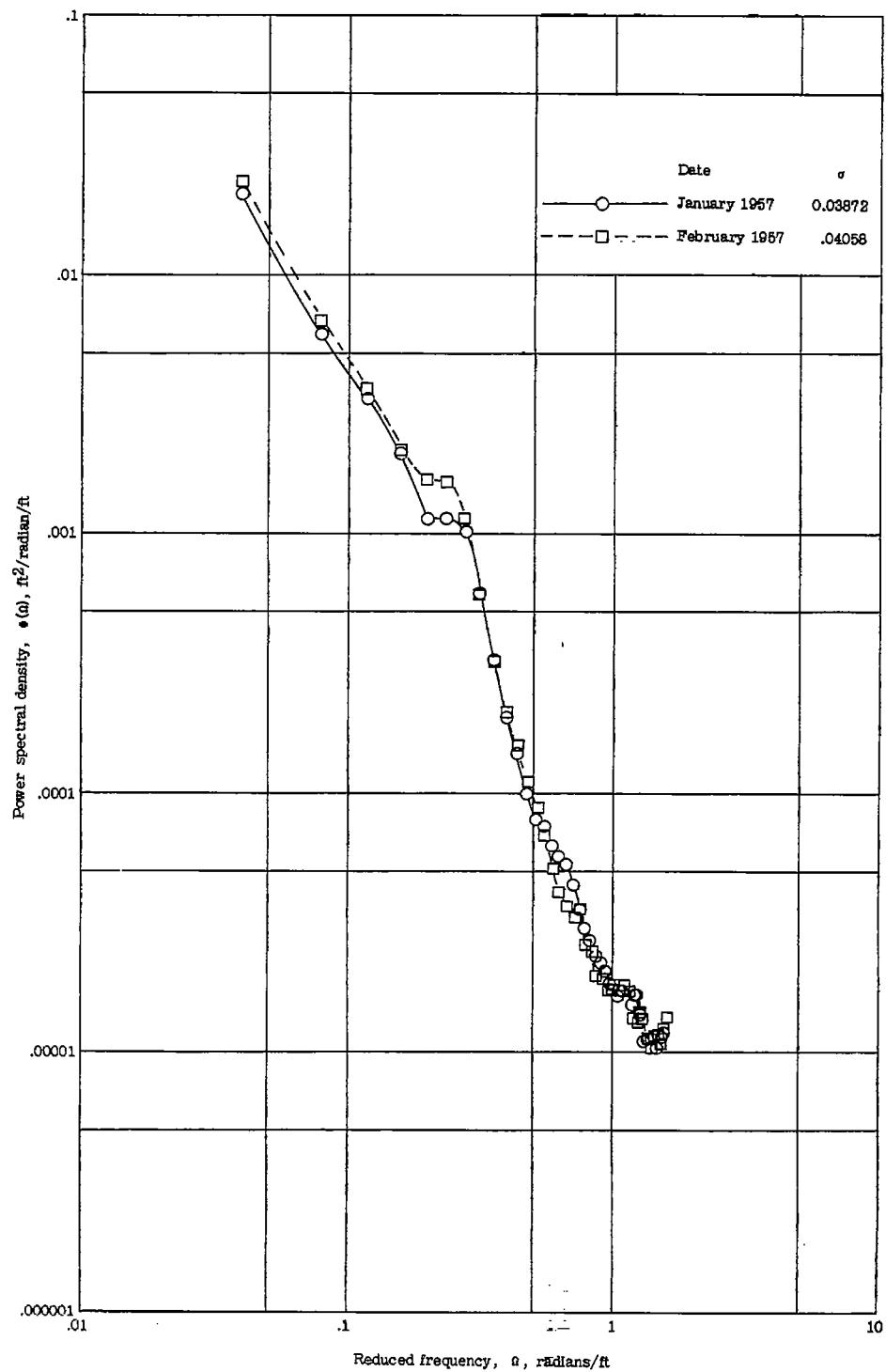


Figure 56.- Continued.

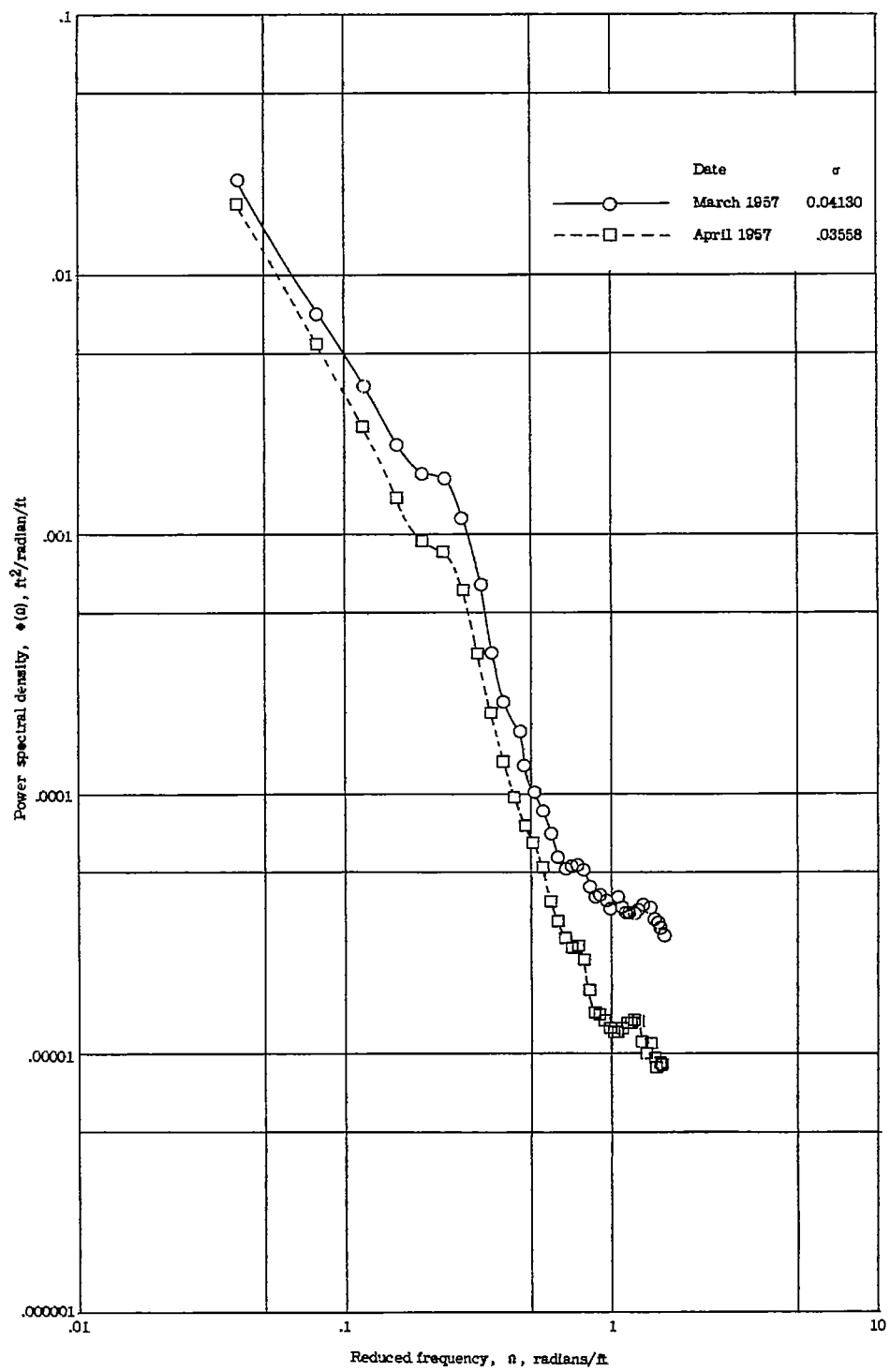


Figure 56.- Continued.

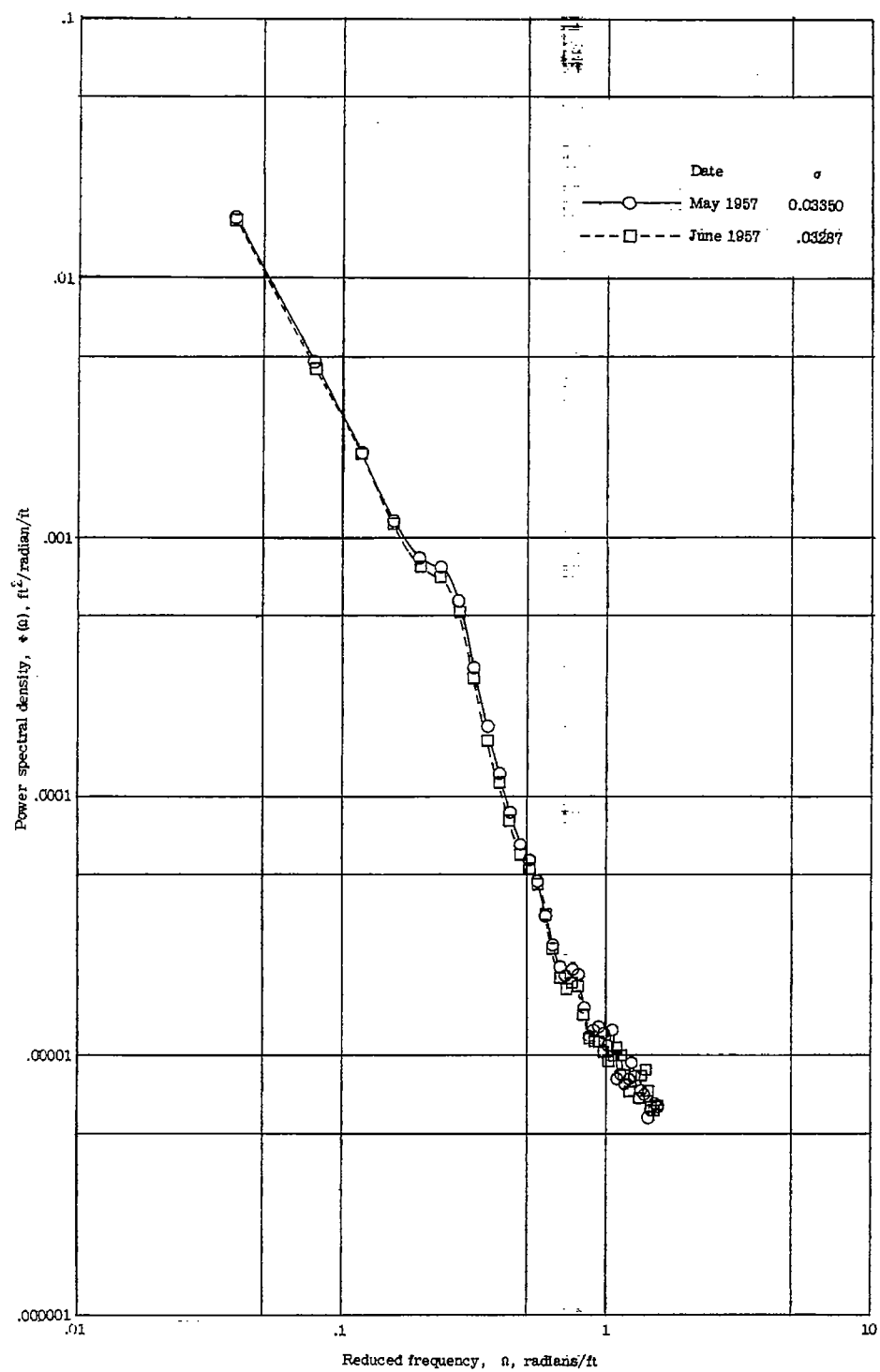


Figure 56.- Continued.

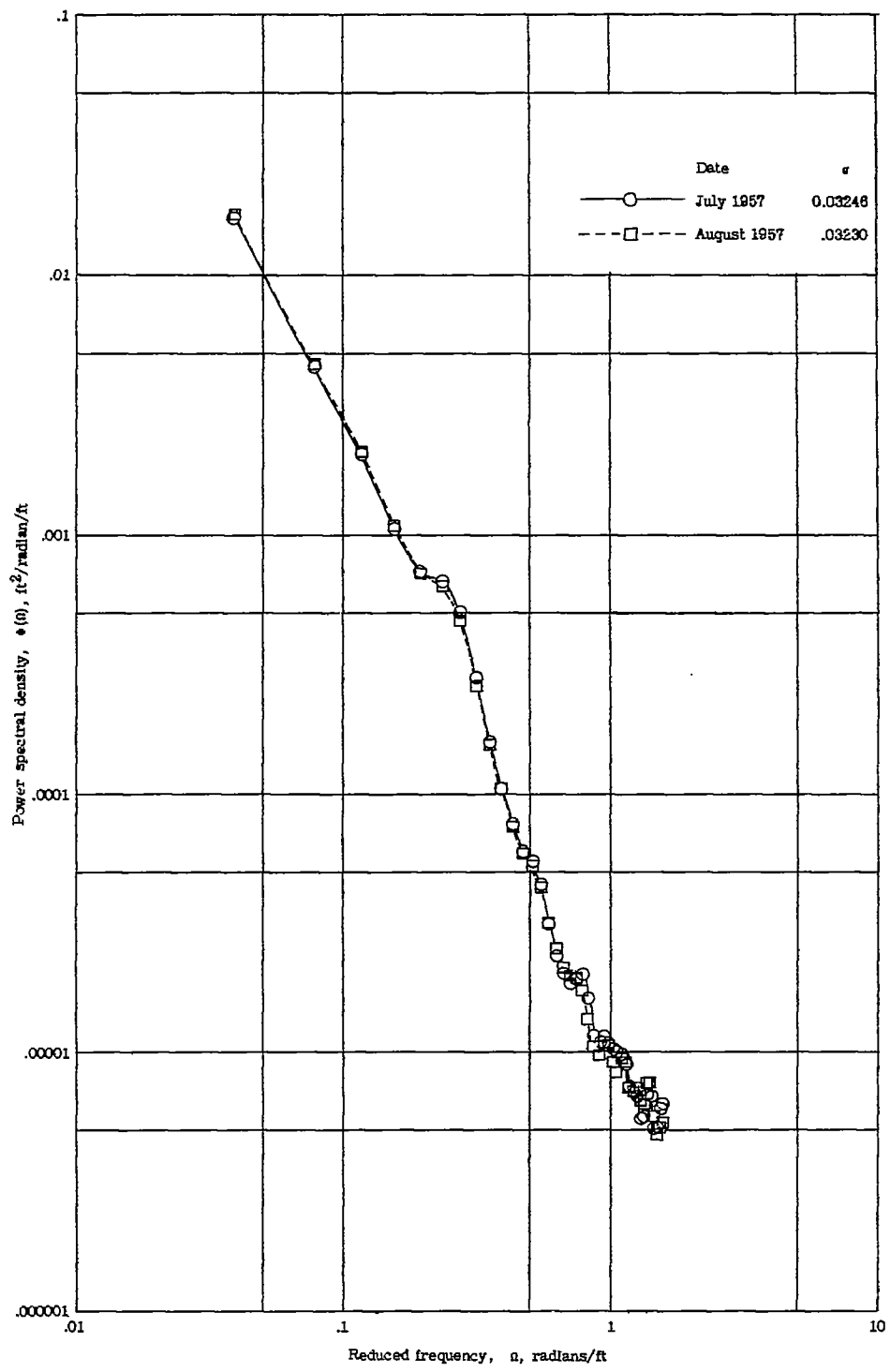


Figure 56.- Concluded.